NTNU

Norwegian University of
Science and Technology

# Analysis and Verification of a Rheological Servomechanism

**Dag Sverre Grønmyr**

Master of Science in Engineering Cybernetics
Submission date: May 2008
Supervisor: Geir Mathisen, ITK
Co-supervisor: Øyvind Stavdahl, ITK

Norwegian University of Science and Technology
Department of Engineering Cybernetics

# Problem Description

In servo applications where significant mechanical power is combined with strict limitations in size and weight, hydraulic motors are generally preferred. In reality, the proportions of the instrumentation (i.e. the size of control valves etc.) often limit the achievable power/size ratio. In this assignment you are to study actuator solutions where magnetorheological fluid, i.e. fluid whose rheological parameters vary with the magnetic field strength, is used both as a hydraulic medium and in order to realize the valve function. The aim of the assignment is to compare alternative principle solutions, optimize the geometry of the mechanism and if possible evaluate the theoretical results by means of physical experiments.

1. Outline some relevant methodologies for the development of electromechanical/mechatronic systems, and make a justified choice of methodology for this assignment.
2. Based on a traditional electrohydraulic servo valve, describe one or more derived solutions where the electromechanical parts of the servo valve are partly or completely replaced by magnetorheological solutions.
3. Perform a simulation based analysis of selected solutions with emphasis on the correspondence between geometry, material properties, and mechanical performance.
4. If necessary and as far time permits, verify the theoretical findings by doing physical experiments.

Assignment given: 07. January 2008
Supervisor: Geir Mathisen, ITK

**Abstract**

This thesis is an investigation into a small hydraulic actuator based on magnetorheological fluids. Magnetorheological fluids are "smart", synthetic fluids with the ability to change their viscosity from liquid to semi-solid state within milliseconds if a sufficiently strong magnetic field is applied. The actuator should be smaller than $5mm$ in diameter.

The thesis first gives a review of three different product development methodologies, before different actuator concepts are investigated and a concept is chosen for further exploration. Mathematical models and simulations in Comsol are used in order to find the optimal geometry and material, and to find the performance of the actuator. Finally, real tests are carried out in order to investigate some of the properties with the models and simulations that was linked to some uncertainty.

The main principle for creating a movement of the actuator is pressure distribution caused by addition and subtraction of magnetic fields over the magnetorheological fluid. It seems from the tests that subtraction of magnetic fields has a very little effect on the fluid flow. A theory is that the magnetic fields, instead of getting "subtracted", are deflected and placed parallel to the flow direction. Still, the subtraction does work the intended way, but with an extremely small effect. This can probably be improved by finding ways to lead the deflected field away from the fluid.

Even though the dimensions should be quite small (in the order of millimeters), it seems as if there should be no problem in achieving the required magnetic field from an electromagnetic coil without it going into saturation. It is a question, though, how large effect the windings of the coil will have on its size.

From the results of the calculations and simulations it seems as if the actuator can achieve both a stiffness of $0.5N/mm$ and a movement of over $5mm$, even if subtraction of magnetic fields does not work the intended way. This is with an actuator diameter of $4mm$. A higher stiffness will give a smaller movement, and vice versa.

It is recommended to either do more extensive simulations in three dimensions in Comsol, with the permanent magnets and electromagnetic coil incorporated, or to build a full-scale prototype of the actuator.

## Preface

This is a master thesis in Engineering Cybernetics, at the Norwegian University of Science and Technology in Trondheim. The year(s) has gone by quite fast, and this is now my final work as a student. It has been quite rewarding to work with this thesis since it is an exploration into something that has never been made before. I kind of feel like a pioneer. Nevertheless, it will also be quite rewarding to be able to enjoy the nice weather that always seem to turn up when there is work to be done.

As a finishing comment before the acknowledgements, I would like to share two things I have learned through five years of studies: First, always save what you are doing as often as possible, especially when you are working with time-consuming things that are not easy/quick to redo. If you do so, you can avoid losing hours of work if the program (or Windows) suddenly decides you have done enough work that day, and commits suicide right in front of your eyes, without notice, and taking everything you have done to the grave. Second, do not to drop magnets into a magnetorheological fluid. They are very difficult to get clean again. Still, it is a lot of fun! The fluid looks and feels like clay in the vicinity of the magnet, but becomes liquid as soon as it moves away from the magnet. Fun, but a bit messy.

During the course of this thesis, I have received invaluable help from a number of persons. First and foremost I would like to thank my advisor Øyvind Stavdahl for all his ideas and help concerning the thesis, and for always being positive. I would also like to thank the guys at the workshop for building the test rig, especially Hans Jørgen Berntsen. I would also like to thank Jan Leistad for his help in acquiring the simulation tool Comsol 3.4 and the additional module, Knut Einar Aasland for recommending litterature concerning product development methodologies, and John Olav Horrigmo for lending me the Teslameter. Finally, I am grateful for the help I have received from the Comsol support team.

# List of Figures

# List of Tables

## Nomenclature

| | |
|---|---|
| $kg/cm^2$ | Kilogram-force per square centimetre – a unit of pressure using metric units. Also called *technical atmosphere* $[at]$. $1kg/cm^2 = 98.0665kPa$ |
| B | Magnetic flux density, also called magnetic field, unit Tesla [T] |
| bar | Unit of pressure. $1bar = 100kPa$ |
| Dynamic viscosity | A viscosity coefficient determining the dynamics of an incompressible Newtonian fluid. $\eta$ $[Pa \cdot s]$ |
| H | Magnetic field intensity, $[N/A^2]$ |
| Mechatronics | The combination of mechanical, electronic and software engineering |
| Metric | A standard unit of measure, or more generally, part of a system of parameters, or systems of measurement. |
| Neodymium magnet | A powerful magnet made of a combination of neodymium, iron, and boron – $Nd_2Fe_{14}B$. Also called NIB magnet or, less specifically, a *rare-earth magnet*. |
| Pa | Pascal – SI derived unit of pressure or stress. $1Pa = 1N/m^2$ |
| Relative permeability | The ratio of the permeability of a specific medium to the permeability of free space given by the magnetic constant $\mu_0 = 4\pi \cdot 10^{-7} N/A^2$. $\mu_r = \frac{\mu}{\mu_0}$ |
| Rheology | The science of the deformation and flow of matter |
| Shear | The movement of a layer of material relative to parallel adjacent layers |
| Shear rate | The change of shear strain per unit time, also called strain rate. $\dot{\gamma}$ [1/s] |
| Shear strain | Relative deformation in shear. $\gamma$ |

| | |
|---|---|
| Shear stress | The component of stress parallel to (tangential to) the area considered. $\tau$ [Pa] |
| Strain | The measurement of deformation relative to a reference configuration of length, area or volume. Also called relative deformation. |
| Stress | A force per unit area. [Pa] |
| Yield stress | The stress corresponding to the transition from elastic to plastic deformation. $\tau_y$ [Pa] |

# Contents

# 1 Introduction

In servo applications where significant mechanical power is combined with limitations in size and weight, hydraulic motors are generally preferred. This thesis will continue the work done in [5], where a new type of tiny actuators based on a technology of fluids that exhibit rapid and reversible increase in flow resistance through the application of a magnetic field (magnetorheological fluids) was modelled and simulated. The design considered in [5] turned out to have some drawbacks that was devastating to its ability to meet the requirements. The worst problem was the magnetic saturation that, if left unsolved, would make the servomechanism virtually useless due to its inability to supply enough magnetic field to the fluid. Another drawback that was not thought of in [5] is the fact that the magnetic field probably would contribute to dragging the pin down, especially at the relatively high magnetic fields required for the fluid to perform at its maximum.

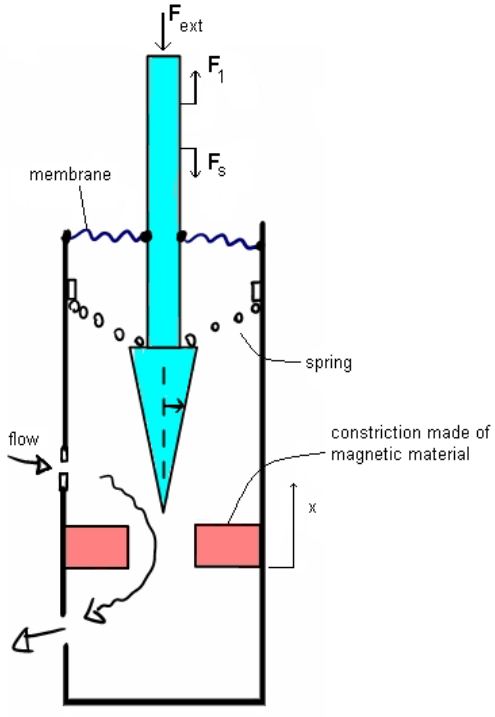


**Figure 1:** Sketch illustrating the initial design of the concept in [5], which proved to have some flaws that made it necessary to explore new concepts.

Therefore, rather than further exploring a design that could prove to be useless, it was decided to investigate other concepts that possibly could remedy the problems and perhaps improve the stiffness of the actuator and lead to a larger movement. This might take more time than just refining the previous concept, but will no doubt increase the probability of success.

As before, the servomechanism should have no sensors, making it a *sensorless* actuator. This has several advantages, such as less wires, it can be made smaller, and easier control. The fact that it should be sensorless implies that disturbances must have no, or at least very little, impact on the system. It should go to the desired reference value almost irrespective of what happens. For instance, the actuator should be "stiff" enough to stay at the same displacement even with a certain applied external force. In addition, it should be as small as possible, preferably with a diameter smaller than $5mm$.

If the new design should turn out to be successful, the actuator will produce considerable mechanical power compared to its size, and will have a vast potential market, as the world is moving towards smaller and smaller actuators at the same time as demanding a significant power. Conventional mechanisms often fails in providing necessary power when being in millimeter dimensions. A possible area of application could be tactile displays, for instance like the one considered in [13].

Notice that the terms "actuator" and "servomechanism" will be (and has been) used interchangeably throughout the report.

## 1.1 Background

The *magnetorheological fluid* was chosen in [5, Chapter 2] because of its higher performance and considerable smaller voltage needed, compared to its "counterpart", electrorheological fluids. Magnetorheological fluids are colloidal suspensions of particles in inert carrier liquids. The particles, typically in the order of 1 to $10\mu m$ in size, are magnetizable in such a way that they form chains in the appearance of a magnetic field. As the fluid flows these chains will be broken down and reformed, which creates a resistance against the flow. The magnetorheological fluid may be continuously and reversibly varied from a state of free flowing liquid in the absence of an applied field to that of stiff semisolids in a moderate field, with a response time in the order of milliseconds. [16]

In the absence of a magnetic field, the magnetorheological fluid may be characterized as Newtonian, i.e. as resisting shear strain $\gamma$ with a shear stress

$\tau$ proportional to the product of the strain rate $\dot{\gamma}$ and (dynamic) viscosity $\eta$:

$$\tau = \eta\dot{\gamma}$$

With a magnetic field present, the behaviour of the magnetorheological fluid can be approximated by the *Bingham plastic model*:

$$\tau = \tau_y(H) + \eta\dot{\gamma} \quad , \tau > \tau_y \tag{1}$$

where the difference compared to the Newtonian model is the yield stress $\tau_y$, which is dependent on the magnetic field intensity $H$. *How* the yield stress varies is dependent on various variables, such as fluid and particle composition. An example is shown in the technical data sheet in Appendix D. In [5], the yield stress was approximated by $\tau_y = 0.3H$, but other linear or nonlinear approximations might certainly provide a better approximation. The best possible approximation should be found for each specific range of magnetic fields.

In [5], the pressure drop over a certain distance was calculated by using a parallel plates approximation. The pressure drop of a Bingham fluid between parallel plates is given by an equation depending on the flow regime. A variable $T^*$ is used to decide which equation to employ:

$$T^* = \frac{bh^2\tau_y}{12Q\eta} \tag{2}$$

where $b$ is the width of the plates, $h$ is the distance between the parallel plates (see Figure 2), $\tau_y$ is the field-induced yield stress, $Q$ is the flow rate and $\eta$ is the dynamic viscosity. The pressure drop equations are:

$$\Delta p = \frac{12\eta QL}{bh^3} + 3\frac{L}{h}\tau_y \quad , T^* < 0.5 \tag{3}$$

$$\Delta p = \frac{8\eta QL}{bh^3} + 2\frac{L}{h}\tau_y \quad , T^* > 200 \tag{4}$$

where L is the length of the plates. An adjustment can be done to these equations by saying that $bh = A$, with $A$ then being the cross-sectional area in the flow direction. The denominator in the first part of the equations then becomes $Ah^2$ instead of $bh^3$.

Please see [5] for more information about the modelling and simulation of the previous concept and for more information concerning magnetorheological (and electrorheological) fluids.

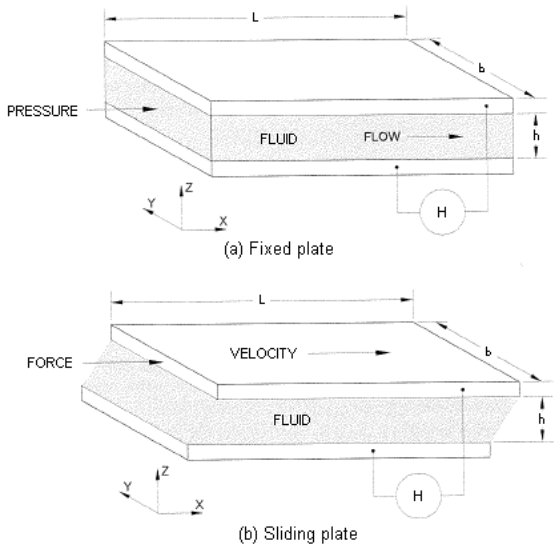


**Figure 2:** Gap geometries and fluid shear modes, from [16]. (a) is also called 'Flow Mode' while (b) illustrates the 'Shear Mode'.

## 1.2 Outline

Chapter 2 explores three different product development methodologies, and a methodology that will be used in this thesis is found.

In Chapter 3 different servomechanism concepts are developed and described, before a concept is selected for further investigation.

The next chapter, Chapter 4, deals with some modelling of the behaviour of the servomechanism, in addition to simulations and tests in order to explore the performance and viability of the concept.

The following chapters include discussion, conclusion, and a prospective.

## 1.3 Contributions

Most of my contribution to this project has been adapting existing equations and models to the specific problem, extracting information from the literature, and performing simulations.

The majority of ideas concerning the concepts come from others than me, but some of the changes brought by the simulations and calculations such as the cylinder constriction concept was my idea. The test rig was mostly my design, with great help from the staff at the workshop.

# 2 Product Development Methodologies

## 2.1 Introduction

A sensible product development methodology is of great help in attaining a both cost efficient and time efficient development process. In addition it is a lending hand to structuring the development process and making sure that the probability of success is at a maximum. In this chapter some product development methodologies will be reviewed before eventually one of them is selected and applied to the following development process.

Bearing in mind that this is not a commercial product in the way that production costs, sales price, and potential market will not be considered, and that there is no large "team" involved in developing the product, some of the theories presented in the litterature are not entirely relevant. The design (appearance/shape) of the product is not of any concern either. The focus is on getting a functioning "product" with its geometry and material decided by performance criteria rather than the looks and cost of it. Therefore this will not be a complete review of the different methodologies. Only the parts that might be relevant are chosen and repeated. If more detailed descriptions are needed, please see the literature.

The following sections are short compilations of the most important and *relevant* elements in the different methodologies described in [3, 14, 17], and are, as earlier mentioned, not meant as a thorough investigation into each methodology. For instance, some of the parts involving software methods have either been omitted or very superficially commented on due to the fact that software/programming is not a part of this assignment. To keep the overview, each methodology has its own section. Some might not be entirely relevant, but is referred to nevertheless in order to maintain consistency with the literature. In the end of the chapter, the methodology that fits best for the purpose will be chosen and adapted to fit the properties of this project.

Note that although some has been rewritten, a major part of this chapter is partly or completely taken from the references. As far as possible, this will be cited with references to the respective pages.

## 2.2 Shakeri Methodology

In [14], Ahmad Shakeri has proposed a methodology he calls "The Mechatronic Methodology"(TMM), used for the development of mechatronic systems, with the main focus on the abstract views, as opposed to the concrete views being the main concern in most methodologies. A few concrete views are also considered, with the concrete part being based on the results of the abstract part. The abstract part consist of the problem domain analysis, the requirements analysis (both part of the *initial analysis*) and the *abstract design*. The bridge connecting the abstract part to the concrete part is the *principle design*. In the concrete part, the physical behaviour design and the detail design resides, being part of the *physical design*, see Figure 3. The difference between the abstract and concrete part will gradually get clearer.

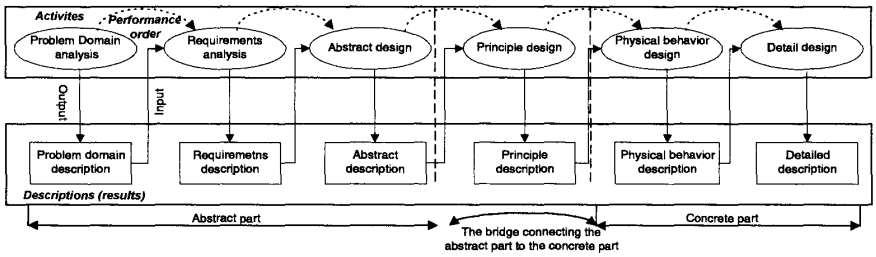


**Figure 3:** The activities and their results shown in a sequential manner. Figure from [14].

The proposed activity set of Shakeri's methodology has six main elements [14, p.41]:

- *Initial analysis* – where the problems and needs are studied, the system is identified and its properties are specified. Consists of the *problem domain analysis* and the *requirements analysis*.
- *Abstract design* – where the system is designed in an abstract manner without considering how to realize it. A term used for both *logical behaviour design* and *logical structure design*.
- *Principle design* – where the trade-off between different technologies is performed and cost-effective principle solutions are found.
- *Physical design* – where the system is designed by taking the physical and non-functional aspects of the system into consideration.

- *Implementation* – where the software part, electronic part, and mechanical part of the system are implemented.
- *Integration* – where implemented software, electronics and mechanics are integrated in order to provide the resulting physical mechatronic system or product.

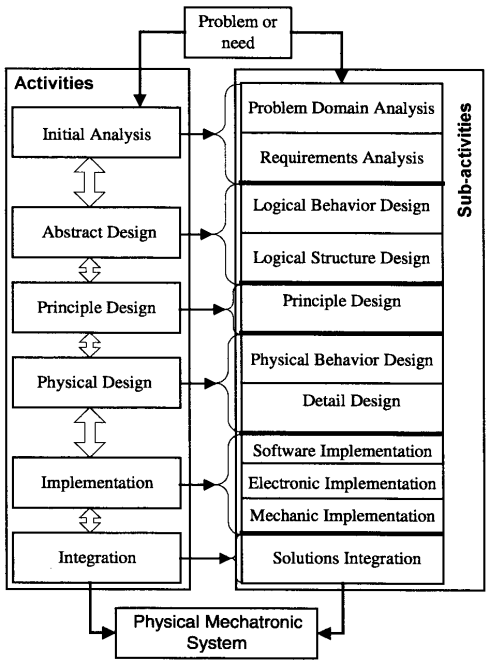


**Figure 4:** The activities and sub-activities in The Mechatronic Methodology. Figure from [14].

After the accomplishment of each activity, verification and validation should be performed. *Verification* is done in order to confirm that the system is developed correctly or according to the specifications, while *validation* assures that the system under development is one that the customer or end-user really needs. Iteration is an integral part of the development process.

Identifying a complete set of activities is, according to Shakeri, *very important*. The approaches, methods and tools may change over time but the set of activities and descriptions are more stable against changes.

Since Shakeri in [14] focuses mainly on the abstract part, the *abstract part* of the activity set will be described more thoroughly, while the concrete part is left to the other sections.

### 2.2.1 Initial analysis

The initial analysis, which is the first element in the activity set of the methodology proposed by Shakeri, is an investigation into the problems, needs, requirements and other factors that may have an impact on the quality and business value of the product or system.

The initial analysis is divided into two sub-activities:

- *Domain analysis* – seeks to understand the underlying needs, and to describe the problem *independent* of any particular system solutions. This analysis is *not* technology oriented.
- *Requirements analysis* – performed in order to analyze needs and to develop specifications. A critical stage of the development process.

The aim of domain analysis is to understand the needs within a problem domain independently of the particular system that is intended to be developed. Therefore, the borderlines between the system and the environment should not be drawn at this stage. Instead, the focus should be on the concepts, the terminology and the tasks of the domain with a wider scope than the future system. The fact that the domain analysis is not technology oriented means that the analysis should be performed *independently* of any technology and system solutions.

Requirements on a mechatronic system may be divided into *functional* and *non-functional* requirements. The functional requirements determine the behaviour of the system. This is again divided into logical and physical requirements. Logical functional requirements determine those aspects of a system that are relevant for its external representation and use, and are concerned with the system services, i.e. the behaviour as the user will see it. Physical functional requirements are also concerned with the system services and will complement the logical behaviour requirements, as they explain how the system should be realized such that its logical behaviour can be executed satisfactory. Note that the physical behaviour requirements depend on the logical behaviour, thus the logical behaviour requirements must be specified *before* the physical behaviour requirements. Further, the non-functional requirements are those which have no impact on the behaviour of the system, but determine its implementation. This might for instance be the form, shape and colour of the product. Shakeri claims that the requirements analysis is a critical stage in the development process, since it is important to describe the (desired or required) functionality in a way that can be well understood and analyzed by developers, market people and users alike.

Both the domain analysis and the requirements analysis contain more specific activities which will not be further elaborated here. The interested reader is referred to [14, Chapter 5].

### 2.2.2 Abstract design

Abstract design is a general term applied for *logical structure design* and *logical behaviour design*. The purpose of this activity is to design an abstract system that fulfills the logical functional requirements of the system. This differs from later activities in that designing the structure and behaviour of the system is independent of the realization factors or physical parameters.

The objective of the logical structure design is to define a system structure that helps to describe, analyze and simulate the logical behaviour of the system, while the logical behaviour design seeks to explain how the objects cooperate in order to manage their tasks and provide the functionality of the system. Logical structure and behaviour design are related to and dependent on each other.

For more thorough explanation and examples concerning the abstract design phase, please see [14, Chapter 6].

### 2.2.3 Principle design

The principle design is the first step towards realization of the system. In this part the principle solutions that are able to realize the abstract design and satisfy the non-functional and functional requirements will be found. This activity can be thought of as a bridge between the abstract and concrete part of the design process, see Figure 3, and represents the part of the development process which formulate the principle solutions upon which the detail design is based. The approximate major dimensions are determined and major components selected. To do this the non-functional and physical functional requirements on the system are important. These requirements constrain the set of possible principle solutions for a given abstract design. The principle description resulting from the principle design (see Figure 5) consists of four main sub-descriptions, which together make up the documentation for the system's physical construction and describe [14, p.114]:

- *Control principles* – the principle solutions for controlling and providing required services to the system.
- *Mechanical principles* – focus on the principle solutions for the working system part including the principle solutions for the interfaces between this part and the control part.

- *Service interface principles* – the principle solutions for realization of interactions between the system and its environment.
- *Preliminary layout* of the system – the first rough layout of the physical structure of the technical system.

Since modifications at the prototype and production stages of the development generally are very expensive, constraints and trade-offs concerning the logical behaviour (of the system) are considered mainly during the (early) abstract part of the development process. Form, fit and other physical constraints and trade-offs come into consideration in the principle design.

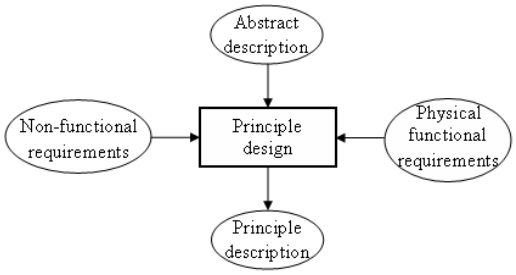


**Figure 5:** The abstract description, non-functional requirements, and physical requirements are the inputs to the principle design which produces a principle description. Figure from [14]

A number of strategies have been suggested for facilitating the procedure of finding and classifying principle solutions. Interface strategy, bottleneck strategy, prototyping strategy, rapid prototyping strategy, morphological strategy, and function/means tree strategy are some of the strategies. The interested reader is referred to [14, Chapter 7].

Shakeri stresses that the *iteration* between the principle design, physical behaviour design and the (realization dependent) logical behaviour design is of *vital importance*. The iteration must go on, if the project time and cost allow, until an acceptable principle system is achieved.

The physical design and implementation following the principle design is not discussed very deeply in Shakeri's methodology, because his focus was on the *abstract* phase, since the concrete phase is thoroughly described by numerous other authors. Therefore, the concrete phase is left for the other methodologies to consider more deeply.

### 2.2.4 Summary

Shakeri [14] has developed a methodology called "The Mechatronic Methodology". This methodology has an activity set consisting of six main elements:

- *Initial analysis*
- *Abstract design*
- *Principle design*
- *Physical design*
- *Implementation*
- *Integration*

There are two main views of mechatronic systems:

- *Abstract views* – let the technology trade-off be possible, and the problem and behaviour understandable.
- *Concrete views* – where the technologies are selected.

"The Mechatronic Methodology" focuses mainly on the abstract part of the development process and the transition from the abstract part to the concrete part, paying little attention to the concrete part. The abstract part consists of two activities: *initial analysis* and *abstract design*. The initial analysis activity is where the problem and needs are studied, the system is identified and its properties are specified. During the abstract design phase, the system is designed in an abstract manner without considering how to realize it. The last activity considered (here) is the *principle design* where the trade-off between different technologies is performed and cost-effective principle solutions are found. This activity is responsible for the transition from the abstract part to the concrete part, and is therefore called the "bridge" between the two parts.

## 2.3 Hildre et al. Methodology

In [3], Hans P. Hildre et al. has developed a methodology for systematic development of mechatronic products. It is particularly developed for the early development stages, as in the later stages (e.g. detail design), procedures and tools known in the different disciplines (mechanical, electronical or software engineering) can be used. The methodology is based on work with joint design models and methods linked to these models. They are interdisciplinary models that can be used and understood by *all* the implicated parties, a fact that is quite important. It is organized in the following three parts:

1. Project execution
2. Descriptions (results)
3. Methods and diagrams

The project execution part is where the development project is planned, i.e. where the designing is done. This part is divided into four phases: the *specification* phase, the *concept* phase, the *design* phase, and the *implementation* phase, see Figure 6. The methodology described in [3] covers mainly the three first phases.

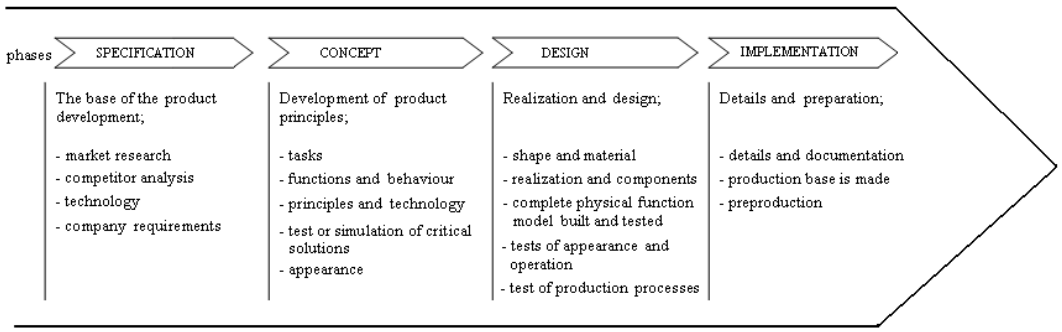


**Figure 6:** Short description of the different project execution phases. Figure translated from [3].

The descriptions constitute the structural element of this methodology. The focus is on the descriptions of various results and the relations between them, and not to that extent on the activities producing the results. The descriptions are structured in seven levels, shown in Figure 7.

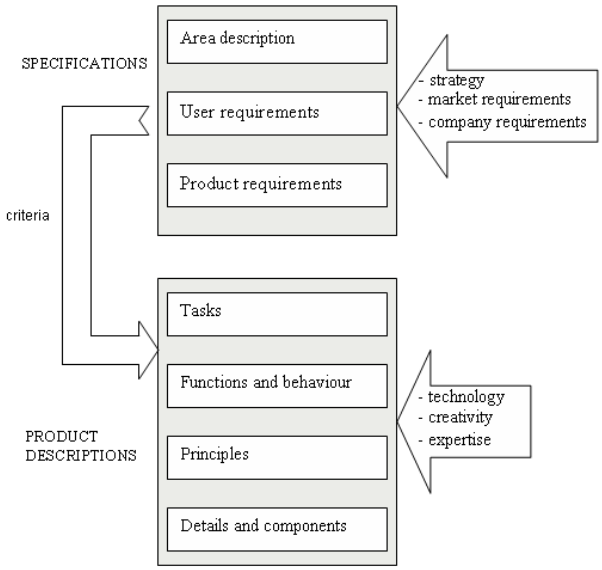


**Figure 7:** Descriptions in 7 levels. Figure translated from [3].

The methods and diagrams part constitute a tool box with independent methods, frameworks, diagrams, languages, models and so on. The various methods in the tool box support particular design activities in the descriptions part.

The following sections will give a slightly more thorough explanation of the different parts.

### 2.3.1 Project execution

The different tasks that should be performed during the project are as follows [3, p.32]:

1. Planning the development project:
    - Set a goal for the project and define milestones. The milestones are defined by documents that should be completed at a given time.
    - Define start/stop criteria for phases and activities within phases. The criteria are linked to the milestones.
    - Revise the plan.

2. Execute the development project:
    - Generate the descriptions, prototypes, documents etc., which are described in the project plan. Product planning is a part of this task.
3. Follow up the plan:
    - Follow up the milestones, i.e. check that the documents come at the right time and has a correct content.
    - Make decisions. Decisions include to start or stop a phase or activity.
    - Identify discrepancies, initiate measures, and report to the management.

As mentioned above, the project should be divided into phases with milestones where decisions have to be made. Check lists can be used to decide whether a milestone has been reached [3, p.35]. The phases are:

- *Specifications phase* – describe the requirements to the product. Note that the specifications will become more detailed during the course of the product development. The specifications will therefore not be complete when the specifications phase is finished.
- *Concept phase* – where the major technology is chosen and the product is designed. First, technology independent functional descriptions should be created. Next, principle solutions should be found and alternative solutions evaluated and selected. If possible, the solutions should be verified by for instance doing simulations.
- *Design phase* – where the different components and details of the concept are determined.

Also see Figure 6.

To achieve a high degree of innovation, creative methods can be of great help in structuring the work and providing optimal working conditions. These creative methods first and foremost aim to generate as many solutions or ideas to a problem as possible. The following three classes of creative methods are identified [3, p.35]:

1. *Associative methods* – encourage spontaneous reactions to ideas. Critisism should be suspended. Example: brainstorming.

2. *Creative confrontational methods* – investigate "analogies" in the search for solutions to a problem. Describe the problem in several ways and look for similarities within for instance other professions or areas of operation.

3. *Analytic-systematic methods* – analysis and systematic descriptions are supposed to contribute to an expansion and overview of the solution space, to give new ideas, new variants and the systematics to combine partial solutions.

For more explanations and investigations into the project execution part, please see [3, Chapter 3].

### 2.3.2 Descriptions (results)

The descriptions are not only used in order to describe completed ideas, but are also an important tool for recording the knowledge that is achieved during the process. They consist of seven different levels, also shown in Figure 7:

1. Area descriptions
2. User requirement specifications
3. Product requirement specifications
4. Task descriptions
5. Functional descriptions
6. Principle descriptions
7. Detail descriptions

In this context, the area in the *area description* coincide with the problem area. The purpose with the area description is to record and to model the requirements without considering how they are to be solved regarding concrete system solutions. The descriptions should therefore *not* be technology oriented. The value in creating these descriptions is that a joint terminology and an understanding of the problem area is established. Good area descriptions may make it easier to find a solution to the (correct) requirements, to work efficiently and to easily involve new persons not having the appropriate knowledge concerning the problem area.

The *user requirement specifications* describe the users, their relations to the system and their requirements and requests for the system. Even if the

user is not capable of precisely elaborating his/her requirements to the system, interactions between the users and the developers will help the developers in obtaining a more profound understanding concerning the situation of the user.

A *product requirement specification* is a specification believed to be the best foundation for the further development of the product. All the requirements not covered in the user requirement specifications should be described in the product requirement specifications. The requirements might for instance include things like production/assembly, laws and regulations and transportation.

Unlike the area description, which relates to the entire problem area and might cover multiple products or product families, the *task descriptions* relates specifically to a certain product or product family. A task description describes the tasks of the system and its environment (users and other systems). The purpose is to create a general understanding of the tasks.They should be expressed in a way both customers and users can understand and decide about. Flow diagrams constitutes the core of the task description, and describe the tasks (transformations) the system and the surroundings should perform. Models of the processes and the behaviour can and should be included in the task description.

A *functional description* is a description of a system, or type of systems, pointing out the functional properties (behaviour) in a *complete* way. This is the first fairly complete system description that is made. One of the major objectives with the functional description is, during the development process, to specify the logical behaviour in a way that is understandable, analysable and, preferably, possible to simulate. In addition it will give a good starting point for the principle descriptions, and in some cases it will generate parts of the implementation automatically. Another major objective is, after the development process, to document the complete logical behaviour of the system. The functional description should be technology independent. All the connections between stimuli and response must be unambiguously described, and this description is therefore one of the most important remedies to ensure that the functionality of the product meet the user requirements.

Next, the *Principle descriptions* document the technical solution down to a detail level where all non-functional properties are determined and the constraints for the detail design and the realization are well defined. The principle descriptions are used both as an aid under the development process, as well as a documentation of the final result. Under the development process they are used to describe alternative solutions and to analyse the non-functional properties of the solution. The principle descriptions allow

for technology, hence they are technology dependent.

Finally, the *detail descriptions* show the actual technical realizations within mechanics, electronics, software and operator controls. What is described is the development from principle solutions for the working system, control and operation down to realizable operator controls, mechanical and electronical components, software modules and their mutual connections. The detail descriptions are highly specific and depend on the choices that are made beforehand.

For examples and systematic methods for each of the levels, please see [3, Chapter 4].

### 2.3.3 Methods and diagrams

This part constitutes a tool box for support during the design process. Particularly interesting are the:

- Method to evaluate different concepts
- Strategy methods in the development of solutions
- Methods to construct mechanisms
- Methods for variation and optimization of solutions
- Method for design variations

A short explanation of each method is very difficult. Therefore, for an investigation into each method, please see [3, Chapter 5].

### 2.3.4 Summary

The methodology of Hildre et al. is organized in the following three parts:

1. Project execution
2. Descriptions
3. Methods and diagrams

During the *project execution*, the development project is planned, i.e. the "design" of the project is performed. This part consists of four phases: the specification phase, the concept phase, the design phase, and the implementation phase.

The *descriptions* part is the structural element of the methodology, focusing on descriptions of various results and relations between them. The focus is not on the activities giving the results.

The *methods and diagrams* part constitute a tool box for support during the design process.

## 2.4 Ulrich & Eppinger Methodology

[17], written by Karl T. Ulrich and Steven D. Eppinger, consists of methods for completing development activities. According to the authors, the structured methods in the book are not intended to be applied blindly, but rather to offer a starting point for continuous improvement. The approaches should therefore be modified to meet the individual needs.

Notice that this methodology has a particularly strong focus on teams, customers, market and management. Some of the points repeated here is therefore not entirely relevant for this thesis, but is included in order to maintain consistency with the litterature.

### 2.4.1 Development processes and organizations

Ulrich & Eppinger gives several reasons to why a well-defined development process is useful. Firstly, it is a way of *assuring the quality* of the resulting product, if the phases and checkponts the project passes through are chosen wisely and followed. Secondly, the *coordination* of the project gets easier, as a clearly articulated development process will act as a master plan defining the roles of each of the "players" in the development team, informing the members of the team when their contributions will be needed and with whom they will need to exchange information and materials. Thirdly, the *planning* is easier since the development process contains natural milestones corresponding to the completion of each phase. Next, the *management* gets better since, by comparing the actual events to the established process, a manager can identify possible problem areas. Finally, the careful documentation of an organization's development often helps to identify opportunities for *improvement*.

A generic product development process consisting of six phases is suggested by Ulrich & Eppinger . The six phases of the generic development process are [17, p.13]:

0. **Planning:** Often referred to as "phase zero" since it precedes the project approval and launch of the actual product development process. This phase begins with corporate strategy and includes assessment of technology developments and market objectives. The output of the planning phase is the project mission statement, which specifies the target market for the product, business goals, key assumptions, and constraints.

1. **Concept development:** Where the needs of the target market are identified, alternative product concepts are generated and evaluated,

and one or more concepts are selected for further development and testing.

2. **System-level design:** The system-level design phase includes the definition of the product architecture and the decomposition of the product into subsystems and components. The final assembly scheme for the production system is usually defined during this phase as well. The output of this phase usually includes a geometric layout of the product, a functional specification of each of the product's subsystems, and a preliminary process flow diagram for the final assembly processes.

3. **Detail design:** This phase includes the complete specification of the geometry, materials, and tolerances of all of the unique parts in the product and the identification of all of the standard parts to be purchased from suppliers. A process plan is established and tooling is designed for each part to be fabricated within the production system.

4. **Testing and refinement:** The testing and refinement phase involves the construction and evaluation of multiple preproduction versions of the product. Prototypes are tested to determine whether the product will work as designed and whether the product satisfies the key customer needs.

5. **Production ramp-up:** In the production ramp-up phase, the product is made using the intended production system. The purpose of the ramp-up is to train the work force and to work out any remaining problems in the production processes.

The *product plan* identifies the portfolio of products to be developed by the organization and the timing of their introduction to the market. This part is therefore not too relevant for this thesis, and will not be further investigated. Please see [17, Chapter 3] for more information.

The *concept development* phase is perhaps the phase of the development process that demands the most coordination among functions than any other, and it is therefore expanded into what is called the *front-end process*. The front-end process generally contains many interrelated activities, which is rarely sequential and often includes iterations. The concept development process includes the following activities [17, p.16]:

- *Identifying customer needs* – the output of this step is a set of carefully constructed customer need statements, organized in a hierarchical list, with importance weightings for many or all of the needs.

- *Establishing target specifications* – the translation of the customer needs into technical terms, and represents the hopes of the development team. Later these specifications are refined to be consistent with the constraints imposed by the team's choice of a product concept. Each target specification consists of a metric, and marginal and ideal values for that metric.
- *Concept generation* – the goal is to thoroughly explore the space of product concepts that may address the customer needs.
- *Concept selection* – where various product concepts are analyzed and sequentially eliminated to identify the most promising concept(s).
- *Concept testing* – done in order to verify that the customer needs have been met, assess the market potential of the product, and identify any shortcomings which must be remedied during further development.
- *Setting final specifications* – the target specifications set earlier in the process are revisited after a concept has been selected and tested.
- *Project planning* – the final activity of concept development. The team creates a detailed development schedule, devises a strategy to minimize development time, and identifies the resources required to complete the project.
- *Economic analysis* – an economic model for the new product.
- *Benchmarking of competitive products* – an understanding of competitive products is critical to successful positioning of a new product and can provide a rich source of ideas for the product and production process design.
- *Modelling and prototyping* – every stage of the concept development process involves various forms of models and prototypes.

These activities are *generic*, and should be adapted to the particular processes, according to Ulrich & Eppinger. Several variants of generic product development processes can be distinguished, but they will not be elaborated here. The interested reader is referred to [17, Chapter 2].

### 2.4.2 Product specifications

In an ideal world, the product specifications would be established once early in the development process and then the design and engineering of the product would proceed to exactly meet those specifications. This is rarely possible in the real world, unfortunately. For most products, specifications are established at least twice, with *target specifications* and *final specifications*. Four steps has been proposed for the process of establishing the target specifications [17, p.75]:

1. *Prepare the list of metrics* – a good way to generate the list of metrics is to contemplate each customer need in turn and to consider what precise, measurable characteristic of the product will reflect the degree to which the product satisfies that need.

2. *Collect competitive benchmarking information* – the relationship of the new product to competitive products is paramount in determining commercial success. The target specifications are the language the team uses to discuss and agree on the detailed positioning of its product relative to existing products, both its own and its competitors'.

3. *Set ideal and marginally acceptable target values* – the ideal value is the best result one can hope for, while the marginally acceptable value is the value of the metric that would just barely make the product commercially viable.

4. *Reflect on the results and the process* – make sure that the results are consistent with the goals of the project.

Finalizing the specifications can be difficult because of trade-offs, i.e. inverse relationships between two specifications that are inherent in the selected product concept. Trade-offs frequently occur between different technical performance metrics and almost always occur between technical performance metrics and cost.

For further explanation and examples, please see [17, Chapter 5].

### 2.4.3 Concept generation

A product concept is an approximate description of the technology, working principles, and form of the product. It is a concise description of how the product will satisfy the customer needs. The concept generation process begins with a set of customer needs and target specifications and results in a

set of product concepts from which a final selection is made. Good concept generation leaves the team with confidence that the full space of alternatives has been explored.

For concept generation, Ulrich & Eppinger presents a five-step method, see Figure 8 [17, p.100]:

1. **Clarify the problem:** Clarifying the problem means developing a general understanding and then breaking the problem down into subproblems if necessary. Once the problem decomposition is complete, initial effort should be focused on the critical subproblems.

2. **Search externally:** External search is aimed at finding existing solutions to both the overall problem and the subproblems identified during the problem clarification step. There are at least five good ways to gather information from external sources: lead user interviews, expert consultation, patent searches, literature searches, and competitive benchmarking. Note that the external search occurs *continually* throughout the development process, and not only at the beginning of the concept generation phase. Implementing an existing solution is usually quicker and cheaper than developing a new solution. The external search for solutions is essentially an information-gathering process.

3. **Search internally:** Internal search is the use of personal and team knowledge and creativity to generate solution concepts. The search is *internal* in that all of the ideas to emerge from this step are created from knowledge already in the possession of the team.

4. **Explore systematically:** Systematic exploration is aimed at navigating the space of possibilities by organizing and synthesizing the solution fragments.

5. **Reflect on the solutions and the process:** Note that this step should be performed throughout the whole process.

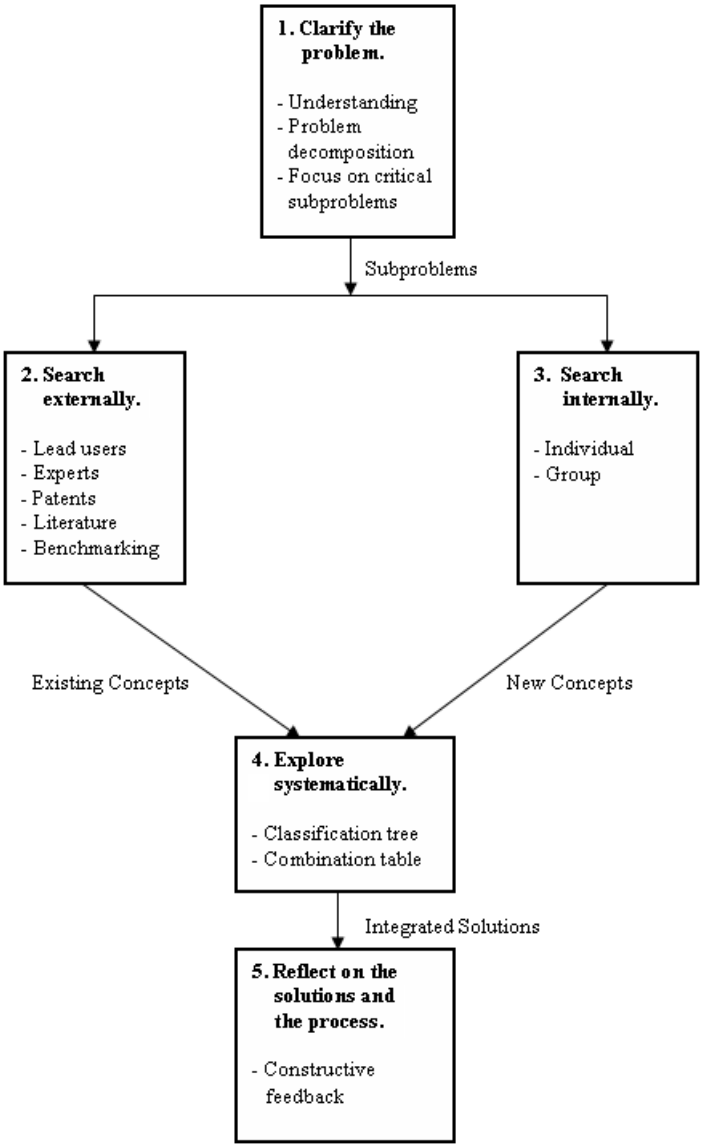


**Figure 8:** The five-step concept generation method. Figure from [17].

When it comes to the "internal search", some guidelines are given that can be useful for improving both individual and group internal search [17, p.108]:

- *Suspend judgment* – no critisism of concepts is allowed.
- *Generate a lot of ideas* – the more ideas a team generates, the more likely the team is to explore fully the solution space.
- *Welcome ideas that may seem infeasible* – ideas which initially appear infeasible can often be improved, "debugged", or "repaired". The more infeasible an idea, the more it stretches the boundaries of the solution space and encourages the team to think of the limits of possibility.
- *Use graphical and physical media* – reasoning about physical and geometric information with words is difficult. Text and verbal language are inherently inefficient vehicles for describing physical entities. Sketching surfaces should be available. Foam, clay, cardboard, and other three-dimensional media may also be appropriate aids.

Some hints are also given for generating concepts, hints that are aimed at stimulating new ideas or encouraging relationships among ideas [17, p.109]:

- *Make analogies* – ask yourself what other devices solve a related problem. Is there a natural or biological analogy to the problem? Does the problem exist in a much larger or smaller dimensional scale? What devices do something similar in an unrelated area of application?
- *Wish and wonder* – beginning a thought or comment with "I wish we could..." or "I wonder what would happen if..." helps to stimulate oneself or the group to consider new possibilities, and cause reflection on the boundaries of the problem.
- *Use related stimuli* – related stimuli are those stimuli generated in the context of the problem at hand. For example, one way to use related stimuli is for each individual in a group session to generate a list of ideas (working alone) and then pass the list to his or her neighbour. Upon reflection on someone else's ideas, most people are able to generate new ideas. Other related stimuli include customer needs statements and photographs of the use environment of the product.
- *Use unrelated stimuli* – an example of such a technique is to choose, at random, one of a collection of photographs of objects, and then to

think of some way that the randomly generated object might relate to the problem at hand.

- *Set quantitative goals* – near the end of a session, individuals and groups may find quantitative goals useful as a motivating force.
- *Use the gallery method* – the gallery method is a way to display a large number of concepts simultaneously for discussion. Sketches, usually one concept to a sheet, are taped or pinned to the walls of the meeting room. Team members circulate and look at each concept. The creator of the concept may offer explanation, and the group subsequently makes suggestions for improving the concept or spontaneously generates related concepts.

For further explanation and examples, the reader is referred to [17, Chapter 6].

### 2.4.4 Concept selection

Concept selection is the process of evaluating concepts with respect to customer needs and other criteria, comparing the relative strengths and weaknesses of the concepts, and selecting one or more concepts for further investigation, testing, or development. There are several different methods for choosing a concept, each varying in their effectiveness, and include the following [17, p.125]:

- *External decision* – concepts are turned over to the customer, client, or some other external entity for selection.
- *Product champion* – an influential member of the product development team chooses a concept based on personal preference.
- *Intuition* – the concept is chosen by its feel. Explicit criteria or tradeoffs are not used. The concept just seems better.
- *Multivoting* – each member of the team votes for several concepts. The concept with the most votes is selected.
- *Pros and cons* – the team lists the strengths and weaknesses of each concept and makes a choice based upon group opinion.
- *Prototype and test* – the organization builds and tests prototypes of each concept, making a selection based upon test data.

- *Decision matrices* – the team rates each concept against prespecified selection criteria, which may be weighted.

The concept selection activity consists of two stages. The first stage is called *concept screening*, which is a quick, approximate evaluation aimed at producing a few viable alternatives, while the second stage is named *concept scoring*, being a more careful analysis of these relatively few concepts in order to choose the single concept most likely to lead to product success.

For further explanation and examples, please see [17, Chapter 7].

### 2.4.5 Prototyping

Prototypes can be usefully classified along two dimensions. The first dimension is the degree to which a prototype is *physical* as opposed to *analytical*. Physical prototypes are tangible models created to approximate the product. Aspects of the product of interest to the development team are actually built into a model for testing and experimentation. Analytical prototypes represent the product in a nontangible, usually mathematical or visual, manner. Interesting aspects of the product are *analyzed*, rather than built.

The second dimension is the degree to which a prototype is *comprehensive* as opposed to *focused*. Comprehensive prototypes implement most, if not all, of the attributes of a product, whereas focused prototypes implement one, or a few, of the attributes.

Because an analytical prototype is a mathematical approximation of the product, it will generally contain parameters that can be varied in order to represent a range of design alternatives. In most cases, changing a parameter in an analytical prototype is easier (and cheaper) than changing an attribute of a physical prototype. In addition, the analytical prototype generally allows for larger changes than can be made in a physical prototype. The analytical prototypes are therefore usually more flexible than the physical prototypes, and mostly precedes the physical prototype. Physical prototypes are, however, required in order to detect unanticipated phenomena. The reason is that the analytical prototypes never can reveal phenomena that are not part of the underlying analytical model on which the prototype is based.

For more information about prototyping, please see [17, Chapter 12].

### 2.4.6 Summary

Ulrich & Eppinger suggest a product development process that consists of six phases:

0. *Planning*
1. *Concept development*
2. *System-level design*
3. *Detail design*
4. *Testing and refinement*
5. *Production ramp-up*

with the planning phase often referred to as "phase zero" since it precedes the project approval and launch of the actual product development process. The output of the planning phase is the project mission statement, which specifies the target market for the product, business goals, key assumptions, and constraints.

The concept development phase is where the needs of the target market are identified, alternative product concepts are generated and evalued, and one or more concepts are selected for further development and testing.

The system-level design phase includes the definition of the product architecture and the decomposition of the product into subsystems and components. The final assembly scheme for the production system is usually defined during this phase as well.

The detail design phase includes the complete specification of the geometry, materials, and tolerances of all of the unique parts in the product. A process plan is established and tooling is designed for each part to be fabricated within the production system.

The testing and refinement phase involves the construction and evaluation of multiple preproduction versions of the product.

In the last phase, the production ramp-up phase, the product is made using the intended production system.

## 2.5 Discussion

The methodology presented by Ahmad Shakeri in [14] is meant for development of highly complex mechatronic systems, where there is a need to structure the development process. The complexity of the logical behaviour and the way the different parts (electronics, mechanics and software) interact make it necessary to use this kind of methodology. The focus is on the abstract part, meaning the realization-independent part and the logical functions. The servomechanism that will be analysed in this thesis does not have a complex logical behaviour or any substantial interactions between mechanics and other areas. The closest relation to electronics is probably an electromagnetic coil, and there will be no software included. The substantial focus on the abstract part of the development process is therefore not necessary. Still, there are some thoughts that can be applied to the project, especially in the initial analysis with the domain analysis and the requirements analysis. But also here, it is clear that the "The Mechatronic Methodology" is intended for "slightly" more complex projects.

[3] by Hildre et al. focuses mainly on the concrete part of the development process, as opposed to Shakeri's abstract focus. The project execution part is divided into a specification phase, a concept phase, a design phase and an implementation phase. This is actually not too far from the methodology proposed by Ulrich & Eppinger, where the phases roughly are a planning phase, a concept development phase, design phases and a test and refinement phase. The phases indicate that this methodology too is meant for slightly more complex development projects. Nevertheless, there are some general ideas that obviously can be used, for instance in the planning of the project by defining milestones and defining start/stop criterias for phases and activities. In addition some creative methods for generating ideas can be of some help even though they are somewhat aimed at development *teams* rather than at one person. The descriptions part also seems to be aimed at more complex problems, with the specifications divided into three parts; the area descriptions, the user requirements and the product requirements. Hildre et al. also provides several checklists that can be used by development teams. The methodology could naturally be adapted to the project by omitting the parts that are irrelevant. However, the project in this thesis is closer to a pure *mechanical* development project than a *mechatronic* project, considering that the only electrical part of the servo mechanism at this stage seems to be the electromagnetic coil, and that no software will be employed. Therefore, a *mechatronic* methodology seems to be somewhat of an overkill, hence excluding both the Shakeri methodology and the Hildre et al. methodology.

The Ulrich & Eppinger methodology, on the other hand, is more focused on general product development and not specifically on mechatronic systems. The methodology has got more similarities with Hildre et al.[3] than with Shakeri [14], the reason probably being the strong focus on the *abstract* part in Shakeri, while the other two focuses more on the *concrete* part. The Ulrich & Eppinger methodology consider several economical and market perspectives, in addition to keeping the focus on development *teams*, but these can easily be omitted or adapted to the project. Most of the theories are universal and can be used in a vast range of problems. In addition, the methodology just feels like it will fit better than the other two. Certainly, not all points and phases can be included, but as the authors point out in the beginning; "(...) the methods are not intended to be applied blindly. (...) Teams should adapt and modify the approaches to meet their own needs and to reflect the unique character of their institutional environment."[17, p.7]. The different phases of the generic development process can easily be adapted by removing what is not relevant. In addition, the methodology gives several activities and methods that can be of great help in the development. Therefore, the Ulrich & Eppinger methodology seems to be the natural choice.

## 2.6 Conclusion – choice of methodology

As already mentioned, the Ulrich & Eppinger methodology seems to be the right choice for this assignment, with relevant methods and procedures chosen and adapted.

Adapting the phases of the generic development process gives the following phases:

0. **Planning** – key assumptions, constraints, assessment of technology developments, in short a background investigation. In addition, a plan of progress should be made.

1. **Concept development** – specifications, alternative product concepts, and selection of concepts for further development and testing.

2. **Testing and refinement** – first create analytical prototypes and optimize these with respect to geometry, choice of materials and mechanical performance. Then create a physical prototype to test in "real-life".

The system-level design phase and the production ramp-up phase is omitted because of the relatively low complexity of the servo mechanism and the fact that it will not be put into production (at least not in foreseeable future). The detail design phase is merged with the testing and refinement phase,

since the test phase will determine what materials should be used and which geometric properties are optimal. The (design and) testing phase should be iterative, since the tests probably will reveal design flaws that will need to be corrected.

The *concept development phase* includes the following activities:

- *Establish target specifications* – initial determination of both the ideal and marginally acceptable values of the specifications.
- *Concept generation* – thorough exploration of product concepts that may meet the specifications.
  - Clarify the problem – develop a general understanding of the problem and then possibly break the problem down into subproblems if necessary.
  - Search externally – patent search, literature search, etc.
  - Search internally – use own knowledge/the knowledge of the "team" to create ideas.
  - Explore systematically – organize and describe thoroughly the different concepts.
  - Reflection – are there any other solutions?
- *Concept selection* – analyze and eliminate concepts in order to identify the most promising concept(s).

Identifying customer needs and an economical analysis will not be done because it is not in the scope of this thesis. The concept testing will be done in the testing and refinement phase.

When it comes to concept generation, almost all the methods described by Ulrich & Eppinger can be used. Some of these methods are: make analogies, wish and wonder, use unrelated stimuli, and use related stimuli. Please see either [17] or Section 2.4.3 for more methods and explanations.

Of the concept selection methods proposed in Section 2.4.4, the "pros and cons" and "prototype and test" methods will be used here, due to the fact that the other methods are aimed at development *teams*.

Both analytical and physical prototypes are needed in order to fully explore the concept. The analytical prototype should precede the physical prototype, and constitute a base for the choice of materials and geometries used in the physical prototype.

The methodology presented here will be used from now on.

# 3 Concept Development

## 3.1 Introduction

The concept development part is where the specifications will be set and where the exploration of different concepts will be done. As a starting point, a traditional servo valve is considered, followed by an exploration of different concepts that can prove to meet the requirements. Finally, the most promising concept will be chosen and further analyzed, developed and tested.

The reason why the traditional servo valve is considered is due to the fact that it has a design that has proven to work well through many years, and it has a design that partly can be transferred to this problem, then particularly with the concept of distributing pressure in mind. This will become more evident further down.

The servomechanism that will be explored in this thesis should essentially work as a hydraulic actuator, with a pin with an adjustable height. It should be as small as possible, with a high stiffness and with no sensors.

Please note that the terms "piston" and "pin" can seem to be used a bit interchangeably. The pin is *part* of the piston.

## 3.2 Specifications

The specifications were set by investigating the different actuators listed in [13, p.69]. The goal must be to create a better working actuator.

Ideal values:

- $10mm$ movement
- Stiffness $5N/mm$
- 2mm diameter

Marginally acceptable values:

- $5mm$ movement
- Stiffness $1N/mm$
- 5mm diameter

There is no particular restriction to the length of the actuator, but it should obviously not be too long. It should have a smallest possible diameter, so the ideal value for the diameter should in fact be $\approx 0$. However, this is very difficult to achieve, so the ideal value was set to $2mm$ because that seems

to be a reasonable goal compared to the actuators considered in [13, p.69]. The maximum movement of the previously mentioned actuators was $5mm$. To be ambitious, the ideal value for this actuator is set to $10mm$. As to the stiffness, it was nearly impossible to find any numerical values for other than the specific actuator considered in [13]. That had a stiffness of $50N/mm$ which is extremely high and an intrinsic property of its screw-based design. Since the design of the actuator in this thesis will not be screw-based, the stiffness will probably be far from that magnitude. Therefore, the ideal value was set to 1/10 of the "screw-based" stiffness ($5N/mm$), and the marginally acceptable value was set to $1N/mm$, 1/50 of the actuator in [13].

## 3.3 A "traditional" servo valve

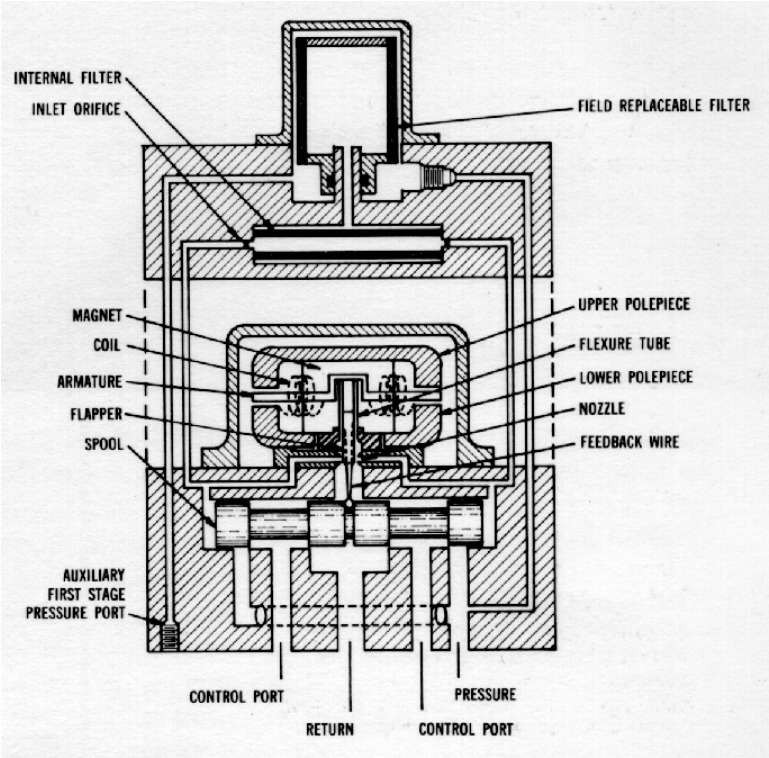


**Figure 9:** Traditional servo valve. [1]

[1] http://www.bmed.mcgill.ca/REKLAB/manual/Common/Hydraulics/figure1.gif Figure retrieved January 22, 2008.

Please note that this explanation concerning the operation of the servo valve is partly taken from [2].

The traditional servo valve shown in Figure 9 works by, simply put, pressure distribution. The armature in Figure 9 can be rotated clockwise or counterclockwise with the presence of a current in the coils. This rotation leads to a movement of the flapper towards one of the sides, and closer to one of the nozzles. This leads to a higher pressure in one passage relative to the other. If, for instance, the armature is rotated counterclockwise as in Figure 10, the right side of the flapper will be moved closer to the right nozzle, creating higher pressure in the right passage and lower pressure in the left passage. The higher pressure in the right passage acts on the right end of the spool applying force to distance the spool to the left. At the same time, lower pressure is acting on the left side of the spool, creating a force imbalance facilitating the spool's movement to the left. As the spool moves to its left, the feedback wire follows and thereby inputting a feedback force on the flapper, counteracting the magnetic forces. This leads to a re-centering of the flapper between the nozzles. Once the flapper is centered, the pressure between each of the nozzles becomes equalized, and so does the pressure acting on the ends of the spool. Hence the spool stops moving, but remains displaced, controlling flow to and from the control ports.

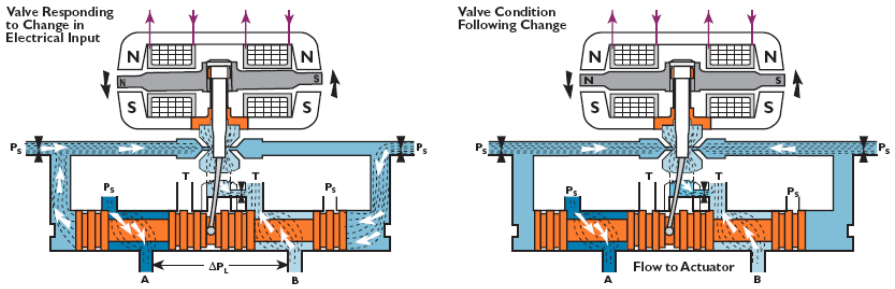


**Figure 10:** Operation of the servo valve. Figure from Moog [10].

## 3.4 Concept Generation

The main purpose with the actuator is that it should be small, and utilize the magnetorheological fluid to create the movement of the pin with a relatively large stiffness. In addition, the actuator should be *sensorless* to make it as small as possible and to have less wires and easier control.

The (new) concepts should be improved compared to the concept in [5]. One of the main problems with that concept was the magnetic saturation in the walls that made it impossible to supply the required magnetic field to the fluid. Therefore, the new concepts should have a better solution for supplying the magnetic field to the fluid.

### 3.4.1 External search

The external search includes patent searches and literature searches, and is aimed at finding existing solutions to the problem, if any.

The traditional servo valve described above can be used as a basis for the development of new concepts. For instance, some of the mechanisms for distributing the pressure are quite interesting for the purpose. Especially if the spool in the traditional servo valve in Figure 9 is viewed as the pin of the actuator. Then, one can imagine the armature and the flapper of the servo valve being replaced by a magnetorheological solution, with the magnetorheological fluid and an applied magnetic field being responsible for distributing the pressure, and something else than the feedback wire being responsible for the feedback.

When it comes to existing devices using magnetorheological fluids, patent and literature searches discovered nothing new from the applications considered in [5]. Brakes and adaptive dampers are the major applications for magnetorheological fluids. A patent has been found for a method and device for producing a tactile display using an electrorheological fluid [4], but this is "just" an "on/off" mechanism and is not providing variable heights for the tactile dots. Therefore, it is probably better to look at the traditional servo valve in order to get ideas for the further development.

### 3.4.2 The concepts

Some of the concepts that will be mentioned are "improvements" of the concept from [5]. Most of them, however, are derivations from the traditional servo valve (see above) with major parts replaced by solutions based on effects created by a magnetic field in the magnetorheological fluid. Actually, the traditional servo valve is more an *inspiration* than a basis for the concepts, since the area of application is a bit different. The inspiration lies in using nozzles that can be unequally constricted, hence causing an unequal pressure distribution and a movement of the spool due to the pressure difference.

The first concept (Figure 11) is thought to be an improvement of the

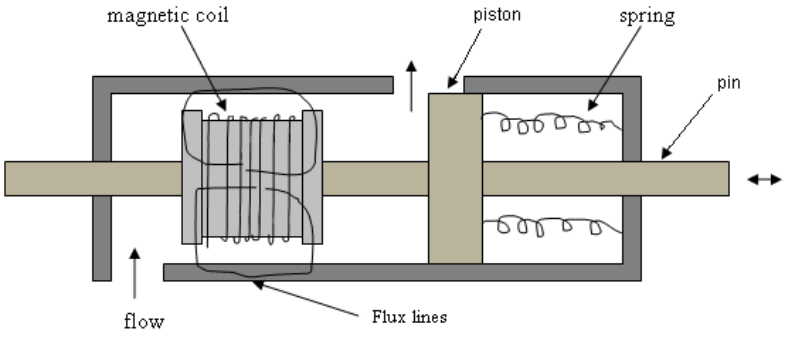


**Figure 11:** The first concept, with the coil mounted on the pin and the outlet partially overlapped by the piston.

concept that was investigated in [5]. That design had major problems with magnetic saturation, which is tried alleviated by having the coil producing the magnetic field closer to the fluid and inside the actuator. This idea comes from the design of magnetorheological dampers [8, 12, 15]. However, the saturation problem might still be present, because the magnetic field still has to go through the "walls" of the actuator, and it was the walls that were the bottleneck in [5]. The improvement from before consists in a relocation of the coil closer to the fluid, as previously mentioned, and possibly an improvement of the stiffness of the system, due to a partial overlap of the outlet by the piston. Supposing the pin is pushed down (to the left in the figure) from an equilibrium state, the outlet will be constricted, and consequently the internal pressure will increase, increasing the upwards force. Apart from this, the principle is similar to the one described in [5], with the forces being created by the shear stress in the fluid at the piston (the coil in this case) and partially by the internal pressure at the piston. However, there is at least one problem with this design: As the magnetic field intensity increases in the fluid, the shear stress will increase, but then also the pressure drop will increase making the pressure after the coil smaller and hence the upwards pressure force smaller. This means that as the shear force increases, the pressure force decreases. Whether these effects cancel each other or if one is much stronger than the other is an element of uncertainty before it is modelled and tested. Please notice that the pin does not have to protrude at both sides, but it might be advantageous for e.g. carrying the wires to the coil. Also notice that the rightmost "chamber" must not be completely sealed, because then the movement of the piston would be difficult, if not

impossible, especially if the content of the "chamber" is incompressible, a fact that is true for most fluids. The spring is present in order to create a counter force and to act as a stabilizing mechanism together with the constriction of the outlet.

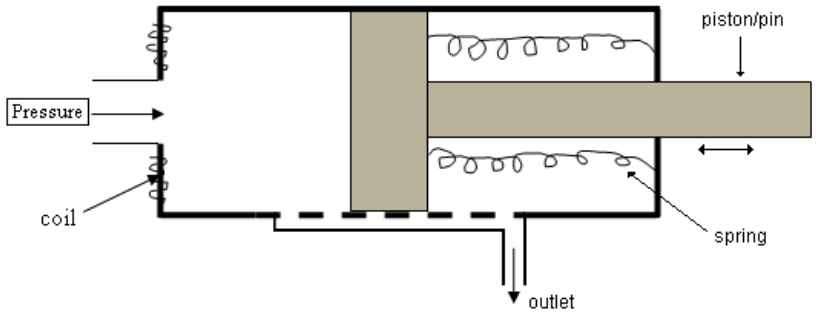


**Figure 12:** The second concept, a concept with multiple partially overlapped outlets.

The second concept has some similarities with the previous, with an outlet that is partially covered by the piston, see Figure 12. The outlet consists of an area with many holes, sort of like a sieve. As the piston moves up (to the right in the figure), more of the holes are exposed and hence the internal pressure will get smaller. With a downwards movement (to the left in the figure), less holes will be exposed and hence the internal pressure will increase. The pressure force is what drives the piston, and the pressure can be controlled by for instance a magnetic coil at the inlet, controlling the magnetic field over the fluid at the inlet. More magnetic field intensity at the inlet leads to a higher pressure drop, less internal pressure, and a movement of the piston downwards. The covering/uncovering of the outlet holes will act as a stabilizing feedback mechanism in addition to contributing to a higher gain if the pin is pushed down (a higher stiffness). The springs will create a counter force, and act as a stabilizing mechanism together with the covering/uncovering of the oulet, and set the initial height of the pin, as in the previous concept.

The next concept has a radically different design compared to the previous, instead of just being an "improvement" of the concept in [5]. The thought is to use nozzles both as a means to distribute the pressure and to serve as a feedback mechanism. The choking of nozzles in order to distribute pressure is utilized in the traditional servo valve shown in Figures 9 and 10, and is the inspiration for this design. The main idea was to replace the flapper, the ar-

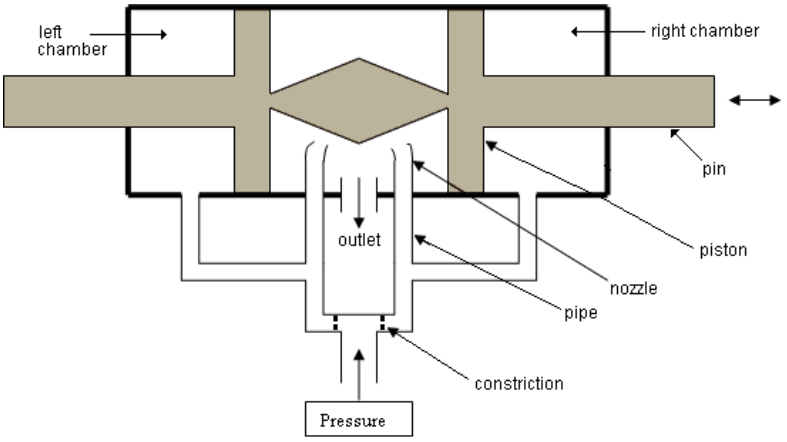


**Figure 13:** A new concept based on nozzle choking.

mature and the feedback wire in the servo valve with something based on the magnetorheological fluid in such a way that the complexity and size would become considerably smaller, and of course to make some changes to the spool in order to adapt it to the functionality that is required. If the nozzles are placed as in Figure 13, and if a magnetic field is used in order to create a different flow resistance in the two pipes, the pressure difference that arise will lead to a movement of the piston. Say, for instance, that the right pipe is choked (higher flow resistance) and the left is "opened"(less flow resistance), the pressure in the rightmost chamber will increase and the pressure in the leftmost chamber will decrease. This leads to a movement of the piston to the left. As this movement goes on, the left nozzle will be increasingly choked due to the the wall of the piston closing in. Accordingly, this also leads to an opening of the right nozzle since the wall is moving away from it. Eventually, this results in an equalization of the pressure in the left and right chamber, and consequently the piston is brought to a halt at a certain displacement from the centre position. The pipes can be choked and opened by means of a magnetic field, as previously mentioned. Increasing the magnetic field intensity leads to an increase of shear stress in the magnetorheological fluid; in other words the flow resistance is increased and the pipe is "choked". Opening the pipe can be done if there is an offset in the magnetic field in the fluid. A permanent magnet can take care of this offset, and an electromagnetic coil can be used to either weaken or strengthen that field. How this can be done will be explored later. The different concepts of creating the magnetic

field can partially be examined detached from rest of the design to see which will convey the most field intensity to the fluid, but in the end everything must be tested together. The constrictions at the beginning of each pipe branch are there in order to reduce the "travel of pressure" from the left to the right branch and vice versa. When the pressure in the left branch is reduced, the flow rate over the left constriction will increase and hence the pressure drop increases. When the pressure in the right branch increases, the flow across the right constriction will decrease and hence the pressure drop decreases. This will contribute to reducing the effects of the pressure "travelling" between the two branches, something that might become a problem to the performance of the servomechanism since the increase of pressure at one side would "travel" to the other side and hence reducing the pressure difference. Having two separate supply pipes could of course be a solution to that problem, but is probably not feasible in reality, or would at least lead to more parts than strictly necessary. There are no springs attached since the constriction of the nozzles should contribute to stopping the piston with almost the same effect as a spring (the counter force grows larger as the displacement increases). The constriction of the nozzles will also provide for the (hopefully high) stiffness of the system by constricting the nozzles and creating a counter force if the piston should be displaced by an external force.

Please notice that the pin does not necessarily have to protrude both sides of the actuator, but the huge advantage with this bilateral protrusion is that the area which the pressure acts on is the same at both sides, in such a way that $\Delta p = 0$ means equilibrium for the piston. If the areas of the piston were different in the left and right chamber, the forces acting on the piston would be different at the left and right side when the pressure difference was zero, and hence the piston would move even though $\Delta p = 0$. It could of course be possible to take this offset into account, but the *easiest* solution is to have the same cross-sectional area of the piston at both sides.

In order to get sufficient space for the coil and the permanent magnet(s), the wall that the nozzles are pointing at should be moved as far up as possible, as shown in Figure 14. The electromagnetic coil can be placed between the two pipes while the permanent magnet(s) can be located at the opposite side of the pipes as in the figure, but other arrangements are certainly possible. Considering the requirement that the diameter should be as small as possible, while the length has no particular restrictions, the best idea will probably be to have a lying magnetic coil as shown in the figure. Other solutions to both the placement of the magnets and to the internal geometry will be illustrated and described below. Note that the north pole of the per-

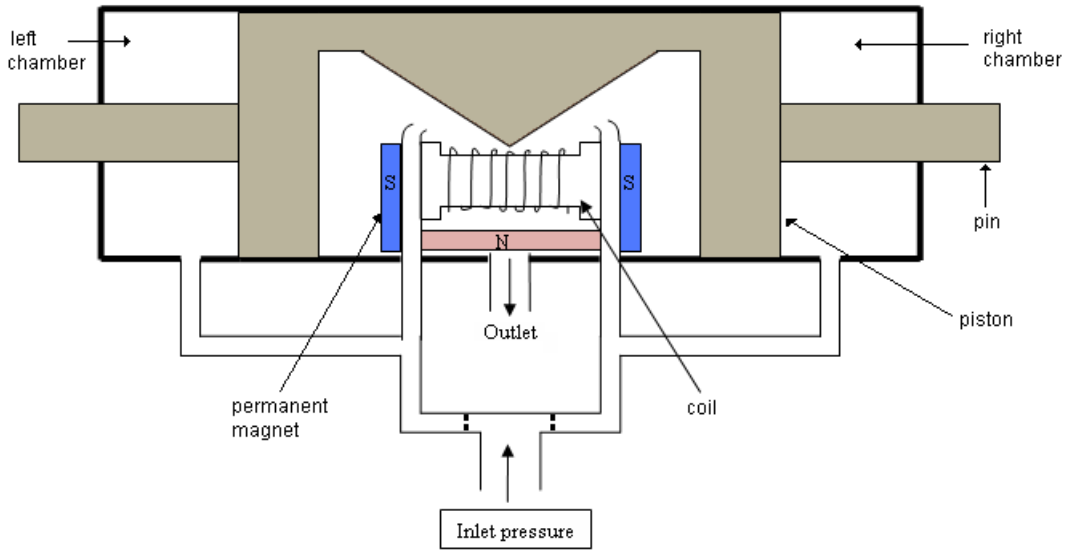


**Figure 14:** A slight revision of the shape of the piston, and an illustration of how the placement of the permanent magnet(s) and the coil can be done.

manent magnet does not have to lie where it does in the figure, it was just placed there for illustration purposes. In fact, it would probably be a bad idea to have the north pole that close to the pipe because the magnetic field might have an undesirable influence on the fluid.

The nozzles does not necessarily have to be turned towards each other. Figure 15 shows how the design might be with the nozzles pointing in other directions. For instance in a) and c) where the nozzles are pointing away from each other, outwards. Notice that the right pipe then must be connected with the leftmost chamber and vice versa in order to get the negative feedback effect. If the connections were *not* changed, and the right pipe was connected to the right chamber and the left pipe to the left chamber as before, an increase in magnetic field over the right pipe would lead to an increase in the pressure in the right chamber, and a movement to the left. Then, the *right* nozzle would become more constricted and hence the pressure in the *right* chamber would increase even more. Hence there would be a positive feedback effect, which obviously is undesirable. Figure 15 b) shows a view from above the nozzles and the piston with the nozzles not turning outwards or inwards, but laterally. An advantage with this design might be that the actuator can become slightly shorter, but this is not certain before more thorough investigations are made. Other than that, the difference is rather

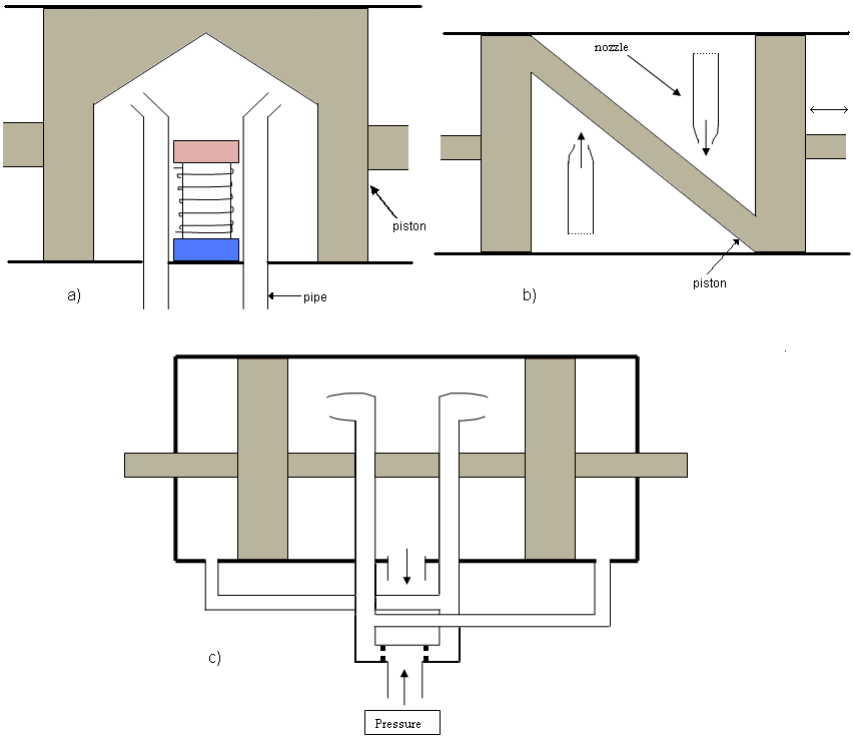


**Figure 15:** Some other variations of the concept. a) with the nozzles turned outwards. b) is viewed from above, the nozzles pointing laterally. c) is similar to a) but with straight piston walls. Notice the alterations of the connections between the pipes and the right and left chamber in c) compared to before. The coil in a) is merely for illustration purposes.

small compared to the other concepts.

Figure 16 illustrates different solutions to the distribution of the magnetic field. The best way is probably to constrict the flow *before* the outlet of the nozzles in order to keep the outlet unaffected by the magnetic field. The very best would probably have been to have the coil and magnets at the outside of the actuator to save space, but for now everything will be placed inside the actuator.

The first magnetic concept to be considered is the "standing" coil in Figure 16 a). The permanent magnet is placed with a south pole at the right-hand side of the right pipe and a north pole at the left-hand side of the left pipe (it can of course also be placed the opposite way). If the current in the electromagnetic coil is applied in such a way that its magnetic north pole

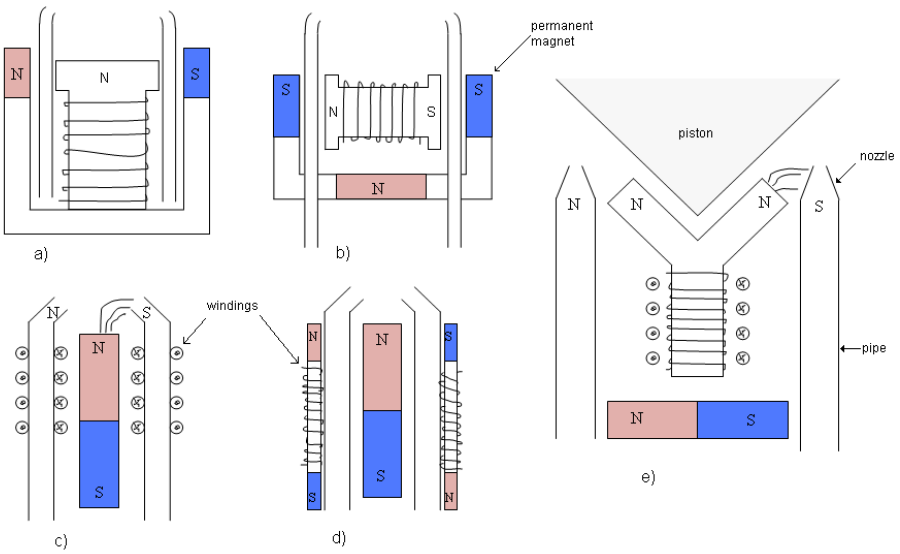


**Figure 16:** Different concepts for distributing the magnetic field, with coils and permanent magnets. The placing of the permanent magnet in e) is merely for illustration purposes, which by the way also concerns the other concepts to some extent.

is at the top of the coil, then the right nozzle will get an increase of magnetic field while the left nozzle will get its field weakened. Hence the right nozzle will be choked while the left nozzle will be "opened".

The permanent magnet can also be placed as shown in Figure 16 b), with south poles (or north poles) at each side of the pipes and the electromagnetic coil in between the two pipes. Then, if a current is applied in such a way that the left-hand side of the electromagnetic coil becomes the north pole while the right-hand side becomes the south pole, then the magnetic field will increase in the left pipe and decrease in the right, and hence the left nozzle is choked while the right nozzle is "opened". As explained earlier, this leads to an increase of the pressure in the leftmost chamber and a decrease of pressure in the rightmost chamber and a movement of the piston to the right. Please note that the exact design of the permanent magnet will not be like in the figure. Most probably, there will be two *separate* permanent magnets, and not a single one. In addition, the north pole should not be that close to the pipe since it might affect the fluid. Remember that these concepts are only *ideas* to how the design should be, and that more thorough investigations must be carried out concerning the detail design of the concepts.

A third possibility is having the permanent magnet in the middle and winding the coil around the pipes as done in Figure 16 c). However, due to the requirement that the magnetic field should be perpendicular to the flow direction, a better alternative must be to wind the wires around two pieces of iron and mount them at the side of the pipes as shown in d). These two coils can have the same current source provided the winding is done the right way; in such a way that the two coils have "opposite poles" (as illustrated). The same concept can be realized with two permanent mangets, one on each side, and the electromagnetic coil in the middle (the permanent magnets must in that case be positioned as in the example with opposite poles). In that case the design is similar to the one in a), but with the effect of field weakening and strengthening happening at two places rather than just one. By changing the direction of the current it is possible to shift the magnetic field from the right pipe to the left pipe. The advantage with this design is that there is a magnetic field at two places.

The last concept is shown in Figure 16 e). The principle is the same as in a), only with an adjustment of the geometry of the electromagnetic coil. The intention with this design was to get the magnetic field as close to the nozzles as possible. Pay no attention to the placement of the permanent magnet, as it was only placed for illustration purposes.

As to the placement of the permanent magnet(s) and the coil(s), this should not be restricted to between and at the side of the pipes. It is important to make the most of the space that is available inside the actuator, since most of the space between and at the side of the pipes is not needed for the movement of the piston. A larger magnet/coil generally leads to a larger magnetic field. There must be enough space for the piston to move freely, but other than that the space can and should be used for the magnets. Figure 17 shows a possible utilization of the space inside the actuator, with the coil and the permanent magnet occupying the "free" space. Note that the permanent magnet might have to be split into two separate magnets. The pipes could also be "flattened", as shown in the figure, in order to get the fluid gap between the magnet and the coil as small as possible, and to minimize the amount of air between the magnet and coil. In between the two pipes there might be possible to place a "flux return path", i.e., a magnetic material that can guide the magnetic field away from where it should not be, for instance when there is two "opposite" poles (e.g. south pole vs. south pole) and the magnetic field might get deflected and move to other parts of the pipe. It might actually be important to pay some attention to this "return path" of the magnetic field, since it is important both to guide the magnetic field away from the regions where it should not be and perhaps

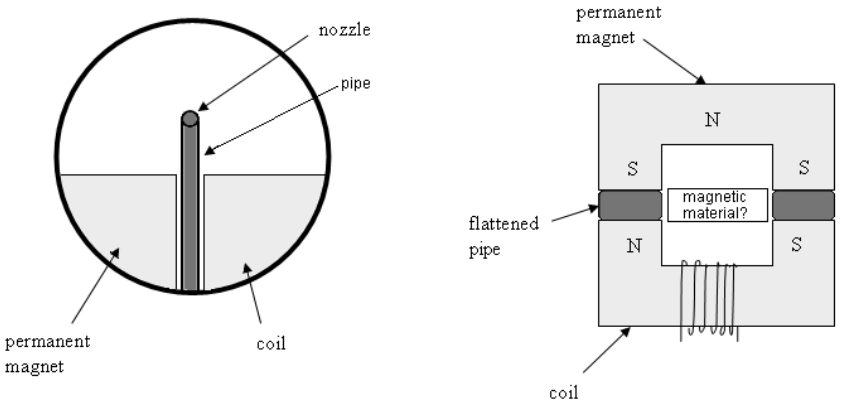


**Figure 17:** Utilizing the space inside the actuator. Note that the design is purely conceptual, and hence it is not certain whether the magnet and the coil can look like that.

also to guide it to where it should be.

Another idea that emerged was to mount the permanent magnets on the piston (Figure 18) in such a way that e.g. moving the piston to the left would decrease the magnetic field at the left pipe and increase the magnetic field at the right pipe. This weakening and strengthening of the field would cause an additional feedback effect. To explain this, take for instance the situation shown in Figure 18, where the permanent magnets have their south poles closest to the pipes and the coil has got a north pole to the left and a south pole to the right. This would lead to a higher magnetic field at the left pipe and a lower magnetic field at the right pipe (because the field from the coil would be added at the left pipe and "subtracted" at the right pipe) and hence a higher pressure in the rightmost chamber and a lower pressure in the leftmost chamber (with nozzles pointing outwards – please remember that the left pipe is connected to the right chamber and vice versa). This will cause the piston to move left, thereby weakening the field at the left pipe and strengthening the field at the right pipe since the left permanent magnet moves away from the pipe and the right permanent magnet draws nearer. The result is that the pressure in the right chamber decreases while the pressure in the left chamber increases. Eventually, the piston stops at a certain displacement. Hence, the effect from moving the permanent magnets closer to or farther from the pipes will, in theory, contribute the same way as the nozzle constriction. However, there are some problems with this

concept, especially if the forces between the magnetic poles are taken into consideration. Again say that the nozzles are pointing outwards, as in Figure 18, and that we have the same situation as before. As the piston moves to the left, the magnetic force between the north and south pole at the left side will decrease together with the magnetic field over the fluid, while the magnetic "repulsive force" at the right side will increase since there is a south pole against a south pole. This seems to be okay , since the piston will settle, but the question is whether the magnetic "repulsive" force between the south poles is large enough to hamper the movement of the piston. In addition, the north pole will be attracted by the south pole at the left pipe, and this will lead to a force to the right. It is a fair question to ask whether the magnetic forces are much larger than the forces created by the pressure difference in the two chambers, such that the magnets will just slam together at first chance. Then, what about the gain of the actuator, or its "stiffness". What if the piston is now pushed to the right by an external force? Then, the magnetic field intensity would increase over the left pipe and decrease over the right pipe, making the pressure in the right chamber higher and lower in the left chamber, thereby counteracting the external force. This seems fine so far. But, the forces between the magnetic poles will *counteract* this force again by contributing to a force to the right. The force between the magnets will act *together* with the external force, not against it. The question is whether this magnetic force is much larger than the forces created by the pressure difference, but bearing in mind that quite high magnetic fields are needed in order to "excite" the fluid, the magnetic forces are probably at least as high as the pressure forces. If the magnetic force should prove to be greater than the "pressure force", the result would be devastating to the actuator.

The other possibility with the permanent magnets mounted on the piston is with inwards pointing nozzles (Figure 14). If the previous scenario is repeated, whith north-south poles over the left pipe and south-south poles over the right pipe, the pressure will increase in the left chamber while it decreases in the right chamber, leading to a movement of the piston to the right. This will again lead to both an increase in the magnetic field in the left pipe and an increased magnetic force between the north- and south pole of the magnets, and hence there is a positive feedback effect. The concept with inwards pointing nozzles can therefore *not* be used with the permanent magnets mounted on the piston.

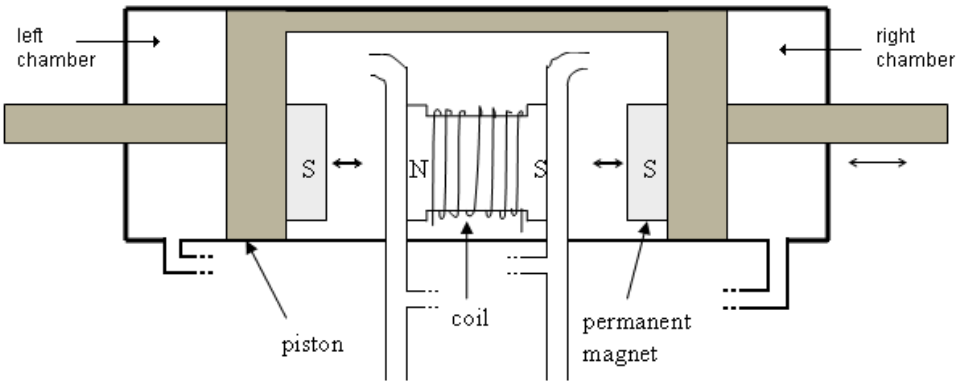


**Figure 18:** Concept with the permanent magnets mounted on the piston.

### 3.4.3 Challenges

One challenge with using a permanent magnet and an electromagnetic coil together, is that of subtraction of magnetic fields and the path of the magnetic field. The question is whether the fields will be subtracted when there are two south poles facing each other (or north poles for that matter) – will the magnetic fields become subtracted and the overall magnetic field move to zero, or will the fields just be deflected? In addition, permanent magnets has got small permeability, close to the permeability of free space, and hence their ability to lead the magnetic field coming from the electromagnetic coil is rather poor. It might become a challenge to find the best possible path for the magnetic field in such a way that the magnetic field in the fluid is optimized, meaning both to "guide" the magnetic field to where it should be and to lead it away from the parts (of the fluid) where it should not be. For instance, in the case of field subtraction, the field should not just be deflected and move to other parts of the fluid, but rather move *away* from the fluid.

Another challenge is the fact that the magnetic material used in the core of the electromagnetic coil has a hysteresis effect, i.e., an increasing magnetic field follows one path while a decreasing field follows another. If this effect is large, the behaviour of the actuator could become somewhat difficult to predict. However, the effect can be avoided if the magnetic material does not reach its saturation limit [7, p.683].

There is also a question whether the permanent magnet will magnetize the core of the electromangetic coil in such a way that there will be an offset

that will lead to an unpredictable behaviour. However, this effect will be disregarded for the time being.

## 3.5 Discussion

The first concept, shown in Figure 11, has got an internal electromagnetic coil that has proved to work well in dampers that experience large forces, then mostly with the electromagnetic coil wired in sections [15]. Wiring the coil in sections could of course be done in this case as well, as shown in Figure 19, resulting in four effective "valve regions" as the fluid flows past the piston. However, one of the reasons why new concepts had to be explored in the

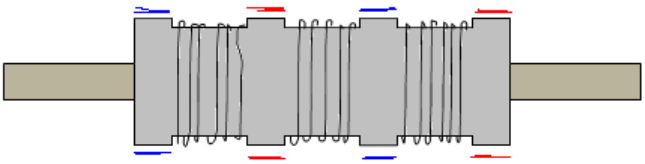

**Figure 19:** Another electromagnetic coil arrangement, with the coil wired in three sections.

first place was the problem encountered in [5] with magnetic saturation in the walls of the actuator that caused huge problems in delivering the needed amount of magnetic field intensity to the fluid. In this new concept, nothing has been done in order to increase the amount of field intensity the wall is able to carry. Therefore, it is reasonable to believe that the same problem with magnetic saturation will be present here as well. In addition, there is the problem that the effect of the shear stress and the pressure acting on the piston might cancel each other – when the shear stress increases, the internal pressure decreases. This effect is clearly not wanted, and might be devastating to the overall performance of the actuator. In addition, there might be a problem with the magnetic field pulling the piston either up or down. Still, it is unknown how large these effects would be. Of course, a possibility would be to think of a solution to these problems, but a better way is to focus the attention on concepts that does not have these problems in the beginning, rather than fixing and making trade-offs with a concept that initially is no good. A good starting point is way better for finding an optimal solution. There is one positive thing about the concept though – the partial overlap of the outlet seems to contribute to a high stiffness.

The "sieve concept" in Figure 12 is essentially the same principle as the previous, but with more outlets and a different placement of the coil. In the

figure, the electromagnetic coils are placed at the inlet, and are responsible for creating a varying pressure drop. The concept relies solely on pressure distribution, and not on shear forces dragging the piston up or down. The problem here is the same as before; the design still is very similar to the one explored in [5]. Multiple partially covered outlets could also be applied to the concept in [5] resulting in a higher stiffness, but would not solve the problem with the magnetic saturation.

The design shown in Figure 14 seems to solve the problems recently stated. Since the electromagnetic coil is as close to the fluid as possible, and is not dependent on the walls in order to transmit the magnetic field, the saturation problem might no longer exist (statement with reservations). The stiffness is not easy to see whether will be large or not, but it should be possible to adjust the stiffness by modifying the geometries concerning the constriction of the nozzles. The question is how large the stiffness can become, and what geometry that will be optimal. Another question is whether the movement will be as large as wanted – the restriction is the space between the nozzles and the wall of the piston. The closer the nozzles are to the wall of the piston, the larger the stiffness might be, but this again restricts the movement of the piston. Hence there seem to be a trade-off between the stiffness of the actuator and the movement of the piston. Further, note that it is important to find ways to separate the left and right pipe branch from each other, in order to prevent the pressure from travelling. Investigations need to be carried out in order to find how the constrictions at the branching of the pipes should be shaped to minimize the "pressure travel", since it might not be feasible to have to separate supply lines. Also note that the fluid jet from the nozzles onto the piston might contribute to pushing the piston against the wall of the actuator, something that could lead to higher friction between the wall of the actuator and the piston and hence a loss of energy. It might therefore be advantageous to make the nozzles perpendicular to the wall of the actuator in such a way that the pressure from the "jet" will act *with* the movement of the piston and not any other direction.

What is the best of having the nozzles pointing inwards or outwards is a bit difficult to say. With the nozzles pointing inwards the pipes must be a certain distance apart, whereas with the nozzles pointing outwards the pipes can in theory be adjacent. The advantage with the last fact is that there is a greater freedom to define whatever distance between the pipes necessary for the electromagnetic coil or the permanent mangets, long or short, whereas with the nozzles pointing inwards the coil or permanent magnet *must* have a certain length. Inwards pointing nozzles might also use a bit more space than the outwards pointing because they need both the space between the

pipes and at the side of the pipes in order for the piston to move. Hence there is a bit more freedom to choose the geometries with the outwards pointing nozzles.

The design in Figure 15 b) with the laterally pointing nozzles might at first sight seem to save some space. However, this is not certain before a more thorough investigation is done. A disadvantage is that the fluid jet from the nozzles will deflect from the slanting wall and move towards the adjacent wall, "creating" a force that might act as a disturbance to the behaviour of the actuator. Also, this jet will force the piston clockwise and perhaps contribute to increasing the friction between the piston and the walls of the actuator.

The other two alternatives in Figure 15 (a and c) are in theory similar in that both the nozzles are pointing outwards, with the only difference being the angle of the piston walls.

It is not easy to tell which of the concepts will provide the largest stiffness before some modelling and simulations are carried out. When it comes to the range of movement, the design in Figure 15 c) will perhaps give the largest movement provided the size(length) is the same as the other concepts. It is also noted that in the concepts with the slanting piston walls (all but the two last figures in Figure 20), the fluid jet from the nozzles will provide a force not only in the direction of movement, but also in lateral directions causing a larger friction between the piston and the wall of the actuator and hence a possible loss of energy, yet unknown how much. At first sight it would therefore seem best to have the nozzles perpendicular to the piston walls, the piston having straight walls, as in the two last sketches in Figure 20. Still, no calculations has been done yet, so it could be careless not to consider the other concepts too, if the gain should prove to be better with slanting piston walls.

Concerning the distribution of the magnetic field, the different concepts in Figure 16 might apply to different geometric designs. For instance, a more compact (shorter) magnetic design can be used with outwards pointing nozzles because the pipes can be placed closer to each other than in the other concepts.

The problem with concept c) in Figure 16 is that the magnetic field not necessarily is perpendicular to the flow direction. This is solved in d) by having the coils at the side of the pipes. This might be a good concept because the magnetic field is distributed at two places and hence the effect is larger. One problem that might be encountered with the design in d) is the saturation problem. The magnetic coils, when mounted at the side of the pipes as shown in the figure, must probably be made smaller than if they

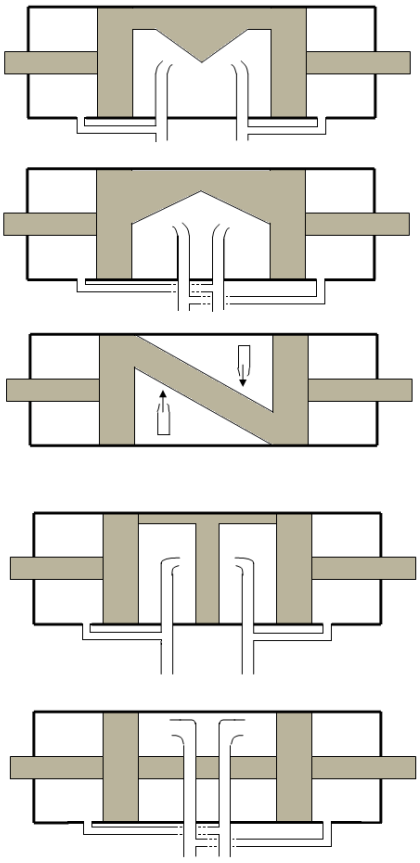

**Figure 20:** Compilation of the various "radically new" concepts.

were placed in between the pipes. Therefore, it is reasonable to think that the coil cores will reach saturation sooner than the other concepts due to their length and comparatively small cross-sectional area.

The concept in e) was invented in order to get the magnetic field as close to the outlet of the nozzles as possible. However, it was soon decided that it would be best to let the outlet be as little affected by the magnetic field as possible, and rather have the "magnetic constriction" further down. In addition, the movement of the piston would be restricted more than strictly necessary, and since the magnets would be closer to the piston, there might arise some problems with magnetic forces dragging the piston.

A problem with the magnetic concept in Figure 16 a) could be that the

magnetic field will not only be present at the top of the electromagnetic coil, but also at the bottom. The solution to this must be the concept in d), only with permanent magnets at the side of the pipes instead of coils. Therefore, the concept in b) could be viewed as a variation of the concept in d), only the other way round with the electromagnetic coil in between the pipes and the permanent magnets at the outside. The design in b) seems to give a

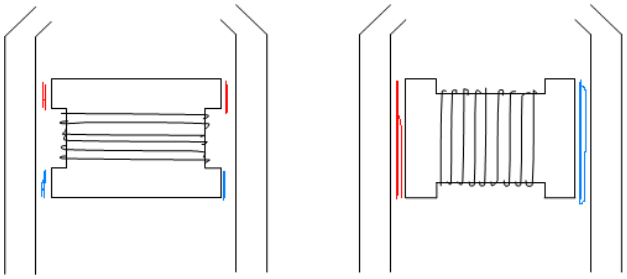

**Figure 21:** Electromagnetic coil comparison, illustrating the difference in "magnetic area"

magnetic field at a larger area than the design in a) and d), see Figure 21. Therefore, for the time being, the design in Figure 16b) seems to be the best due to its ability to supply the magnetic field at a larger area.

Utilizing the space inside the actuator is naturally a good idea, but this has to be done after the modelling and simulations are carried out in order to see what size and shape the different parts should have. It could also be a good idea to investigate what shape the pipes should have. Could it be better to have them slightly flattened rather than circular in order for the magnetic field to have the most influence on the fluid?

When it comes to the concept of having the permanent magnets mounted on the piston, there will probably be a problem with the magnetic force between the permanent magnets and the electromagnetic coil counteracting the effect caused by the weakening/strengthening of the field. The question is whether the magnetic forces will be larger than the pressure forces. In addition, there is the question whether the effect of moving the permanent magnets closer to/further away from the pipes is too large or too small. If the magnetic field decreases too fast with the distance, the movement will be too small, while on the other hand, if the change of the magnetic field with distance is very small, it is no point in mounting the permanent magnets on the piston, as it will only make things more complex and contribute to nonlinear effects because of the magnetic forces and due to the fact that the

magnetic field decreases nonlinearly with the distance. The conclusion is that there is nothing to gain (other than problems) at mounting the permanent magnets on the piston.

## 3.6 Conclusion – Selection of Concepts

The two first concepts (Figures 11 and 12) are somewhat closely related to the design considered in the previous project [5] and will not be further investigated this time. The problems encountered last time has not been explicitly solved, though the concepts at first sight might seem to be better in some areas such as with the stiffness. In addition, in the first concept the increase of shear stress would lead to a decrease of pressure force, something that might be devastating to the performance of the actuator. It would therefore be wiser to investigate some of the other, new concepts rather than trying to improve the concept that has been investigated before.

To cover the concepts best, one concept with outwards pointing nozzles and one with inwards pointing nozzles is chosen for further investigation. One of these should be with slanting piston walls while the other with straight piston walls (to see which provides the highest stiffness). The choice then becomes easy. Straight walls and outwards pointing nozzles are best covered by the concept in Figure 15 c), since it would be space-consuming to have straight walls with inwards-pointing nozzles(see Figure 20, the last but one concept). For the inwards-pointing nozzles the concept in Figure 14 is chosen. Hence the first and the last concepts in Figure 20 are chosen. Simulations should be done with different angles both of the walls and of the nozzles in order to find the optimal geometry. The outwards pointing nozzles can have less space between the pipes, so a compact magnetic design could be utilized. For the inwards pointing nozzles, there must be a certain distance between the pipes, so a wider/longer magnetic coil must be used. Simulations and/or calculations should show what is the best combination.

Of the "magnetic concepts", the one in Figure 16 a) will not be further investigated due to its smaller "magnetic area" compared to the one in b). Further the d)-concept precedes the one in c), due to its far better ability to apply the magnetic field perpendicular to the flow. The concept in e) will not be further considered due to the restriction of movement. Comparing the concept in Figure 16 b) and d), the concept in b) will be able to supply the magnetic field to a larger area than the concept in d), see Figure 21. In addition, the concept in d) might not be able to supply as high magnetic field as the one in b) due to the fact that the electromagnetic coil might have to be smaller. Therefore, the magnetic concept in b) is selected to be further

investigated, but if this concept should encounter any problems, the concept in d) should be the next to be considered.

The magnetic properties can be investigated somewhat separately of the other design. What should be simulated and optimized is the concept's ability to transfer the magnetic field to a largest possible area, and over a wide rage of magnetic fields from zero to maximum, in addition to being as compact as possible.

To conclude, if nothing new appears before the tests are done, these concepts will be further investigated:

- Actuator with nozzles pointing inwards (Figure 14)
- Actuator with nozzles pointing outwards (Figure 15c)
- Magnetic concept in Figure 16b)

It is a question whether it actually is possible to strengthen or weaken a magnetic field by introducing another magnetic field. This has to be further investigated, but till then it is assumed that this is possible.

## 3.7 Summary

The ideal values of the servomechanism are a movement of $1cm$, a very small diameter ($2mm$), and a stiffness of $5N/mm$. The length has no particular restrictions, but obviously it should not be too long.

A traditional servo valve is used as a starting point for most of the concepts, while the other concepts are "improvements" of the design considered in [5]. The conclusion is that the "improvements" are not good enough to proceed with, so the concepts inspired by the traditional servo valve will be further explored. These concepts are based on pressure distribution by nozzle constriction, with magnetic fields and closing walls used to constrict the pipes/nozzles. To produce the magnetic field, a combination of electromagnetic coils and permanent magnets will be utilized, with the electromagnetic coil(s) being responsible for strengthening or weakening the field set up by the permanent magnet(s). The magnets should be fixed relative to the pipes, and not for instance mounted on the piston, due to the magnetic forces that could interfere with the movement of the piston.

Some reservations has to be taken as to whether it actually is possible to strengthen or weaken a field by introducing another magnetic field. This has to be further investigated, but for the time being it is assumed that it is possible.

# 4 Testing and Refinement

## 4.1 Introduction

This chapter consist of some mathematical models and calculations, simulations in Comsol Multiphysics [2] and real tests done in order to investigate properties that cannot be simulated or is to complicated to simulate. The "refinement" word points out the fact that the design of the actuator inevitably will become "refined" or changed as the simulations or models find things that must be improved for the actuator to work properly.

It was decided to use simulations in Comsol Multiphysics for a number of reasons. Reasons that hopefully will become clearer further down. It is more attractive to leave all the complex calculations to Comsol and get a more accurate result than to make a whole lot of assumptions and simplifications in order to be able to calculate this "by hand".

First, some modelling and calculations will be carried out, starting with calculations of the pressure distribution in the pipes of the actuator, and then continuing with calculations of the magnetic field intensity in the fluid. Next, simulations in Comsol will be carried out before some real tests are described and discussed.

The fluid that will be used is the MRF-140CG due to the fact that this is the "strongest" fluid that could be supplied by [9], and in addition it was the fluid that was reviewed in [5]. The technical data sheet of the fluid is shown in Appendix D.

## 4.2 Models and Calculations

### 4.2.1 New constriction concept

After thinking thoroughly about how the nozzle constriction should work, and trying to develop models for it, the concepts probably need to be slightly revised in order to get the appropriate constriction effect. The whole purpose with the constriction is to create a (significant) pressure drop over a certain range of movement. It then seems as if the best way to get this pressure drop will be to have a constriction that reduces the radius of the pipe. This is easily seen by looking at the Poiseuille's law (Equation (6) further down, anticipating events), where the radius is to the power of 4, i.e., the largest effect can be attained by changing the radius of the pipe. If the constriction concepts described in Section 3.4.2 were to be used for constriction purposes, this might make the constriction range smaller (see lowest right sketch in

[2] Comsol 3.4, a multiphysics simulation environment. Web page: http://www.comsol.no

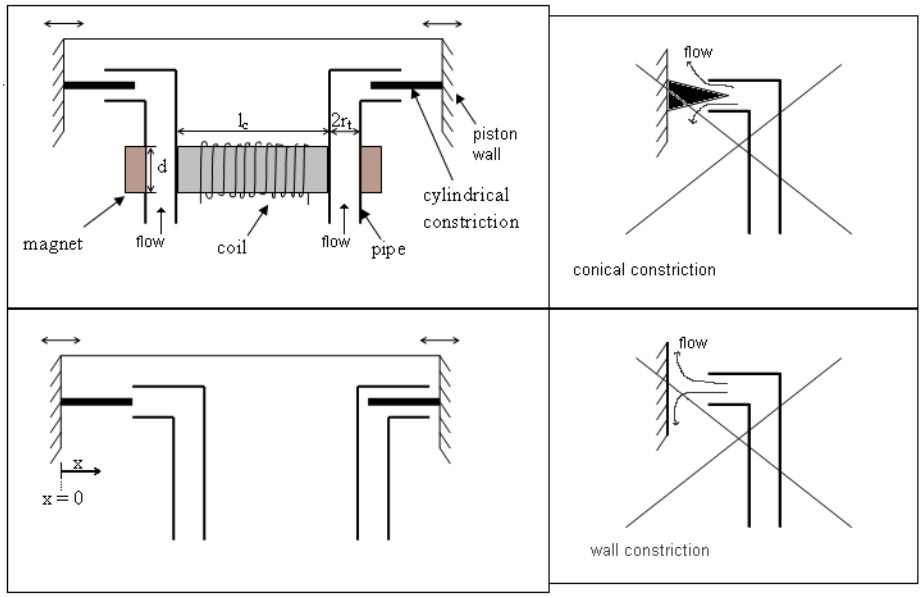


**Figure 22:** Illustration of constriction concepts, with the cylinder constriction concept to the left. The rightmost designs will not be used. The bottom, left figure shows the constrictions at $x = 0$, with no constriction of the left pipe and maximum constriction of the right pipe.

Figure 22), or at least somewhat difficult to calculate because the constriction would be a build-up of pressure in front of the nozzle (or, to be honest, I am not quite sure how the constriction should be modelled). Of course, this works well in the traditional servo valve, but unknown to what degree of control or to what range of movement and how resilient it would be to external forces.

One way to arrange a constriction which reduces the radius of the pipe is to have it moving in and out of the pipe/nozzle. For ease of calculation and length of movement, it is probably best to let this be in the form of a cylindre, as illustrated in Figure 22. It could of course be possible to have a conical constriction (up to the right in Figure 22), but this would lead to a nonuniform behaviour, meaning different radius for different positions of the piston, and perhaps also a shorter movement of the piston.

With a cylindre constriction like in the leftmost sketches in Figure 22, only one of the concepts chosen in Section 3.6 remains, namely that with outwards pointing nozzles and perpendicular piston walls (see Figure 15 c). The constrictions (cylindres) can then be mounted on the piston. This concept is the only one that will be considered in the subsequent sections, since

inwards pointing nozzles would be infeasible with this kind of constriction (see Figure 62 in Appendix C for an illustration).

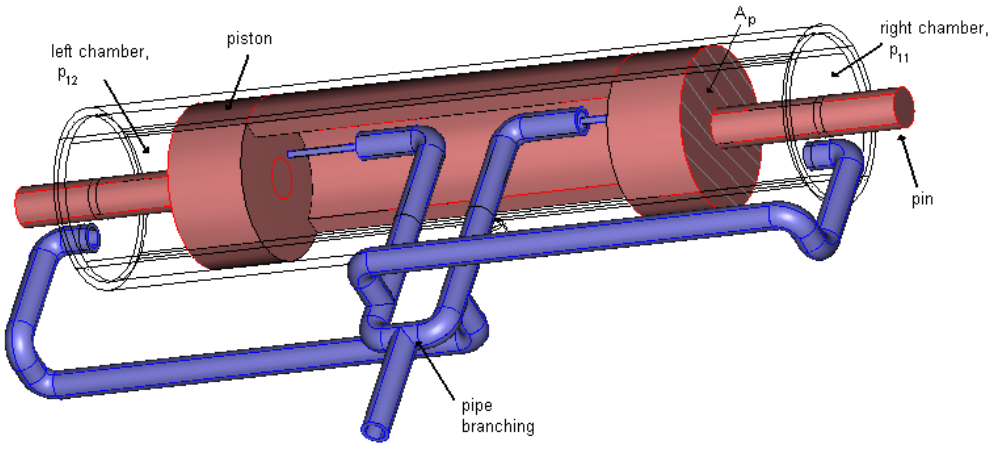


**Figure 23:** Illustration of how the concept could look like in three dimensions, with the pipes and the piston highlighted. Notice how the cylinder constriction is mounted on the piston and is partly inside the pipes, with enough room for the piston to move. The magnets are not included.

### 4.2.2 Pressure calculations

The pressure drop in a pipe filled with fluid under the influence of a magnetic field $H$ is described by the equation

$$\begin{aligned} \Delta p &= \frac{12\eta QL}{\pi r^4} + 3\frac{L}{r}\tau_y \quad , T^* < 0.5 \\ \Delta p &= \frac{8\eta QL}{\pi r^4} + 2\frac{L}{r}\tau_y \quad , T^* > 200 \\ T^* &= \frac{\pi r^3 \tau_y}{12Q\eta} \end{aligned} \tag{5}$$

which is a slight modification of the equations found in [16, p.81], used in [5] and stated again in Section 1.1. $\eta$ is the dynamic viscosity, Q is the volumetric flow rate, L is the lenght of the pipe, r is the radius of the pipe, and $\tau_y$ is the yield stress of the fluid. In [5], the yield stress was linearly approximated with $\tau_y = k_\tau H$ where H is the magnetic field intensity over the fluid and $k_\tau$ a proportionality constant (other approximations might apply). Compared to the equations in Section 1.1, the differences are the denominators. The

first denominator $bh^3$ has become $\pi r^4$, and the second denominator $h$ has become $r$. The first change is justified by looking at Poiseuille's law for a pipe, $\Delta p = \frac{8\eta QL}{\pi r^4}$ [18] (the 8 in the numerator is likely to have the same conditions as the equations above, with a variable deciding whether the numerator should have 8 or 12) – this can be identified as the viscous part in the above equations. Then, by noticing that $bh^3 = bh \cdot h^2 = Ah^2$ where $A$ is the cross-sectional area, and similarly that $\pi r^2 \cdot r^2 = Ar^2$, we can see that $h$ is the equivalent to $r$, hence the second denominator becomes $r$ instead of $h$. The numerator in $T^*$ is adapted the same way, with $bh^2 = bh \cdot h = A \cdot h$ leading to $\pi r^2 \cdot h = \pi r^3$. Note that the equations are (only) valid for flow through a pipe. For other flow regimes, the equations in Section 1.1 must be used or developed to the particular use.

In order to calculate the pressure drop from inlet to outlet, Poiseuille's law, which corresponds to Ohm's law for electrical circuits, can be used [18]. The pressure drop $\Delta P$ is then analogous to the voltage $V$, and the voluminal flow rate $Q$ is analogous to the current $i$. The "resistance" is

$$R = \frac{8\eta\Delta x}{\pi r^4} \tag{6}$$

where $\eta$ is the (dynamic) viscosity as before, $\Delta x$ is the distance in the pipe, and $r$ is the radius of the pipe. As mentioned before, this is nothing else than the viscous expression in Equation (5), and even though this is not mentioned in [18], it is probable that the same conditions as in Equation (5) are valid in such a way that the 8 in the numerator should be changed to 12 provided $T^* < 0.5$, as mentioned before.

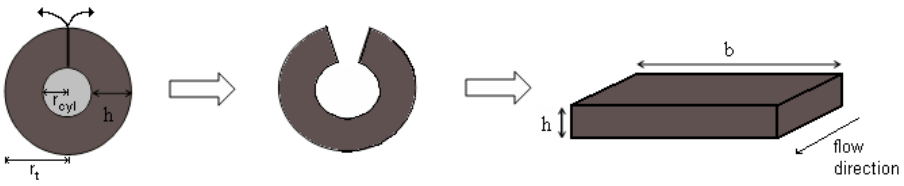


**Figure 24:** Illustration of the pipe with the cylinder constriction inside, and a comparison with a rectangular flow regime

The sketch in Figure 25 shows the placement of the different variables that are used in the modelling and calculations. Before proceeding, please notice that the inlet and outlet pressures are assumed constant and known($p_i$ and $p_o$, respectively). Also notice the definition of $x$; when $x = 0$, the piston

is at its leftmost, meaning that the end of the left cylindre constriction is at the end of the nozzle, while the right cylinder constriction is as deep into the pipe as possible (see Figure 22). In other words, $l_{32} = x$ and $x$ is the length of the constriction inside the left pipe, see Figure 25. Then, by assuming that $T^* < 0.5$ (this is in fact the case for the calculations further down) we get:

$$\begin{aligned}
p_i - p_o &= QR_i + Q_1(R_{ic1} + R_{i1} + R_{11} + R_{21} + R_{31}) \\
&= QR_i + Q_2(R_{ic2} + R_{i2} + R_{12} + R_{22} + R_{32}) \\
R_i &= \frac{12\eta l_i}{\pi r_t^4} \\
R_{ic} &= \frac{12\eta l_{ic}}{\pi r_{ic}^4} \\
R_{i1} &= R_{i2} = \frac{12\eta l_{i1}}{\pi r_t^4} \\
R_{11} &= \frac{12\eta d}{\pi r_t^4} + 3\frac{d}{Q_1 r_t}\tau_{y1} \\
R_{12} &= \frac{12\eta d}{\pi r_t^4} + 3\frac{d}{Q_2 r_t}\tau_{y2} \\
R_{21} &= \frac{12\eta l_{21}}{\pi r_t^4} + \frac{12\eta(l_n - x)}{\pi r_t^4} = \frac{12\eta(l_{21} + l_n - x)}{\pi r_t^4} \\
R_{22} &= \frac{12\eta l_{22}}{\pi r_t^4} + \frac{12\eta x}{\pi r_t^4} = \frac{12\eta(l_{22} + x)}{\pi r_t^4} \\
R_{31} &= \frac{12\eta x}{A_{nc} h^2} = \frac{12\eta x}{\pi(r_t^2 - r_{cyl}^2)h^2} = \frac{12\eta x}{\pi(r_t^2 - r_{cyl}^2)(r_t - r_{cyl})^2} \\
R_{32} &= \frac{12\eta(l_n - x)}{\pi(r_t^2 - r_{cyl}^2)(r_t - r_{cyl})^2}
\end{aligned}$$

where $r_t$ is the radius of the pipe, $d$ is the length of the magnetic field influence, $r_{ic}$ is the radius of space inside the constriction at the inlet, $r_{cyl}$ is the radius of the cylinder constriction, $h = r_t - r_{cyl}$ is the height between the cylinder constriction and the pipe wall, and $A_{nc} = \pi r_t^2 - \pi r_{cyl}^2 = \pi(r_t^2 - r_{cyl}^2)$ is the cross-sectional area of the fluid in the constriction region (see the leftmost figure in Figure 24). It is assumed that the length of the pipe from $p_{11}$ and $p_{12}$ to the magnetic region is close to zero, in such a way that there is no resistance and hence no pressure drop. Notice that $l_{32} = x$ in $R_{22}$ and $R_{32}$.

There is one problem; there are three unknowns $(Q, Q_1, Q_2)$ and only two equations, assuming the magnetic field intensity $H$ ($\tau_y = \tau_y(H)$) and

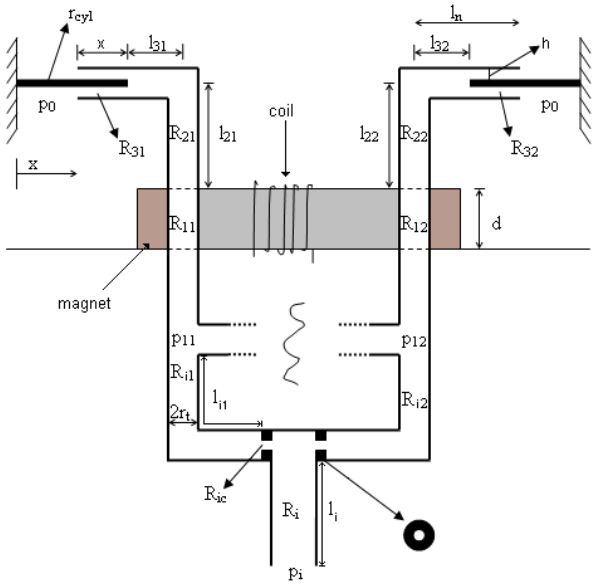


**Figure 25:** Sketch of the pipes with the different "resistances" and constrictions. Note that with x defined as before, $l_{32} = x$. The inlet constrictions (index "ic") are placed at the branching of the pipes.

the displacement $x$ is known. However, if $R_i$ is assumed to be close to zero, meaning that the length from the inlet and to the branching of the pipes is assumed to be close to zero, the flow rate $Q$ can be removed from the equations. Hence we get:

$$
\begin{aligned}
&Q_1(R_{ic1} + R_{i1} + R_{11} + R_{21} + R_{31}) \\
&= Q_1 \left( R_{ic1} + R_{i1} + \frac{12\eta d}{\pi r_t^4} + 3\frac{d}{Q_1 r_t}\tau_{y1} + \frac{12\eta(l_{21} + l_n - x)}{\pi r_t^4} + \frac{12\eta x}{\pi(r_t^2 - r_{cyl}^2)(r_t - r_{cyl})^2} \right) \\
&= Q_1 \left( R_{ic1} + R_{i1} + \frac{12\eta d}{\pi r_t^4} + \frac{12\eta(l_{21} + l_n - x)}{\pi r_t^4} + \frac{12\eta x}{\pi(r_t^2 - r_{cyl}^2)(r_t - r_{cyl})^2} \right) + 3\frac{d}{r_t}\tau_{y1} \\
&= Q_1 R_{p1} + 3\frac{d}{r_t}\tau_{y1} \\
&= p_i - p_o \\
&\Rightarrow Q_1 = \frac{p_i - p_o - 3\frac{d}{r_t}\tau_{y1}}{R_{p1}}
\end{aligned}
$$

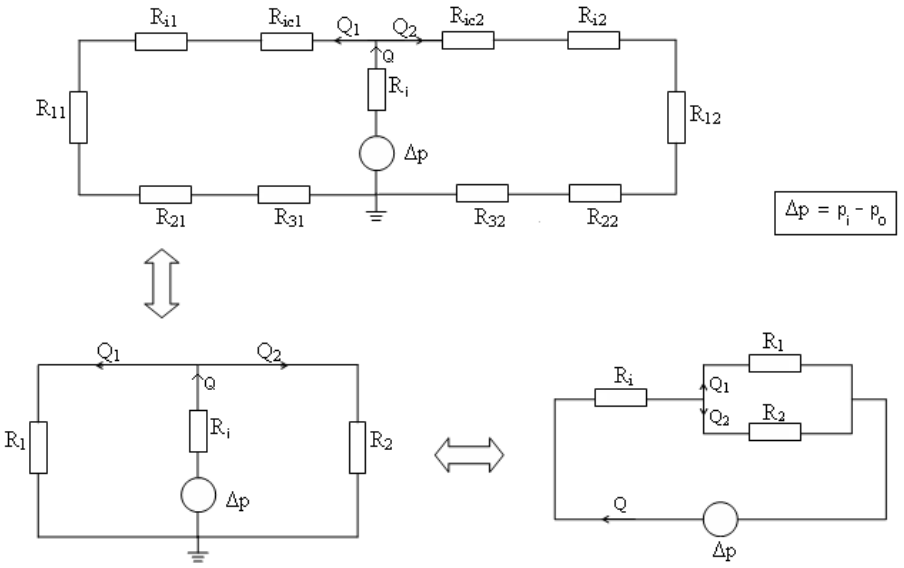


**Figure 26:** Electrical circuit analogy to Figure 25.

and

$$
\begin{aligned}
&Q_2(R_{ic2} + R_{i2} + R_{12} + R_{22} + R_{32}) \\
&= Q_2 \left( R_{ic2} + R_{i2} + \frac{12\eta d}{\pi r_t^4} + 3\frac{d}{Q_2 r_t}\tau_{y2} + \frac{12\eta(l_{22}+x)}{\pi r_t^4} + \frac{12\eta(l_n - x)}{\pi(r_t^2 - r_{cyl}^2)(r_t - r_{cyl})^2} \right) \\
&= Q_2 \left( R_{ic2} + R_{i2} + \frac{12\eta d}{\pi r_t^4} + \frac{12\eta(l_{22}+x)}{\pi r_t^4} + \frac{12\eta(l_n - x)}{\pi(r_t^2 - r_{cyl}^2)(r_t - r_{cyl})^2} \right) + 3\frac{d}{r_t}\tau_{y2} \\
&= Q_2 R_{p2} + 3\frac{d}{r_t}\tau_{y2} \\
&= p_i - p_o \\
&\Rightarrow Q_2 = \frac{p_i - p_o - 3\frac{d}{r_t}\tau_{y2}}{R_{p2}}
\end{aligned}
$$

see Figure 26 for the electrical circuit analogy used to find these equations. Now, with expressions for the flow rates, it is time to direct the attention towards the pressures $p_{11}$ and $p_{12}$. $p_{11}$ will become the pressure in the rightmost chamber, while $p_{12}$ is the pressure in the leftmost chamber (remember that the left pipe is connected to the right chamber and vice versa with

outwards pointing nozzles, see Figure 23), since the fluid is nearly static in the pipes to these chambers and will only move when the piston moves. The pressure difference between $p_{11}$ and $p_{12}$ is responsible for the movement of the piston. These pressures can be found by calculating the pressure drop over the "resistances" from $p_{11}$ and $p_{12}$ to the outlet pressure $p_o$, please see Figures 25 and 26:

$$\begin{aligned} p_{11} - p_o &= Q_1(R_{11} + R_{21} + R_{31}) \\ &= Q_1 \left( \frac{12\eta d}{\pi r_t^4} + \frac{12\eta(l_{21} + l_n - x)}{\pi r_t^4} + \frac{12\eta x}{\pi(r_t^2 - r_{cyl}^2)(r_t - r_{cyl})^2} \right) + 3\frac{d}{r_t}\tau_{y1} \\ \Rightarrow p_{11} &= Q_1 \left( \frac{12\eta d}{\pi r_t^4} + \frac{12\eta(l_{21} + l_n - x)}{\pi r_t^4} + \frac{12\eta x}{\pi(r_t^2 - r_{cyl}^2)(r_t - r_{cyl})^2} \right) + 3\frac{d}{r_t}\tau_{y1} + p_o \\ &= p_{11}(x) \end{aligned}$$

and

$$\begin{aligned} p_{12} - p_o &= Q_2(R_{12} + R_{22} + R_{32}) \\ &= Q_2 \left( \frac{12\eta d}{\pi r_t^4} + \frac{12\eta(l_{22} + x)}{\pi r_t^4} + \frac{12\eta(l_n - x)}{\pi(r_t^2 - r_{cyl}^2)(r_t - r_{cyl})^2} \right) + 3\frac{d}{r_t}\tau_{y2} \\ \Rightarrow p_{12} &= Q_2 \left( \frac{12\eta d}{\pi r_t^4} + \frac{12\eta(l_{22} + x)}{\pi r_t^4} + \frac{12\eta(l_n - x)}{\pi(r_t^2 - r_{cyl}^2)(r_t - r_{cyl})^2} \right) + 3\frac{d}{r_t}\tau_{y2} + p_o \\ &= p_{12}(x) \end{aligned}$$

assuming $p_i$ and $p_o$ known and constant and $Q_1$ and $Q_2$ calculated from the equations found above.

It could be possible to find the displacement $x$ at equilibrium from these equations by setting $\Delta p = p_{12} - p_{11} = 0$, but this would be a lot of work because it would lead to a quadratic equation with heaps of elements. Therefore, it is easier to do the calculations in a step-by-step manner finding the particular $x$ that leads to zero pressure difference.

There is one problem with these equations – they do not take into account that the two pipe branches will affect each other, with the pressure "travelling" between the pipes. This is meant to be alleviated by the inlet constrictions, but with the inlet resistance $R_i$ assumed to be zero, the model is equivalent to having two *separate* pipe branches with separate inlet pressures, and not having a *common* inlet pressure. Therefore, it is impossible to find the effect of the inlet constrictions. A larger constriction will only lead

to a decrease in pressure in the relevant pipe, and will not affect the pressure in the other pipe in any way.

The force acting on the piston can be expressed by

$$F_p = (p_{12} - p_{11})A_p \tag{7}$$

where $p_{11}$ is the pressure in the rightmost chamber, $p_{12}$ is the pressure in the leftmost chamber, and $A_p$ is the cross-sectional area of the piston (the area the pressure is acting on). Note that a positive force is towards the right, in the positive x-direction.

The following values will be used in the calculations:

- Piston "effective" area: $A_p = \pi \cdot (0.002m)^2 - \pi \cdot (0.0005m)^2 \approx 1.18 \cdot 10^{-5} m^2$, meaning the pin has a diameter of $1mm$ and the piston a total diameter of $4mm$ ($A_p$ is the area the pressure will act on, see Figure 23).
- Inlet pressure: $p_i = 10 \cdot 10^{-5} Pa = 10bar$, unless otherwise stated.
- Outlet pressure: $p_o = 100000Pa = 1bar$ (near atmospheric pressure).
- Pipe diameter: $2r_t = 0.5mm$
- $l_{21} = l_{22} = 1mm$ (see Figure 25)
- $\tau_y = k_\tau H$ with $k_\tau = 0.3$, the same linear approximation as in [5].
- Length of inlet constriction: $l_{ic} = 0.2mm$
- Diameter inside inlet constriction: $2r_{ic} = 0.1mm$
- Fluid viscosity: $\eta = 0.28Pas$ (see Appendix D).
- Nozzle length, $l_n$, will be stated for each calculation.
- Magnetic field interaction length: $d = 1.5mm$ unless otherwise stated.

$\Delta x$ is the displacement to either side of the initial centre position of the piston, meaning the position of the piston with no magnetic field at the pipes or possibly equal magnetic fields at both pipes.

Figure 27 shows the effect of the cylinder constriction. Please note that even though only positive values are shown in the figure, the results are valid for both directions. The displacement $\Delta x$ is thought to be happening due to an external force displacing the piston to one of the sides. The forces shown in the figure is the "*counter force*" to this external force. This counter force

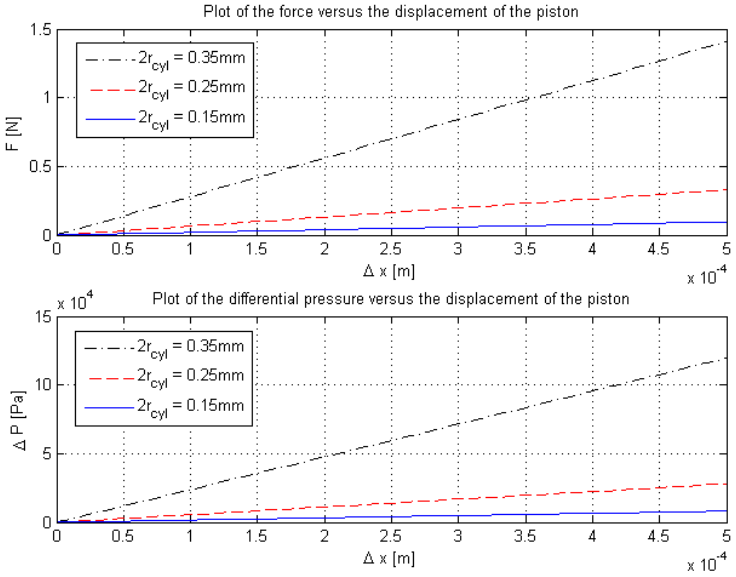


**Figure 27:** Plots of how the displacement of the piston affects the pressure difference and hence the force – this is the *stiffness* of the actuator. The calculations were made without any magnetic field. The force was calculated by assuming a cross-sectional area of the piston, $A_p$. $d = 1mm$ (no influence since there is no magnetic field), nozzle length $l_n = 1mm$.

should be as large as possible, since this means that the *stiffness* of the actuator is large. With the piston "effective" area chosen above ($A_p$), the force at a piston displacement of $0.5mm$ and a 70% constriction ($2r_{cyl} = 0.35mm$ with the pipe diameter $2r_t = 0.5mm$) is about $1.4N$, indicating a stiffness of $2.8N/mm$. With a 50% constriction ($2r_{cyl} = 0.25mm$) and the same displacement, the force is about $0.3N$ ($0.6N/mm$) which is considerably smaller. Hence it is easy to see that a larger constriction gives a "stiffer" actuator. The bottom plot in Figure 27 shows the pressure differences at the different displacements. Please note that there is no magnetic fields present in these calculations, so the pressure differences are purely due to the constriction of the pipes.

The next simulations were carried out with magnetic fields at the pipes, and with longer pipes in order to see how this would affect the stiffness. First, the maximum effect from the magnetic field was tested, with a maximum difference of magnetic field intensity between the two sides. It is assumed that the maximum total magnetic field intensity that can be achieved is

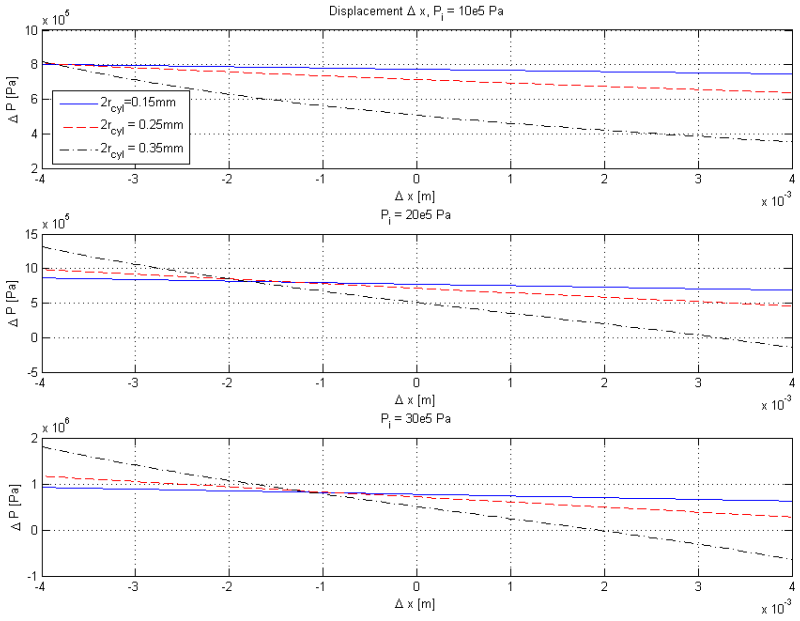


**Figure 28:** Simulations with $H_1 = 0$ and $H_2 = 160000A/m$, with varying inlet pressure and longer pipes than before, $l_{i1} = l_{i2} = 8mm$ (was $4mm$ before), and nozzle length $l_n = 8mm$(was $1mm$ before).

$160000A/m$ (which brings the yield stress of the fluid close to the saturation limit, see the technical data in Appendix D), and that it is possible to subtract and add magnetic fields such that the field at the left pipe is $H_1 = 0A/m$ and the field at the right pipe is $H_2 = 160000A/m$. With these magnetic field intensities at the pipes, the pressure difference at various displacements from the centre position $\Delta x$ was plotted in Figure 28. When $\Delta P = 0$, the piston is at equilibrium and will stay there until the magnetic fields are changed. A smaller difference, $\Delta H$, between the magnetic field intensities in the two pipes will lead to a smaller displacement of the piston. The plots show that different constriction sizes will lead to different equilibrium positions; a smaller constriction leads to a larger displacement and vice versa (see Figure 28). A somewhat surprising result can be seen. As expected, the force (or more precisely the pressure difference) increases with an increasing inlet pressure. But, as the inlet pressure increases, the *movement* of the piston is *reduced*. This means that a higher inlet pressure leads to higher forces, but comes at the expense of the movement of the piston.

One can also read the stiffness from the plots in Figure 28 by finding the pressure difference $\Delta P$ over $1mm$ movement. For instance, in the upper plot with $P_i = 10 \cdot 10^5 Pa$ and a constriction diameter of $0.35mm$, the pressure difference over $1mm$ seems to be approximately $0.5 \cdot 10^5 Pa$, which corresponds to a force of $0.59N$ (with the assumed $A_p$ above), hence a stiffness of $0.59N/mm$. This is far from the stiffness above, almost five times smaller, and shows the importance of having the pipes as short as possible.

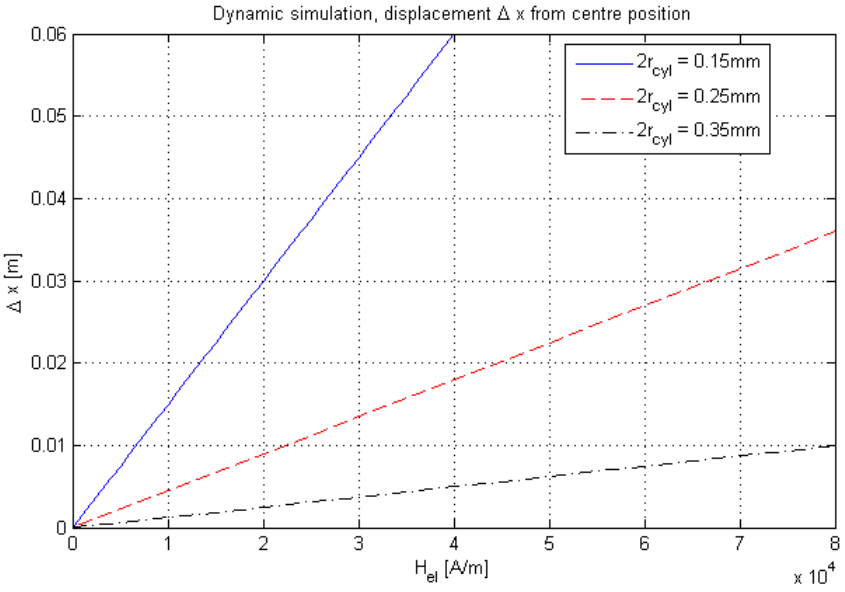


**Figure 29:** Figure illustrating the displacement of the piston with a certain magnetic field intensity from the electromagnetic coil, $H_{el}$. Note that this is the displacement to *one* of the sides, and that it is possible to get the same displacement to the other side by "reversing" $H_{el}$.

Figure 29 shows the range of movement to one of the sides for the piston, with the electromagnetic coil providing a certain magnetic field intensity $H_{el}$. It is assumed that addition and subtraction of magnetic fields is possible, and that the permanent magnets contribute to a constant magnetic field intensity of $H_{pm} = 80000A/m$ at each pipe and over a certain length $d$. To find the magnetic field intensity in each pipe, it was decided that an increase in magnetic field from the electromagnetic coil would lead to a decrease in the left pipe and an increase in the right pipe, i.e. $H_1 = H_{pm} - H_{el}$ and $H_2 = H_{pm} + H_{el}$. This way, an increase in the magnetic field from the electromagnetic coil will lead to a smaller flow resistance in the left pipe

and a greater flow resistance in the right pipe, leading to an increase of pressure in the leftmost chamber and a decrease of pressure in the rightmost chamber and hence a movement of the piston to the right (remember that the left pipe is connected to the right chamber and vice versa). Note that the displacements at $H_{el} = 80000A/m$ are the same as shown in the upper plot of Figur 28 (if the range had been long enough). Also note that Figure 29 shows the displacement to *one* of the sides, and that it is possible to get a similar displacement to the other side by turning the direction of the magnetic field (negative $H_{el}$ by changing the direction of the current in the electromagnetic coil).

The displacement is proportional to the magnetic field intensity (probably due to the linear approximation of the yield stress), with equations:

- $\underline{2r_{cyl} = 0.15mm} : \Delta x = 1.5 \cdot 10^{-6} \cdot H_{el}$ [m]
- $\underline{2r_{cyl} = 0.25mm} : \Delta x = 4.5 \cdot 10^{-7} \cdot H_{el}$ [m]
- $\underline{2r_{cyl} = 0.35mm} : \Delta x = 1.25 \cdot 10^{-7} \cdot H_{el}$ [m]

which gives the following maximum displacement of the piston (assuming $H_{elmax} = 80000A/m$):

- $\underline{2r_{cyl} = 0.15mm} : \Delta x_{max} = 1.5 \cdot 10^{-6} \cdot H_{elmax} \cdot 2 = 0.24m$
- $\underline{2r_{cyl} = 0.25mm} : \Delta x_{max} = 4.5 \cdot 10^{-7} \cdot H_{elmax} \cdot 2 = 0.072m$
- $\underline{2r_{cyl} = 0.35mm} : \Delta x_{max} = 1.25 \cdot 10^{-7} \cdot H_{elmax} \cdot 2 = 0.02m$

which also can be seen in Figure 29 by knowing that the same displacement is possible in the negative direction too. Be aware that these equations are *only* valid with the given variables and with $H_{pm} = 80000A/m$. The equations must *not* be used in other contexts.

As you might have noticed, *assumed* magnetic fields have been used. In the next section, calculations will be carried out in order to see whether it is possible to reach the required magnetic fields with an electromagnetic coil. As to the permanent magnets, they are assumed to be able to supply at least as high magnetic fields as the electromagnet.

### 4.2.3 Magnetic field calculations

This section is aimed at finding out whether it is possible to get the required magnetic field intensity from the electromagnetic coil. It is assumed that the

permanent magnets will manage to supply at least as high field intentity as the electromagnet.

In order to find the magnetic field intensity in the fluid gap, $H_f$, the equivalent to Ohm's law will be used, where the voltage is replaced by the magnetomotive force $F_{mmf}$, the current replaced by the magnetic flux $\Phi$ and the resistance replaced by the *reluctance* $R$ [7, p.673],

$$F_{mmf} = R\Phi \tag{8}$$

$$R = \frac{l}{\mu A} \tag{9}$$

please see Figure 30. To model the magnetic properties of the actuator,

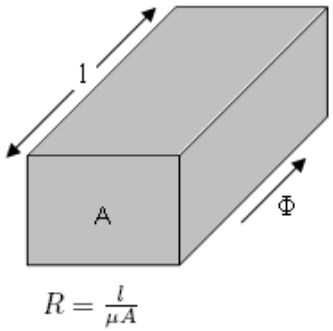


**Figure 30:** The reluctance $R$ of a magnetic path depends on the mean length $l$, the area $A$, and the permeability $\mu$ of the material. [7]

three different reluctances can be identified: the reluctance of the fluid between the magnets, $R_f$ (consisting of two equal reluctances, one for each gap; $R_f = \frac{\frac{1}{2}l_f}{\mu_f A_f} + \frac{\frac{1}{2}l_f}{\mu_f A_f} = \frac{l_f}{\mu_f A_f}$), the reluctance of the flux return path (meaning the return path of the magnetic field), $R_{ret}$, and the reluctance of the electromagnetic coil core, $R_{core}$, see Figure 31. The layout and geometry might not be entirely correct, but the results will give a hint as to whether it is possible to achieve the required magnetic field intensity.

The magnetomotive force of an N-turn current-carrying coil is given by $F_{mmf} = Ni$ [7]. Since the magnetic field intensity $H$ is needed in order to relate the yield stress to a magnetic field, a relationship between the magnetomotive force and this field intensity is required. From [5, p.28], $F_{mmf} = Hl$ where $l$ is the length of the material, as in Figure 30. Then, if "common voltage division" is employed, an expression for the magnetomotive force over

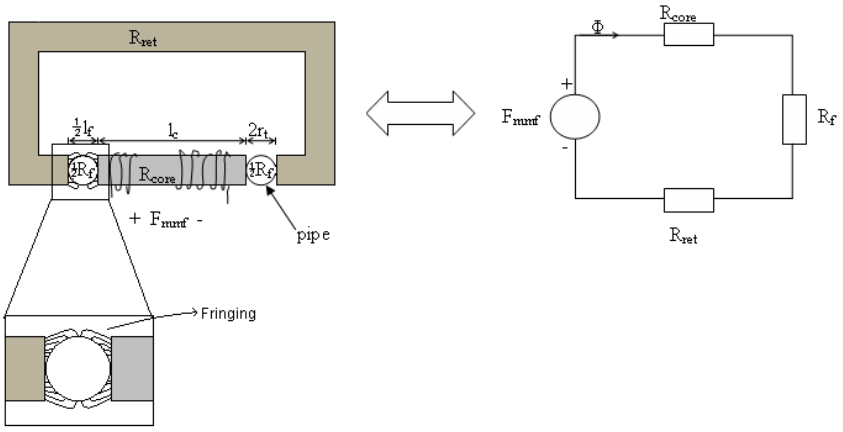


**Figure 31:** Illustration of the "magnetic circuit" in the actuator, the permanent magnets not taken into account.

(one of) the fluid gaps can be obtained (see Figure 31):

$$F_{mmff} = \frac{\frac{1}{2}R_f}{R_f + R_{ret} + R_{core}} F_{mmf} = \frac{\frac{1}{2}\frac{l_f}{\mu_f A_f}}{\frac{l_f}{\mu_f A_f} + \frac{l_r}{\mu_r A_r} + \frac{l_c}{\mu_c A_c}} F_{mmf} \tag{10}$$

and by using that $F_{mmf} = Hl$,

$$\begin{aligned} H_f \frac{1}{2} l_f &= \frac{\frac{1}{2}\frac{l_f}{\mu_f A_f}}{\frac{l_f}{\mu_f A_f} + \frac{l_r}{\mu_r A_r} + \frac{l_c}{\mu_c A_c}} Hl \\ \Rightarrow H_f &= \frac{\frac{l_f}{\mu_f A_f}}{\frac{l_f}{\mu_f A_f} + \frac{l_r}{\mu_r A_r} + \frac{l_c}{\mu_c A_c}} H \frac{l}{l_f} \end{aligned} \tag{11}$$

where $H_f$ is the magnetic field intensity in the fluid at each of the fluid gaps (equal for both fluid gaps), $\frac{1}{2}l_f$ is the length of *one* fluid gap, $A_f$ is the cross-sectional area of the fluid gap, $\mu_f$ is the permeability of the fluid. The constants with index r are related to the flux return path and the constants with index c are related to the electromagnetic coil core. The same calculation

applies to the magnetic field intensity in the electromagnetic coil core:

$$\begin{aligned} F_{mmf,core} &= \frac{R_{core}}{R_f + R_{ret} + R_{core}} F_{mmf} \\ \Rightarrow H_c l_c &= \frac{R_{core}}{R_f + R_{ret} + R_{core}} Hl \\ \Rightarrow H_c &= \frac{R_{core}}{R_f + R_{ret} + R_{core}} H \frac{l}{l_c} \end{aligned} \tag{12}$$

Equations (11) and (12) will be used to examine whether it is possible to get the required magnetic field intensity over the fluid from the small electromagnetic coil.

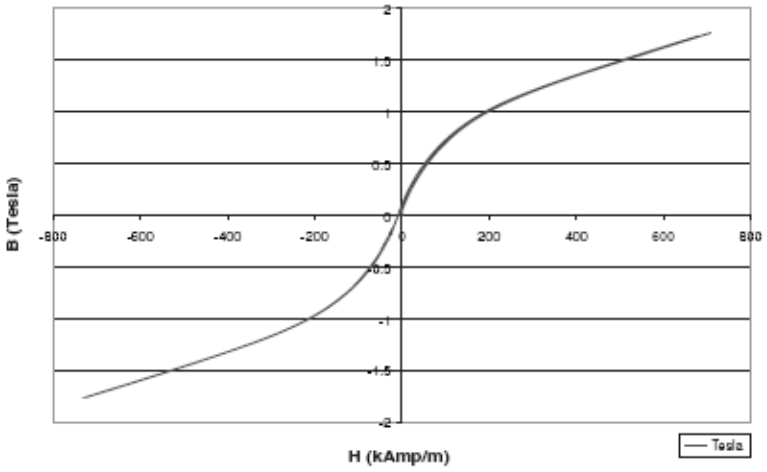


**Figure 32:** Typical magnetic properties for the MRF-140CG fluid, taken from the technical data sheet in Appendix D.

Since the permeability of the fluid is quite low (relative permeability $\mu_r$ from about 2 to about 20 depending on the magnitude of the magnetic field, see Figure 32 and calculations below) a phenomenon called "fringing", the fact that the flux lines tend to bow out in an air gap thus making the effective area of the gap larger than that of the iron core, should be taken into account. Customarily, this is taken into account by adding the length of the gap to each of the dimensions of the air-gap (fluid-gap in this case) cross section [7, p.675]. However, as illustrated in Figure 31, since the gap consists of a pipe assumed to be made of a magnetic material, the fringing

effect is probably neglectable. The flux lines does not necessarily bow out to the same extent as if the gap between the magnets had been only filled with air. Hence, the cross-sectional fluid area is assumed to be $A_f = d \cdot 2r_t$ with $d$ being the "height" of the fluid gap under the "magnetic influence"(see Figure 25), and $2r_t (= \frac{1}{2} l_f)$ is the diameter of the pipe. In other words, the effective area is assumed to be the same in the fluid gap as in the iron core. Note that this might only work if the pipe is made of a magnetic material, since the magnetic material is a necessity for the magnetic field to bow as in Figure 31. If the material in the pipes had been non-magnetic, it is probable that fringing should have been taken into account.

In order to perform the calculations, the following constants and variables were decided:

- Current: $i = 1A$, unless otherwise stated.
- # windings: $N = 50$, unless otherwise stated.
- Radius of the pipe: $r_t = 0.5mm$ (diameter $1mm$)
- Radius of the electromagnetic coil core: $r_c = 0.5mm$ (diameter $1mm$)
- Magnetic influence length: $d = 1mm$
- Total length of fluid gap: $l_f = 2mm$ (the diameter of two pipes)
- The permeability of the fluid: $\mu_f = 5 \cdot 10^{-6} N/A^2$ (relative permeability $\mu_{fr} \approx 4$), average permeability at $1T$, see Figure 32 and note that $\mu = \frac{B}{H}$.
- Cross-sectional area of fluid gap, with no fringing: $A_f = d * 2r_t = 1 \cdot 10^{-6}$
- Length of flux return path: $l_{ret} = 20mm$
- Permeability of the flux return path: $\mu_{ret} = 5000 \cdot 10^{-6} N/A^2$ (relative permeability $\mu_{retr} \approx 4000$)(iron, [19])
- Cross-sectional area of the flux return path: $A_{ret} = 1mm * 1mm = 1 \cdot 10^{-6} m^2$
- Length of the electromagnetic coil core: $l_c = 5mm$
- Permeability of the electromagnetic coil core: $\mu_c = 5000 \cdot 10^{-6} N/A^2$ (iron, relative permeability $\mu_{cr} \approx 4000$)

- Cross-sectional area of the electromagnet core: $A_c = \pi r_c^2 = \pi \cdot (0.0005m)^2 \approx 7.85 \cdot 10^{-7} m^2$ (assuming cylindrical core)

The diameter of the pipe is made larger than in the previous simulations in order to find "worst-case" parameters. If this list should be incomplete for any reason, please see Appendix F.2 for the matlab script used in the calculations.

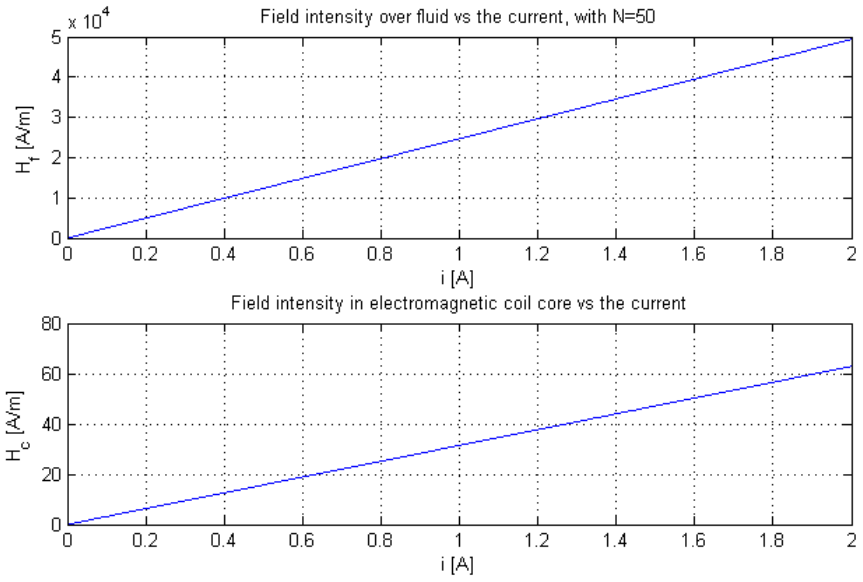


**Figure 33:** Plot of the magnetic field intensity over the fluid, $H_f$, and the field intensity in the electromagnetic coil core, $H_c$, with increasing current in the coil.

The plots in Figure 33 shows how the magnetic field intensity in the fluid gap and in the electromagnetic coil core changes with the current. As the current increases, so does the magnetic field intensity both in the electromagnetic coil core and in the fluid gap. The magnetic saturation of iron is assumed to be about $440 A/m$ (with a permeability of $\mu = 5000 \cdot 10^{-6} N/A^2$ [19] and saturation at $B = 2.2T$ [20], with $B = \mu H$, and assuming that the magnetic properties are linear for the magnetic fields considered). In Figure 33, the saturation limit is not reached. At a current of about $1.6A$, the magnetic field intensity in the fluid is about $40000 A/m$ while the field intensity in the electromagnetic coil core is about $50 A/m$. The hope was to get up to $80000 A/m$ from the electromagnet such that, with a "preload" from a permanent magnet of about $80000 A/m$, it should be possible to get a total

field of about $160000A/m$ at which point the fluid is close to its maximum yield stress (see Appendix D). This will apparently be no problem to reach provided it is possible to further increase the current and/or the number of windings in the coil.

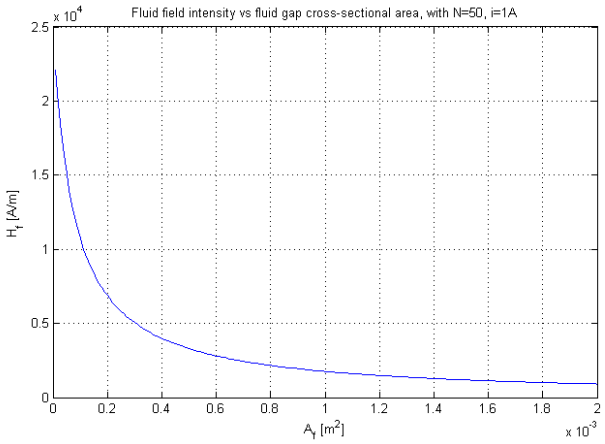


**Figure 34:** Plot of the magnetic field intensity over the fluid, $H_f$, when the cross-sectional area over the fluid gap changes.

Figure 34 shows how the magnetic field intensity over the fluid, $H_f$, chances with the cross-sectional area of the fluid gap, $A_f$. It is obvious that the cross-sectional area should be as small as possible, preferably below $0.2 \cdot 10^{-3} m^2$. Figure 35 is a plot of the magnetic field intensity in the fluid vs. the length of the fluid gap. As in [5], the result is that the fluid gap should be as short as possible in order to get the most field intensity over the fluid.

The magnetic field intensity in the electromagnetic coil core can be adjusted by changing its geometry, such as the length $l_c$ and the cross-sectional area $A_c$, or by changing the material it is made of and hence its permeability $\mu_c$. Figure 36 shows that the magnetic field intensity decreases in both the fluid gap and in the electromagnet core when the length of the core increases, hence the core length should be as small as possible. However, the change is not very large so the length of the core is not that essential to the performance. Next, Figure 37 shows that the field intensity in the core decreases as its cross-sectional area increases, while the magnetic field intensity in the fluid increases. It is clear that the cross-sectional area should be at least above $0.2 \cdot 10^{-6} m^2$, preferably as large as possible but the effect of increasing the cross-sectional area is smaller beyond that point. In Figure 38, the results of changing the permeability of the electromagnetic coil core is

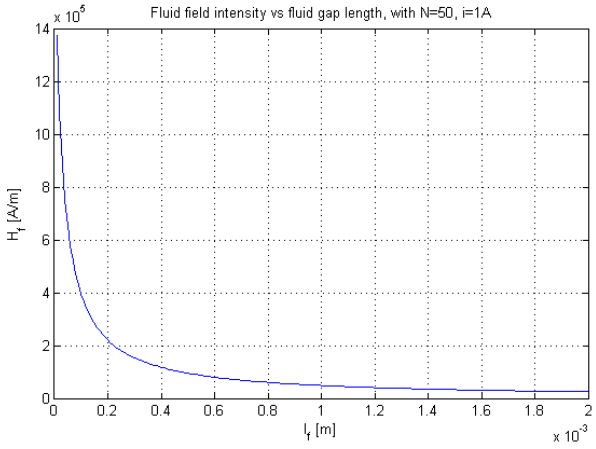


**Figure 35:** Plot of the magnetic field intensity over the fluid, $H_f$, with a changing fluid gap length $l_f$, i.e. with changing pipe diameter. ($\frac{1}{2}l_f = 2r_t$)

shown. The magnetic field intensity in the core decreases when the permeability increases, with the opposite happening in the fluid gap. Obviously, there is little to gain in having a permeability above $0.005N/A^2$, being the permeability of iron [19]. Still, the results show that it is advantageous to have the permeability of the core as large as possible. Note that the simulations were carried out with a constant current at $1A$ and with a constant number of windings in the coil.

When it comes to the flux return path, it is obvious from Figures 40, 41, and 42, that its length should be as short as possible, the cross-sectional area should be as large as possible (but there is little to gain at having the area larger than about $0.5 \cdot 10^{-6}m^2$), and finally that the permeability should be as large as possible (but again – there is little to gain at having the permeability larger than that of iron, i.e. larger than about $0.005N/A^2$). However, the cross-sectional area is limited by the diameter of the actuator, which should be as small as possible. Still, as can be seen in Figure 41, the area of the return path should not be much smaller than $0.2 \cdot 10^{-6}m^2$. Note that Figure 39 shows that the magnetic field intensity in the return path will not exceed the magnetic field intensity in the electromagnetic coil core, so as long as the core does not saturate, the return path will not either. Still, it is important to bear in mind that this might change if the reluctance of the return path is increased by for instance increasing the length or decreasing the cross-sectional area or permeability. Nevertheless, with the geometries used here, the magnetic field intensity in the return path is about $10A/m$

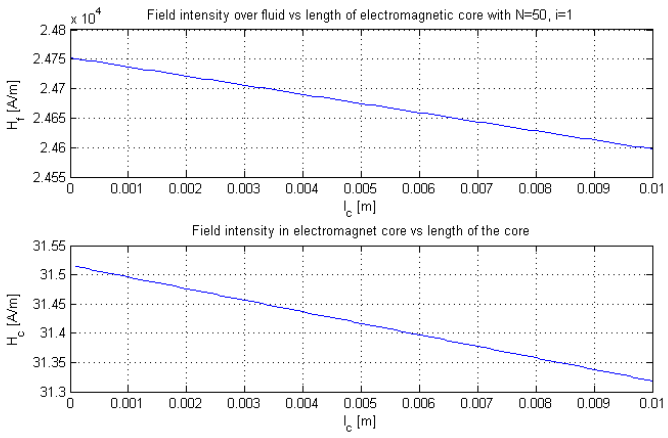


**Figure 36:** Plot of the magnetic field intensity over the fluid, $H_f$, and the field intensity in the electromagnetic coil core $H_c$ with a changing electromagnetic coil core length $l_c$.

below the field intensity in the electromagnetic coil core.

If it is taken into account that the permeability of the permanent magnets is close to that of vaccuum, i.e., $\mu_{pm} \approx \mu_0 = 4\pi \cdot 10^{-7} N/A^2$, and that they have a total length of $1.5mm$, the plot of the magnetic field intensity vs. the current becomes like in Figure 43. The magnets are placed in the flux return path. As can be seen both the magnetic field intensity in the fluid and in the coil core decreases in such a way that either more current or more windings in the coil is needed in order to get the required field intensity in the fluid. However, the magnetic field intensity in the coil core still will be far from the saturation level even if the magnetic field intensities should be 10 times higher, so the result is not too bad. The drawback is that the electromagnet inevitably must have either more windings or more current, making it more bulky since more current means thicker wires and more windings obviously leads to a thicker coil.

Note that these figures must be plotted again if some of the parameters are changed. The plots are made with the assumed parameters in the above list.

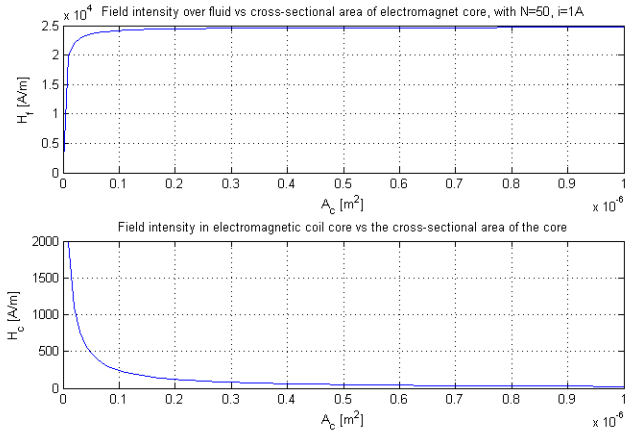


**Figure 37:** Plot of the magnetic field intensity over the fluid, $H_f$, and the field intensity in the electromagnetic coil core $H_c$ with a changing electromagnetic coil core cross-sectional area $A_c$.

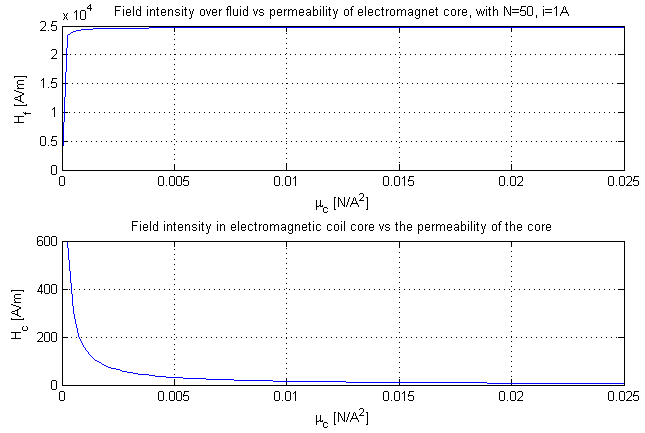


**Figure 38:** Plot of the magnetic field intensity over the fluid, $H_f$, and the field intensity in the electromagnetic coil core $H_c$ with a changing electromagnetic coil core permeability $\mu_c$.

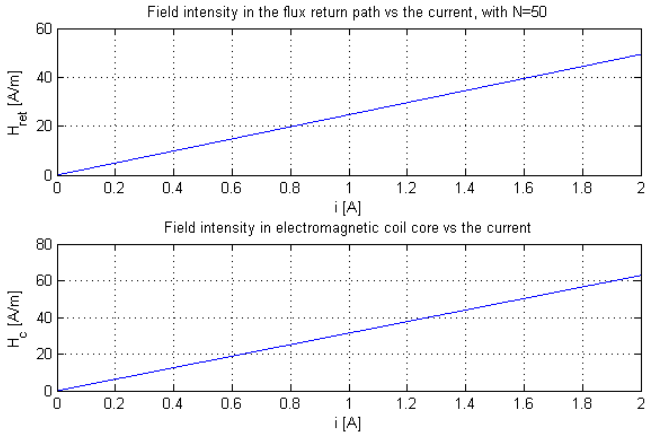


**Figure 39:** Plot of the magnetic field intensity in the flux return path, $H_{ret}$, and the field intensity in the electromagnetic coil core $H_c$ with a changing current.

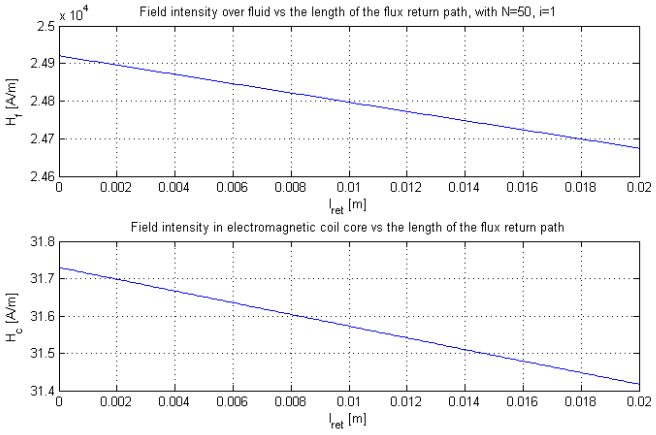


**Figure 40:** Plot of the magnetic field intensity over the fluid, $H_f$, and the field intensity in the electromagnetic coil core $H_c$, with an increasing length of the "flux return path".

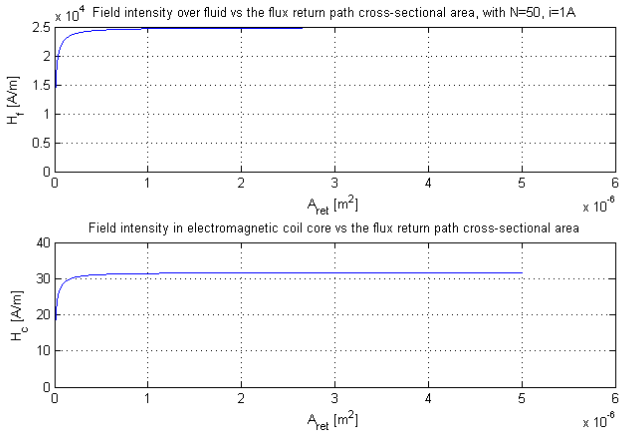


**Figure 41:** Plot of the magnetic field intensity over the fluid, $H_f$, and the field intensity in the electromagnetic coil core $H_c$, with an increasing cross-sectional area of the "flux return path".

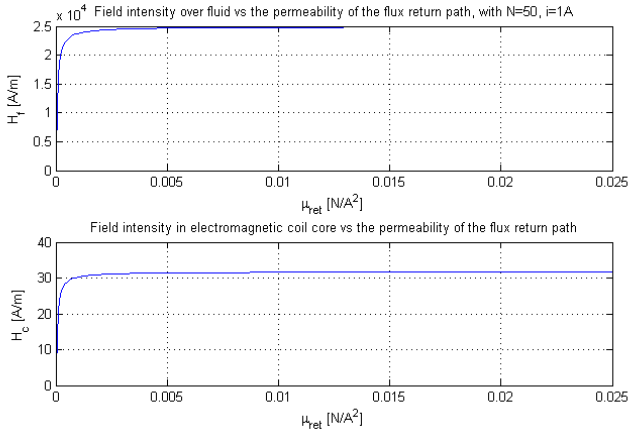


**Figure 42:** Plot of the magnetic field intensity over the fluid, $H_f$, and the field intensity in the electromagnetic coil core $H_c$, with an increasing permeability of the "flux return path".

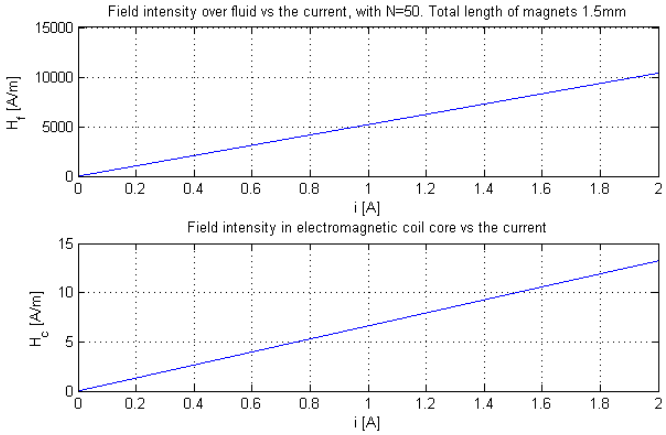


**Figure 43:** Plot of the magnetic field intensity over the fluid, $H_f$, and the field intensity in the electromagnetic coil core $H_c$, with an increasing current in the coil, and with the permeability of the permanent magnets taken into account.

### 4.2.4 Discussion

The cylinder constriction concept was "invented" during the modelling phase, which is the reason why it was not mentioned in the concept development chapter. Judging by the results, the cylinder constriction seems to fit perfectly for the purpose.

The calculations related to the behaviour of the actuator are not too bad. At a 70% constriction, the stiffness is about $0.59N/mm$ while the total movement of the piston is about $2cm$. This is way over the ideal movement of $1cm$, and it should therefore be possible to increase the constriction of the pipe giving a higher stiffness and still reach the required ideal movement. It seems as if the ideal stiffness of $5N/mm$ cannot be reached without going under the ideal movement of $1cm$, but the marginally acceptable stiffness should be within reach even with the ideal movement. The results also show that shorter pipes will lead to a higher stiffness, an example showing a stiffness of up to $2.8N/mm$ for the 70% constriction. This indicates that a higher stiffness can be achieved without reducing the movement (as long as the pipes can be made shorter). Shorter pipes might actually both lead to a larger stiffness *and* to a longer movement, because the constrictions (both the cylinder constriction and the constriction by the magnetic field) would have a greater influence on the pressure drop from the inlet to the outlet. With longer pipes, a larger part of the pressure drop would happen at other places than at the constrictions.

The inlet resistance $R_i$ is not taken into account, and therefore it is not easy to tell how large the effect of "pressure travel" will be, meaning the travel of pressure from one pipe to the other. The way the calculations are done is similar to having a separate inlet pressure for each pipe. Therefore, the calculations might be a bit optimistic. Comsol simulations are therefore probably necessary in order to find the effect of "pressure travel" between the two branches, and to act as a verification as to whether the mathematical model is close to reality or not.

Actually, it could be an idea to drop the leftmost pin. This way, the pressure in the leftmost chamber would have a larger cross-sectional area of the piston to act on, and hence a potentially larger force and stiffness provided the only way the piston can be moved by an external force is by pushing it to the left. However, this would lead to an initial position a bit to the right of the centre, depending on how large the difference in the cross-sectional area of the piston at the left side and at the right side is. This would perhaps also lead to a need for a larger magnetic field at one of the pipes compared to the other in order to get the same movement as before.

Still, this is an idea to have in mind if the stiffness should prove to be too small.

The pressure at the outlet of the nozzles, $p_o$, is assumed constant and equal to the atmospheric pressure. This is not entirely true because there will be some pressure drop from the outlet of the nozzles to the outlet of the actuator. Still, this is thought to have no large effect on the results since this pressure drop would be relatively constant and small compared to the other pressure drops.

The geometry of the pipe is a potential source of error for the calculation of the magnetic field intensities. For instance, the length of the fluid gap has been set to $l_f$, even though this length is valid only for the middle of the pipe. Still, the flux lines are probably not far from this length even at the side of the pipes (see Figure 31). In addition, the permeability of the fluid is much closer to the permeability of air than the permeability of iron (iron has a relative permeability of about 4000 while the fluid has a relative permeability below 20), so the fact that there is some air in the fluid gap might not lead to a very large error.

In addition, fringing has not been taken into account, based on a qualified "guess" that the effect is not prominent when the pipe is magnetic, and hence that the cross-sectional area of the flux lines is nearly the same as in the magnetic material, illustrated in Figure 31. This might lead to a small error.

The magnetic properties of the fluid are assumed linear, with a constant permeability, which probably is the reason why the plot of the magnetic field intensity vs. the current in the coil is linear (Figure 33). The plots will therefore probably not be linear in reality. The permeability was approximated at a magnetic field of $B = 1T$, see Figure 32. Below this particular magnetic field, the permeability is a bit higher. Note that reading the typical magnetic properties graph in Figure 32 is somewhat difficult because the graph seems not to go through the origin ($B = H = 0$), even though it should.

The windings in the coil should have been taken into account when thinking about the size. With as many as 50 windings, they will inevitably have some influence on the size of the coil. In addition, the size of the wires is paramount when increasing the current. A larger current leads to a larger diameter of the wires in order for them to handle the current. This has not been taken into account.

It still is an open question how the magnetic field will behave when having two "magnetic sources" – both a permanent magnet and an electromagnetic coil. Will for instance the magnetic fields get perfectly added or subtracted, or will the magnetic fields influence each other in some other way? And will the magnetic field from the permanent magnet lead to an offset in the elec-

tromagnetic coil core leading to a nonuniform behaviour, meaning a varying behaviour depending on what direction the current in the coil has and hence what the direction of the magnetic field in the electromagnet is. Nevertheless, for now it is assumed that perfect addition and subtraction of magnetic fields is possible.

It seems as if the flux return path will not saturate, as long as its reluctance is kept reasonably small implying a small enough length and large enough cross-sectional area and permeability.

Since the electromagnetic coil should be as short as possible, and with a largest possible cross-sectional area, the best place to fit it must be in between the pipes, as illustrated in Figure 31. It could also of course be possible to place it like in Figure 17 if the result is a larger cross-sectional area without increasing the length too much. Note that the permanent magnets are not taken into account in Figure 31, but the difference is a higher permeability in the flux return path since permanent magnets has a permeability close to free air, leading to a lower field intensity in the fluid gap, and more "power" needed from the coil in order to maintain the same field intensity (Figure 43). There might of course be some effects due to the magnetic field of the permanent magnets perhaps leading to a deflection of the fields, but this has been neglected in the calculations of the magnetic field intensities. This is a potential source of error, and might lead to other results in reality. Nevertheless the coil core is far from being saturated even with the permeability of the permanent magnets taken into account, so it should be possible to reach the required magnetic field intensity provided it is possible to have the required current and number of windings in the coil.

Ideally, the permanent magnets should not be in the same path as the flux return path, due to the fact that their permeability is close to that of free air. But, if they have to be placed in the way of the magnetic flux, they should be as small (short) as possible.

It could actually be an idea to flatten the pipes a bit, like in Figure 17, leading to a shorter fluid gap and a higher field intensity in the fluid. However, at the same time the cross-sectional area becomes larger, which has the opposite effect on the field intensity in the fluid. But this might not be a problem as long as the change of cross-sectional area is less than the change of the fluid gap length (see Figures 34 and 35).

Note that the illustration and calculations of the "magnetic circuit" in Figure 31 might not be entirely correct if the magnets and the coil are placed as in Figure 17. Still, the *qualitative* results are still valid, with the electromagnetic coil core having as large cross-sectional area and small length as possible, the fluid gap being as small as possible etc. The exact shape and size

of the permanent magnets and the electromagnetic coil must be optimized to the geometry of the final prototype.

It might be be a bit obvious, but is included nonetheless: There will also be a trade-off between the diameter of the actuator and the force, since the pressure force will increase with a larger area to act on.

Note that the permeability of the pipe has not been taken into account. It has been assumed that the width of the pipe walls are small enough in order for their reluctance to be negligible.

### 4.2.5 Conclusion

A stiffness of about $0.59N/mm$ is not too bad when the movement is $2cm$. It should be possible to increase the stiffness at the expense of the movement and still reach the ideal movement of $1cm$. The stiffness can also be improved by reducing the length of the pipes. The results might be a bit optimistic due to the simplification of separate inlet pressures, and the diameter of the actuator was set to be $4mm$ (a smaller actuator leads to a smaller movement and stiffness), so it is better not to pop the champagne before more tests are done.

It could be an idea to remove the left pin from the actuator. This can lead to a larger stiffness. Note that the behaviour of the actuator would become a bit different.

When it comes to the magnetic field calculations, it seems as if there will be no problem with magnetic saturation, and hence one of the problems with the concept in [5] has been solved. This also means that the required magnetic field intensity of $H_{el} = 80000A/m$ is well within reach, even if some of the assumptions should prove to be wrong.

To conclude, more simulations are needed, preferably in Comsol, in order to take the inlet flow resistance $R_i$ into account, in such a way that it is possible to see the effect of the "pressure travel" that inevitably will happen between the two pipe branches.

### 4.2.6 Summary

A new constriction in the shape of a cylinder has been "invented", a concept that seems to work rather well. The results from the mathematical model indicates a stiffness of $0.59N/mm$ with a 70% constriction and a movement of about $2cm$ for the same constriction. With a smaller constriction, the stiffness decreases while the movement increases. Shorter pipes leads to a larger stiffness.

There will be no magnetic saturation neither in the electromagnetic coil core nor in the flux return path. The results from the calculations show that the optimal geometries for maximum magnetic field intensity in the fluid are:

- Fluid gap length $l_f$ as short as possible
- Fluid gap cross-sectional area $A_f$ as small as possible
- Electromagnetic coil core as short as possible ($l_c$)
- Electromagnetic coil core cross-sectional area $A_c$ as large as possible
- Electromagnetic coil core permeability $\mu_c$ as high as possible (but higher than the permeability of iron is not necessary)
- Flux return path cross-sectional area $A_{ret}$ as large as possible
- Flux return path as short as possible ($l_{ret}$)
- Flux return path permeability $\mu_{ret}$ as large as possible (but higher than the permeability of iron is not necessary)

## 4.3 Simulation in Comsol

### 4.3.1 Introduction

Comsol is a finite element multiphysics simulation environment suitable for simulating complex physical behaviour. When the geometry is drawn and the initial conditions and perhaps some equations are specified, the rest of the modelling and calculation is left to Comsol.

This section show the results from simulating the actuator in Comsol. Appendix C consists of some screenshots from the simulations.

### 4.3.2 Nozzle constriction simulation

The purpose of the constriction is to act as both a feedback mechanism and to provide the stiffness of the actuator. If the piston is pushed by an external force, for instance a finger, the constriction of the pipes should lead to a considerable counter force in such a way that the actuator feels stiff.

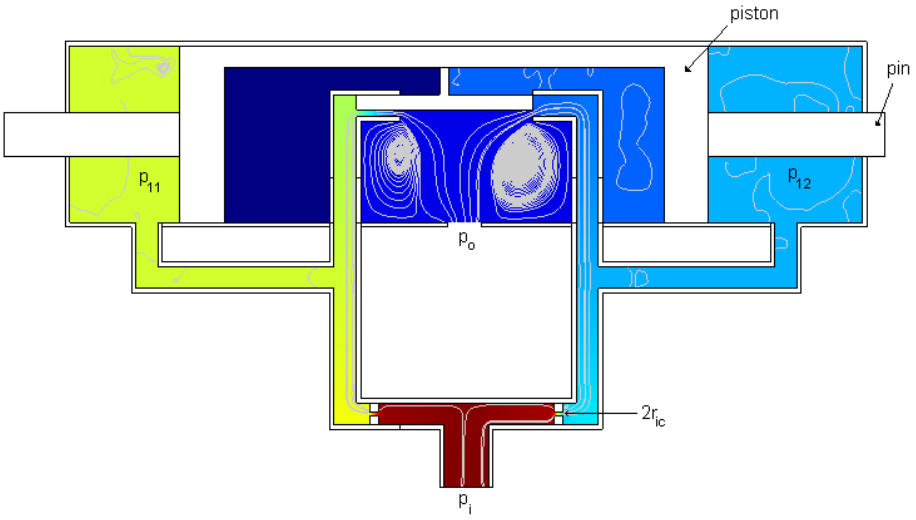


**Figure 44:** Screenshot from the Comsol constriction simulations (from Appendix C). The colour shows the pressure distribution, while the streamlines show the velocity field of the fluid.

Following the mathematical model above, it will be useful to find the effect of the "pressure travel" between the two pipe branches since this could not be calculated with the above assumptions. The constriction tests are carried out in two dimensions without any influence of a magnetic field, and

done in a step-by-step manner, moving the piston slightly for each simulation. As in the mathematical model calculations above, the constriction simulations are carried out with shorter pipes than the dynamic simulations later, in order to see the effect of the length of the pipes. For all the following simulations, some geometry parameters are fixed:

- Pipe diameter $2r_t = 0.5mm$.
- Piston diameter $4mm$
- Pin diameter $1mm$
- Piston "effective area": $A_p = \pi \cdot (0.002m)^2 - \pi \cdot (0.0005m)^2 \approx 1.18 \cdot 10^{-5} m^2$ (the area of the piston minus the area of the pin).
- Inlet constriction internal diameter: $2r_{ic} = 0.1mm$, unless otherwise stated.
- Inlet pressure $P_i = 10 \cdot 10^{-5}$, unless otherwise stated.

with the other parameters close to those in the mathematical model calculations above. For other parameters, though somewhat difficult to read, please see Figure 60 in Appendix C. The piston "effective area" is the area of the piston minus the area of the pin, and is used to calculate the forces acting on the piston due to the pressure difference in the leftmost and the rightmost chamber.

This is what was tested:

- Different diameters of the constrictions at the inlet ($2r_{ic}$): $0.1mm$, $0.2mm$ and no constriction ($0.5mm$).
- Different inlet pressures $p_i$: $10 \cdot 10^5 Pa$, $20 \cdot 10^5 Pa$, and $30 \cdot 10^5 Pa$.
- Different cylinder constriction diameters ($2r_{cyl}$): $0.15mm$, $0.25mm$, and $0.35mm$.

The diameter of the constriction at the inlet ($2r_{ic}$) is the diameter of the "pipe" the fluid is flowing through (see Figure 25), kept at $0.1mm$ when other tests are performed.

The "equilibrium state" of the actuator without any magnetic field is when the piston is centred, i.e., when the cylinder constrictions are equally long into the pipes. If the displacement from "equilibrium" is $0.5mm$ with a pipe diameter of $2r_t = 0.5mm$ and a cylinder constriction diameter of $2r_{cyl} = 0.35mm$ (70% constriction), the simulation shows a difference in

| $\Delta x$: | 0.1mm | 0.2mm | 0.3mm | 0.4mm | 0.5mm |
|---|---|---|---|---|---|
| $2r_{cyl} = 0.15mm$ *(30%)* | $0.059N$ | $0.130N$ | $0.201N$ | $0.283N$ | $0.330N$ |
| $2r_{cyl} = 0.25mm$ *(50%)* | $0.224N$ | $0.448N$ | $0.673N$ | $0.897N$ | $1.097N$ |
| $2r_{cyl} = 0.35mm$ *(70%)* | $0.625N$ | n.a. | $1.864N$ | n.a. | $3.304N$ |

**Table 1:** Constriction force table with area $A_p = 1.18 \cdot 10^{-5}m^2$ used to calculate the force. The diameter of the pipe is $0.5mm$, and the percentage stands for how much the pipe is constricted relative to its diameter. n.a. = not available.

pressure of $\Delta p = p_{11} - p_{12} = 2.80 \cdot 10^5 Pa$, which means, with a cross-sectional area of the piston $A_p = 1.18 \cdot 10^{-5}m^2$, the force acting on the pin is $F_p = 2.80 \cdot 10^5 Pa * 1.18 \cdot 10^{-5}m^2 \approx 3.30N$, which indicates a *stiffness* of $6.6N/mm$, over the double of the results from the mathematical model above ($2.8N/mm$ with short pipes). Forces at other constriction diameters are shown in Table 1. It is easily seen that the stiffness is increased by increasing the constriction. A larger piston area leads to a larger force. Notice that, as opposed to before, the pressure $p_{11}$ is now the pressure in the leftmost chamber while the pressure $p_{12}$ is in the rightmost chamber since the left pipe now is connected to the left chamber and vice versa. This is a result of having the nozzles pointing inwards as opposed to the outwards pointing nozzles before, in the modelling chapter. However, the force is still defined as positive when acting in the positive x-direction which means that the pressure difference is defined the same way as before – the difference between the pressure in the leftmost and the rightmost chamber. The reason why the nozzles point inwards is the fact that the simulations in Comsol are two-dimensional – crossing pipes does not work well in two dimensions. Still, there should not be a huge difference compared to the previous calculations as long as the pipes has approximately the same length.

Figure 45 shows the test results from the simulations; how the pressure difference between the leftmost and the rightmost chamber, $\Delta P$, changes with the displacement of the piston from equilibrium, $\Delta x$. It is quite clear that the constrictions at the inlet do decrease the influence of the "pressure travel" as the pressure difference between the two branches increases with an increasing inlet constriction. This is shown in the upper plot of the figure. Hence the constrictions at the branching of the pipes should be as small as possible, however not to the extent that the flow stops of course. The other results are quite obvious – the pressure difference $\Delta P$ increases with increasing inlet pressure, and with increasing constriction diameter. It seems as if the effect of increasing the constriction diameter is larger the closer to

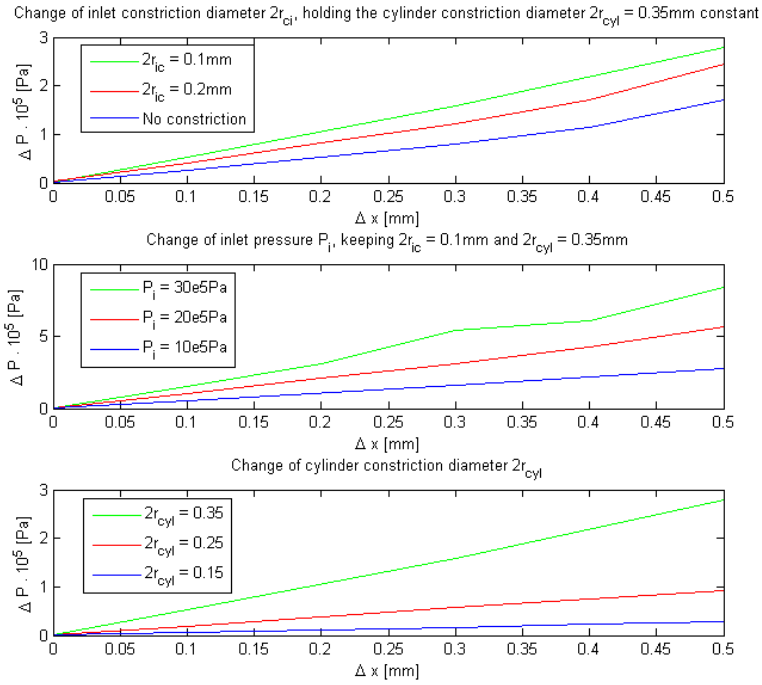


**Figure 45:** Figure visualizing the results from the constriction-simulations performed in Comsol. $\Delta x$ is the displacement from equilibrium.

the pipe diameter it gets. This might have something to do with the fact that the radius is to the power of 4 in Poiseuille's law (see Section 4.2.2).

### 4.3.3 Magnetic field change simulation

When simulating the magnetorheological fluid with an applied magnetic field, the Bingham model is used (see Section 1.1). The implementation of the Bingham-model is done using the "Chemical-Engineering Module" in Comsol, as in [11]. The Bingham model is

$$\tau = \tau_y + \eta_0 \dot{\gamma} \tag{13}$$

where $\tau$ is the shear stress, $\tau_y$ is the yield stress at a certain magnetic field intensity ($\tau_y = \tau_y(H)$), $\eta_0$ is the dynamic viscosity (at zero field) and $\dot{\gamma}$ is the shear rate. In order to use this equation in Comsol, which requires a *viscosity* model, the equation must be rearranged to give the "apparent viscosity" $\eta_{ap}$.

As in [1, p.991], this is easily done:

$$\eta_{ap} = \frac{\tau}{\dot{\gamma}} = \frac{\tau_y}{\dot{\gamma}} + \eta_0 \tag{14}$$

where $\tau_y$ is determined by the magnetic field intensity $H$(see Figure 46), $\dot{\gamma}$ is a built-in variable in the "Chemical Engineering Module", and $\eta_0$ is a property of the fluid ($\approx 0.28 Pa \cdot s$ for the MRF-140CG fluid, see Appendix D). In the simulations, the linear approximation of $\tau_y$ that was used in [5] is used, i.e., $\tau_y = k_\tau H$ with $k_\tau = 0.3$ (see Figure 46).

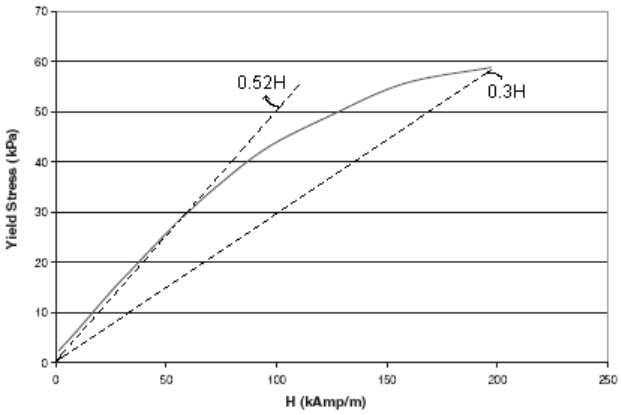


**Figure 46:** Yield strength vs. magnetic field intensity for the MRF-140CG fluid, with some linear approximations shown dotted. Taken from the technical data sheet in Appendix D.

The original idea was to have one permanent magnet at each side of the pipes, and an electromagnetic coil in between the two pipes. The permanent magnets should be responsible for establishing an initial magnetic field in the fluid, and the coil should then be responsible for strengthening or weakening these fields (addition and subtraction of the field depending on what side of the coil each pole were; addition with north pole vs. south pole, and subtraction with south vs. south). The coil, however, had to be simulated as a permanent magnet with an assumed magnetic field, since an extra module (that cost money), the AC/DC- module, is needed in order to simulate the electromagnetic coil with wires and currents. At first sight the concept seemed to work, as the magnetic field was weakened at one side and strengthened at the other side. However, as the magnetization in the permanent magnets was changed, the results became somewhat inconclusive. It

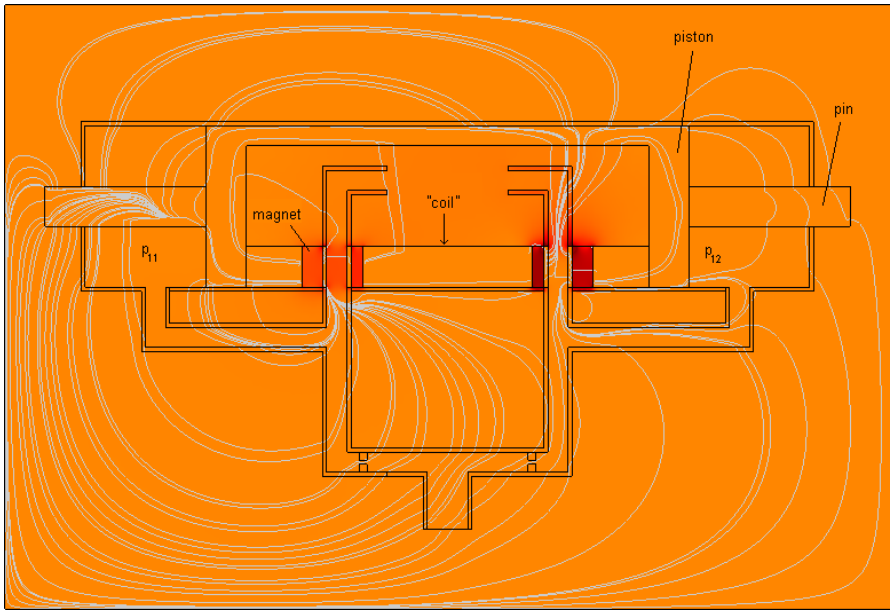


**Figure 47:** Screenshot from the Comsol simulation with *simulated* magnetic field (from Appendix C). Left pipe: North pole vs. south pole. Right pipe: North pole vs. north pole. The colours visualize the norm of the magnetic field intensity H, while the streamlines symbolize the magnetic field lines.

seemed as if the field, at the side it should be weakened, got deflected to other parts of the fluid, thereby creating more field altogether at that side than at the other, and hence resulting in a totally opposite behaviour. Figure 47 shows a screenshot of one of the simulations, with equal magnetization in the permanent magnets and in the coil (simulated as two permanent magnets with the same direction of the magnetic field). In the pipe at the left-hand side, the poles are north vs. south, and the magnetic field intensities are "added" to about $70000 A/m$, with the field rapidly decreasing above and below where the magnets are situated. In the pipe at the right-hand side, the poles are north vs. north, and the fields seems to be subtracted; in between the magnets, the magnetic field intensity is about $100 A/m$, increasing up to about $6000 A/m$ close to the magnets. However, directly *above* this area, and presumably where the magnetic field is deflected, the magnetic field intensity is as high as about $80000 A/m$, most of the field *tangential* to the flow direction (in the y-direction). This field is highly probable to have an influence on the magnetorheological fluid, but it is unknown how large effect

this will have on the performance. Therefore the addition and subtraction of fields should be tested in (real) experiments. Bear in mind that these simulations are carried out in *two* dimensions, and it is therefore a bit difficult to model for instance the flux return path and other geometrical properties that might have an influence on the magnetic field. This might be the reason to the somewhat inconclusive results.

It was then decided to specify certain areas in the pipes, and *assume* the magnetic field intensities there in order to find the ideal performance of the actuator. The magnetic field intensity set up by the permanent magnets should be $H_{pm} = 80000A/m$ and equal at both pipes, as in the previous section with the mathematical model. The magnetic field intensity originating from the electromagnetic coil, $H_{el}$, should be responsible for increasing the field intensity over the left pipe and decreasing the field intensity over the right pipe (which means its north pole should be to the left and its south pole to the right, if the permanent magnets has south poles next to the pipes). Assuming that magnetic fields can be perfectly added and subtracted, the magnetic field intensity over the left pipe is $H_1 = H_{pm} + H_{el}$, while the magnetic field intensity over the right pipe is $H_2 = H_{pm} - H_{el}$. This assumption was made in order to simulate the influence of the magnetic fields under ideal conditions, to find out whether the concept is viable. If the tests then turn out to be negative, there is no doubt that the concept will not work "in the real world".

### 4.3.4 Dynamic simulation

In the following simulations, longer pipes was used in order to see the difference from the previous calculations with shorter pipes (compare Figure 60 and Figure 62 in Appendix C to see the difference in the pipe lengths).

Figure 48 show the displacement $\Delta x$ from the centre position of the piston for a given magnetic field intensity originating from the electromagnetic coil. The simulations in Comsol were conducted, as already mentioned, by assuming perfect addition and subtraction of the magnetic fields, i.e. $H_1 = H_{pm} + H_{el}$ and $H_2 = H_{pm} - H_{el}$ with $H_{pm} = 80000A/m$. At the particular magnetic field intensity from the electromagnetic coil, the constriction was moved until equilibrium was reached, i.e., until $\Delta P = 0$ (the pressure in the leftmost and the rightmost chamber was equal). The behaviour seems to be linear, with expressions:

- $\underline{2r_{cyl} = 0.15mm}$: $\Delta x = 9 \cdot 10^{-8} \cdot H_{el}$ [m]
- $\underline{2r_{cyl} = 0.25mm}$: $\Delta x = 3 \cdot 10^{-8} \cdot H_{el}$ [m]

- $2r_{cyl} = 0.35mm$: $\Delta x = 1 \cdot 10^{-8} \cdot H_{el}$ [m]

giving the displacement $\Delta x$ from the centre position of the piston. When there is no current in the electromagnetic coil, the magnetic field from the coil is zero, i.e., $H_{el} = 0$. Then, the only "magnetic contribution" is from the permanent magnets, $H_{pm}$, and this contribution is equal at both pipes. Hence, the displacement when $H_{el} = 0$ is $\Delta x = 0$. Since $H_{el}$ can be both negative and positive, the total displacement is twice the maximum movement in one direction. Also see Figure 48, where the displacement to *one* side is plotted – the piston can be moved an equal distance to the other side, so the total displacement is twice the displacement in the figure. The following list shows the maximum movement for the different constriction diameters, calculated from a maximum total field of $H_{tot} = 160000A/m$, i.e., $H_{elmax} = 80000A/m$ and $H_{pm} = 80000A/m$:

- $2r_{cyl} = 0.15mm$: $\Delta x_{max} = 9 \cdot 10^{-8} \cdot H_{elmax} \cdot 2 = 14.4mm$
- $2r_{cyl} = 0.25mm$: $\Delta x_{max} = 3 \cdot 10^{-8} \cdot H_{elmax} \cdot 2 = 4.8mm$
- $2r_{cyl} = 0.35mm$: $\Delta x_{max} = 1 \cdot 10^{-8} \cdot H_{elmax} \cdot 2 = 1.6mm$

It is easily seen that there is a trade-off between the stiffness (nozzle constriction) and the maximum length of movement $\Delta x_{max}$, since the movement will decrease as the constriction increases. Notice that $\Delta x_{max}$ is not the maximum displacement to one side, but the *total* maximum movement.

Figure 49 visualizes the results from the various simulations with both assumed magnetic fields and given displacements of the piston from the centre position, $\Delta x$. When $\Delta P = 0$, equilibrium is reached and the piston will stay there. The simulations were conducted at a maximum difference in magnetic field intensity between the two pipes; $H_1 = 160000A/m$ at the left pipe and $H_2 = 0$ at the right pipe. This was done in order to find how the pressure difference changes with changing properties such as the cylinder constriction diameter $2r_{cyl}$ and the inlet pressure $p_i$, and to get a grip at how large forces the actuator will produce if the piston should be displaced from "equilibrium" ($\Delta P = 0$). A positive $\Delta P$ means a higher pressure in the leftmost chamber than in the rightmost chamber, and hence a force "trying to push" the piston towards the right. It can be seen that a larger constriction diameter gives higher forces, but at the expence of the movement: The farther from $\Delta x = 0$ the line crosses $\Delta P = 0$, the larger the movement is. This is exactly what was found above; there is undoubtedly a trade-off between the movement of the piston and the stiffness of the actuator. The stiffness can be

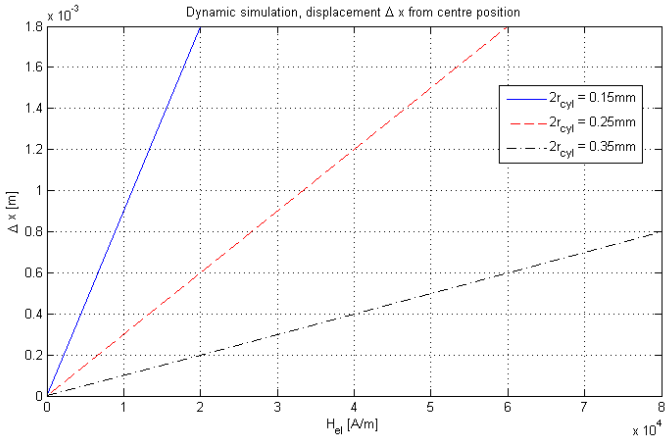


**Figure 48:** Figure visualizing the results from the "dynamic" simulations performed in Comsol. $\Delta P = 0$, $H_{pm} = 80000A/m$, $p_i = 10 \cdot 10^5$. $\Delta x$ is the displacement from the centre position of the piston.

found from Figure 49 by finding the difference in $\Delta P$ over $1mm$ displacement and assuming the same area $A_p = 1.18 \cdot 10^{-5} m^2$ as before. At the lowest inlet pressure ($p_i = 10 \cdot 10^5 Pa$, the upper plot), the stiffnesses are found to be:

- $2r_{cyl} = 0.15mm$: $\approx 0.47N/mm$
- $2r_{cyl} = 0.25mm$: $\approx 1.18N/mm$
- $2r_{cyl} = 0.35mm$: $\approx 1.77N/mm$

which is considerably smaller than the results in the previous section. This shows the importance of having the pipes as short as possible, and hence supports the results found from the mathematical models.

Notice that, as in the mathematical model calculations above, the displacement *decreases* as the inlet pressure increases (the crossing of the line at $\Delta p = 0$ happens at a lower $\Delta x$), and shows that there will be a trade-off also between the force from the actuator and the movement of the piston. This might be due to the fact that the stiffness increases when the inlet pressure increases, see Figure 45.

The interested reader can see Figure 62 in Appendix C for an illustration of how the dynamic simulations from Figure 48 were carried out. The figure shows the piston at equilibrium, when the effect originating from the magnetic field is balanced by the effect from the constriction. The simulations were performed in a "step-by-step" manner, setting up the magnetic fields

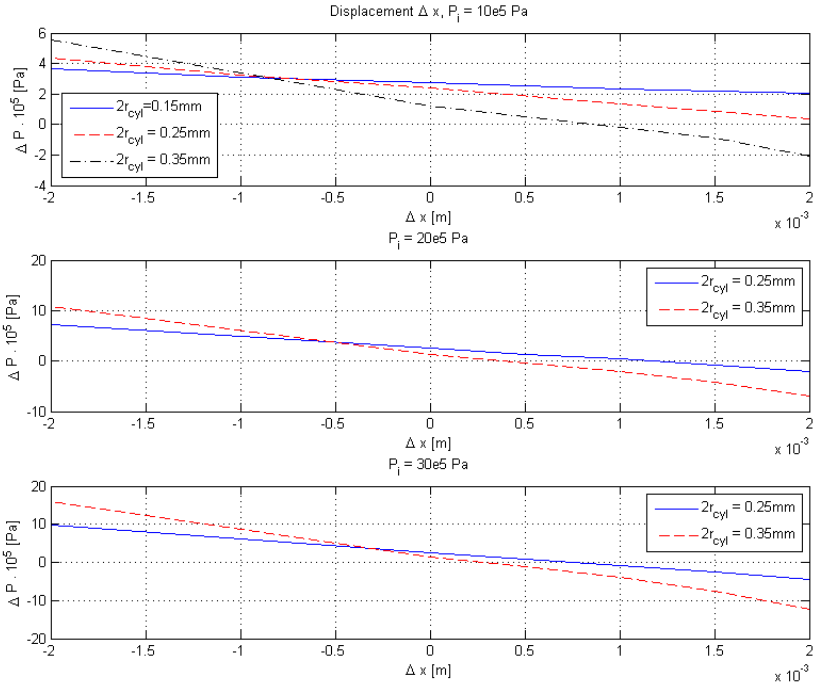


**Figure 49:** Figure visualizing the results from the "dynamic" simulations performed in Comsol. Equilibrium is reached at $\Delta P = 0$. The displacement $\Delta x$ is the distance from the centre position of the piston. The magnetic field intensities are constant, $H_1 = 160000 A/m$ at the left pipe and $H_2 = 0$ at the right pipe.

over the pipes first, and then moving the constriction until the pressure was equal in the leftmost and rightmost chamber.

### 4.3.5 3D simulations

A 3D-model was created, but due to a lack of experience combined with numerous errors and an extremely slow computer, there was not enough time in order to complete the simulations. The preliminary Comsol model can be seen in Appendix C.

### 4.3.6 Discussion

The results from the constriction tests indicate that it is possible to achieve a stiffness of about $1.77N/mm$ for a cylinder constriction with a diameter $0.35mm$, but with a maximum movement of only $1.6mm$, which is rather poor. At 50% constriction ($2r_{cyl} = 0.25mm$), the stiffness is about $1.18N/mm$ and the movement is $4.8mm$, which is not too bad but not extremely good either. With an even smaller constriction, $2r_{cyl} = 0.15mm$, the maximum displacement is actually very good with $14.4mm$, but the stiffness is not that good, approximately $0.47N/mm$. Hence it is easy to see that the movement of the piston comes at the expense of the stiffness of the actuator. In addition, the results show that an increase in the inlet pressure also involves this kind of trade-off: increasing the inlet pressure leads to an increase in the pressure difference and hence a higher force but *decreases* the maximum movement. Hence it is not possible to increase the maximum movement of the piston by increasing the inlet pressure. It seems from the simulations that the marginally acceptable values (stiffness of $1N/mm$ and movement of $5mm$) can be just about reached with a constriction diameter of about $0.25mm$, but the ideal values might seem out of reach. However, it might be possible to increase the stiffness by reducing the length of the pipes. The simulations with shorter pipes indicated a stiffness of up to $6.6N/mm$ for the $0.35mm$ constriction, about four times as high as the other results. In addition, the piston diameter was assumed to be $4mm$. This could be slightly increased in order to get higher forces.

One problem with the Comsol simulations is that the electromagnetic coil had to be simulated as a permanent magnet. When simulating a permanent magnet in Comsol, the magnetization is defined in a certain area. It is not for sure whether this also implies that the area is treated as having a permeability close to zero as in "normal" permanent magnets, but it seems as if this is the case. Therefore, a small area at each side of the coil core was set to be magnetized in such a way that the permeability should have little impact. Inevitably, the low permeability would have had an impact on the magnetic field, since ideally the coil core should have a large permeability. The electromagnetic coil should preferably have been simulated with a current-carrying coil around the core, but due to the fact that the necessary Comsol module (AC/DC) was not installed, this could not be done. In order to get away from those problems, the magnetic field was *assumed* to have a certain magnitude.

As already mentioned, the simulations were conducted in two dimensions and with an assumed field. These facts implies that there might be inaccu-

racies, especially since the magnetic field never is constant over the whole region, it will change relative to the distance from the magnets. In addition, some field will lie above and below the defined region, due to "fringing". It is also possible that, as mentioned above, opposite fields (e.g. south pole vs. south pole) might not get subtracted, but rather be deflected and still have an influence on the fluid. In addition, simulations in two dimensions does not allow for the fact that the pipe is – well – a pipe, and that the magnetic field might "behave" differently with a (round) pipe in between the magnets. There is also the problem of creating a proper "flux return path" in two dimensions (problems with getting enough room). Anyway, in order to simulate the full effect of the magnetic field and the path of the magnetic field, simulations in *three* dimensions should ideally have been performed. Real tests should also be performed in order to find the result of field subtraction.

Comsol was not quite happy about the sudden leap in viscosity model that happened in the fluid with the assumed magnetic field at a certain region. The ideal method would have been to *simulate* the magnetic field, and have the same viscosity model over the whole area. In this case, the viscosity model changed instantaneously from having no field to having the assumed field at a certain part of the pipe. However, due to the problems with simulating the magnetic fields, this was the best solution.

The comsol 2D simulations were carried out with the nozzles pointing inwards. This is due to the fact that Comsol does not deal very well with crossing pipes in two dimensions (but then – who does?). However, it is thought to be no large difference between the inwards pointing nozzles and the outwards pointing nozzles when it comes to the results, the only difference being the total length of the pipes. This actually means that it should be possible to reduce the length of the pipes and hence achieve a greater stiffness.

It seems from the few simulations conducted with permanent magnets that the magnetic field subtraction might not work as well as assumed. The fields might only get deflected, not decreased. Still, it is difficult to know how much influence magnetic fields tangential to the flow direction has on the fluid. The literature states that the best effect is achieved by having the magnetic field *perpendicular* to the flow, but says little or nothing about how large the effect is with the field tangential to the flow direction. However, it is logical that the chains of magnetic particles that are formed along the magnetic field will slow the flow down. Real tests should be performed in order to find out how large this effect really is. A 3D model of the actuator was made (see Appendix C), but due to an exceptionally slow computer (or perhaps a "heavy" application), a lack of experience in Comsol and heaps of

error messages, there was no time to complete it. Still, due to the lack of the AC/DC module, a full-scale test with magnetic fields could not have been made anyway. This could be appropriate for future work.

### 4.3.7 Conclusion

The forces and movements calculated from the simulations indicate that this might work. The marginally acceptable specifications are just about within reach. There will obviously be a trade-off between the movement of the piston and the stiffness of the actuator. According to the results from the simulations, a movement of above $5mm$ can be achieved with a constriction of $2r_{cyl} < 0.25mm$, but then the stiffness would be below $1.18N/mm$. The constriction diameter can be chosen based on a desire to have either a long movement or a large stiffness. The pipes should be as short as possible in order to get the largest possible stiffness.

It still is an open question whether field subtraction really works, but the results from the simulations gives a rather discouraging impression. It will most probably not work as well as wanted, but the effect might still be present in some way. Real tests should give a better indication as to how large the effect of field subtraction really is.

### 4.3.8 Summary

The simulations in Comsol shows that the stiffness increases with the cylinder constriction diameter $2r_{cyl}$:

- $\underline{2r_{cyl} = 0.15mm(30\%)}$: $\approx 0.47N/mm$
- $\underline{2r_{cyl} = 0.25mm(50\%)}$: $\approx 1.18N/mm$
- $\underline{2r_{cyl} = 0.35mm(70\%)}$: $\approx 1.77N/mm$

These forces will increase with increasing inlet constriction and increasing inlet pressure.

The dynamic simulations indicate that the total movement of the piston/pin decreases with an increasing cylinder constriction diameter:

- $\underline{2r_{cyl} = 0.15mm(30\%)}$: $\approx 14.4mm$ movement
- $\underline{2r_{cyl} = 0.25mm(50\%)}$: $\approx 4.8mm$ movement
- $\underline{2r_{cyl} = 0.35mm(70\%)}$: $\approx 1.6mm$ movement

The movement will decrease with an increasing inlet pressure.

## 4.4 Real Tests

### 4.4.1 Introduction

Due to the inevitable question of time (and other existential questions), it was not possible to build a full-scale prototype. Rather it was decided to build a test rig in order to test some of the elements of uncertainty in the simulations, like the interaction of the magnetic field with the fluid and the magnetic field subtraction. The tests will also indicate how good the mathematical model is.

The fluid that will be used is the MRF-140CG with technical data sheet in Appendix D.

### 4.4.2 Description of the tests

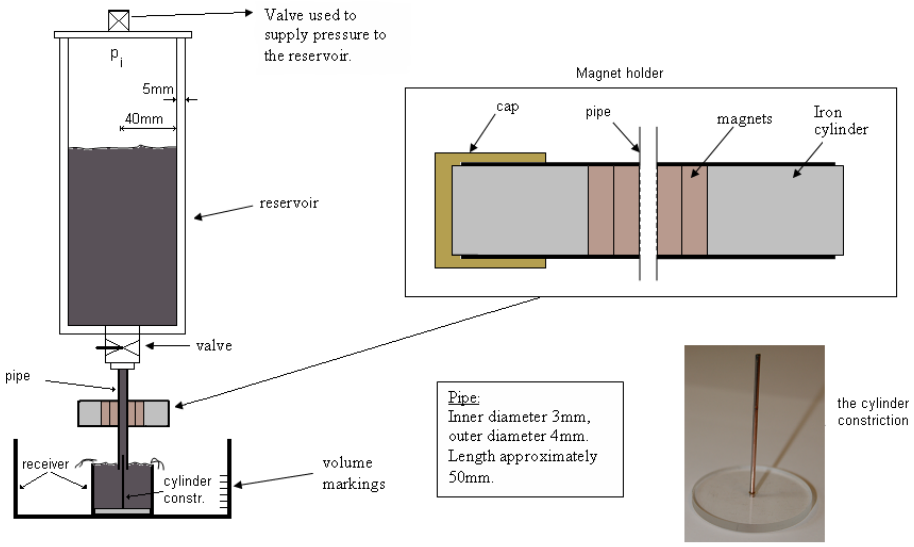


**Figure 50:** Sketch of the whole test rig and a picture of the cylinder constriction.

The test rig consists of a reservoir that can be pressurized using compressed air, the outlet has a valve for starting and stopping the flow, and a pipe mounted on the valve. The pipe has a relatively small diameter in order to simulate the small dimensions that are to be used in the actuator. A magnet holder is used to keep the magnets close to the pipe and at the

same place during the experiments. Finally there is a receiver for collecting the fluid, and a constriction to constrict the pipe.

The reservoir is made of plexiglass and is in the shape of a cylinder. The top is detachable in order to make it possible to refill the fluid. The lid is secured with four screws and sealed with an o-ring. The screws were added to make sure the lid would hold at $5kg/cm^2$ pressure, the equivalent of $250kg$ on the lid (radius $40mm$ gives an area of $\pi r^2 \approx 50.3cm^2$ which consequently leads to $250kg$ pressure). On top of the lid a connector is mounted such that it is possible to mount a tube from a pressure regulator supplying compressed air (the inlet pressure). The maximum pressure of $5kg/cm^2$ is chosen because that is close to the maximum pressure that can be supplied by the pressure regulator.

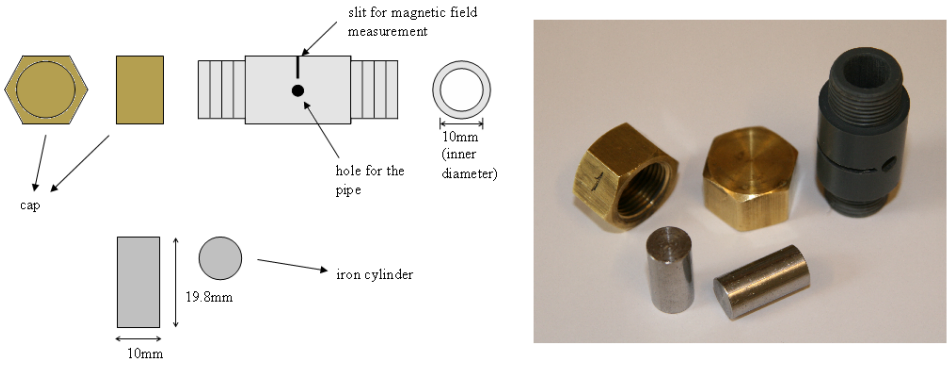


**Figure 51:** Sketch and picture of the magnet holder.

The magnet holder is designed to hold the magnets at certain distances from the pipe and to make it possible to place magnets with equal facing poles at the pipe, i.e. south pole vs. south pole or north pole vs. north pole. Due to forces making it extremely difficult to hold the magnets at a constant distance from each other and making it even more difficult to find the point where the field is completely "zeroed", the need for a magnet holder is rather obvious. Since the magnets acquired to supply the magnetic field are circular (10 magnets with diameter $10mm$ and thickness $2.4mm$), a cylindre-shaped magnet holder seemed to be the best. With an interior diameter of $10mm$, the magnets will fit perfectly. In order to force the magnets towards each other in the event of opposite magnetic poles (south – south or north – north), a cap can be used to screw the magnets towards each other. Two solid iron cylinders with diameter $10mm$ and length $20mm$ were produced such that these can push the magnets all the way in. The reason for the cylinders being

made of iron is to increase the magnetic field, see Section 4.4.3. The magnets that are used are standard neodymium magnets bought at Clas Ohlson.

The receiver consists of two "cylindrical" containers, one placed inside the other, see Figure 52. The end of the pipe will be placed inside the inner "cylinder", see Figure 50, in order to keep the pressure at the outlet of the pipe constant by having a constant volume of fluid over it. What will happen when the fluid starts flowing is that the first and smallest receiver will be filled before the fluid pours over the edge. The stop watch is not started until this happens. The outer volume of the container will then be filled at a certain flow rate measured by measuring the time it takes for the fluid to fill this "outer receiver". The area of the "outer receiver" was calculated to be $A = \pi(0.0695m)^2 - \pi(0.035m)^2 \approx 0.011326m^2$, see Figure 52. Volume marks were drawn on the outside of the receiver in order to make it possible to measure the flow rate. Watching the fluid filling the container, the time should be measured at different volume marks to make sure the measured flow rate is as correct as possible.

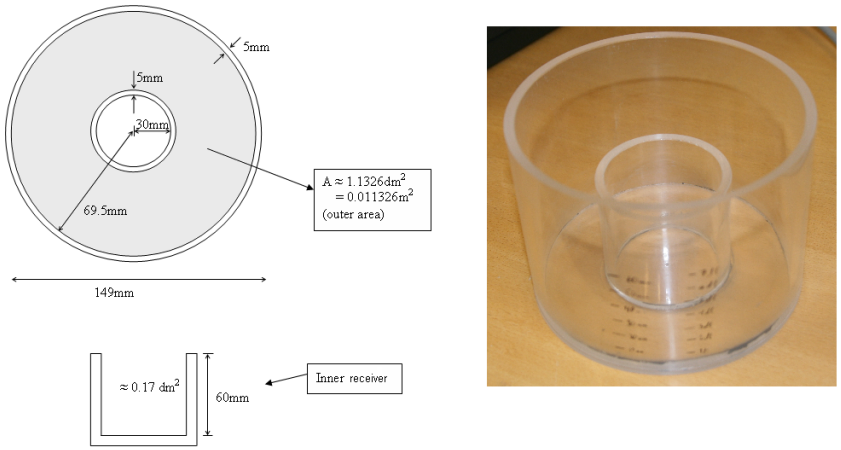


**Figure 52:** Sketch and picture of the receiver.

To supply the inlet pressure, a pressure regulator is connected to the reservoir. This pressure regulator keep a constant pressure in the reservoir. The pressure comes in addition to the atmospheric pressure, so the pressure measured by the pressure regulator is in reality the pressure difference between the inlet and the outlet, $\Delta p$, since the outlet is close to open air with only a small amount of fluid above it. The pressure contribution from the fluid due to the change of volume and height of the fluid in the reservoir,

$p_f = \rho g h$, is neglected due to its small contribution compared to the supply pressure. Say, for instance, that the inlet pressure is $0.5 kg/cm^2$, which corresponds to $47533 Pa$ (see the Nomenclature). With one litre of fluid in the reservoir, the height will be about $20cm = 0.2m$. Then, with $\rho = 3600 kg/m^3$ and $g = 9.81 m/s^2$, the pressure is $p_f = 7063 Pa$, 14% of the inlet pressure. None of the tests were conducted with one litre fluid, mostly the "starting volume" was around $6dl$, and most of the tests were conducted at higher inlet pressures. Therefore, it is safe to say that the pressure originating from the weight of the fluid can be neglected.

To constrict the pipe, solid cylindrical welding rods mounted on a piece of plexiglass is used. The reason why welding rods are used is that they have perfect diameters, $1.1mm$ and $1.9mm$. In order to test at different constriction lengths, the tests will first be conducted with the welding rod a certain length into the pipe before a bit is cut off and another test is done.

The idea is to use the flow rate to measure the influence from the magnetic field and the constrictions, and relate this to the mathematical models.

For more pictures of the test rig, please see Appendix E.

### 4.4.3 Magnetic field tests

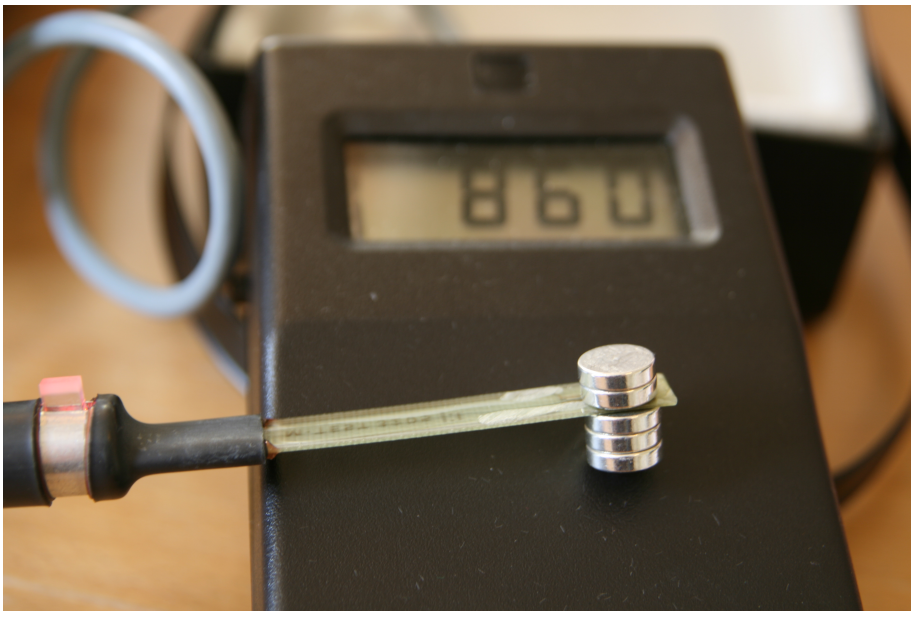

**Figure 53:** How the magnetic field addition and subtraction tests were performed using the teslameter and the permanent magnets.

To see how well the magnetic fields can be added or subtracted, some tests were conducted with the neodymium magnets. First, the field was measured at each magnet, before they were placed at each side of the measuring probe (the Teslameter in Appendix A), see Figure 53. The placement was no problem when the magnets were attracted by each other, i.e., with north pole against south pole. They would then slam together on each side of the sensor, and stay there as shown in the figure. However, the measurement was a bit more tricky when the poles were equal (north vs. north); the magnets then had to be forced together over the probe. This proved to be a bit of a challenge, since the magnets were quite strong, but eventually some results were obtained. The results from the tests are shown in Table 2 and Table 3. The first and second row shows how many magnets were used on each side. The next two rows display the size of the magnetic fields separately while the fifth row shows the measurement of the field when the magnets were put together. The last row tell the difference between the measured magnetic fields of the separate magnets and the magnets together.

As can be seen in Tables 2 and 3, the differences are not large and can be the result of measurement errors, since the position of the measurement sensor was not *exactly* the same for each measurement. A slight change in the position of the magnets would often lead to a $10mT$ change. It seems

| *# Magnets top* | 1 | 2 | 3 | 4 | 5 |
|---|---|---|---|---|---|
| *# Magnets bottom* | 1 | 2 | 3 | 4 | 5 |
| *Top magnets* | $245mT$ | $382mT$ | $433mT$ | $453mT$ | $480mT$ |
| *Bottom magnets* | $249mT$ | $406mT$ | $475mT$ | $470mT$ | $504mT$ |
| *Total magnetic field* | $510mT$ | $807mT$ | $924mT$ | $944mT$ | $1004mT$ |
| *Difference (Tot-top-bottom)* | $16mT$ | $19mT$ | $16mT$ | $21mT$ | $20mT$ |

**Table 2:** Addition of magnetic fields. The total magnetic field is *measured*. Top and bottom points to the place of the magnets at the measurement probe.

as if both field addition and subtraction is possible when looking at the measurements. However, these tests say nothing about whether the magnetic fields are only deflected, or if the fields really are *zeroed* (which by the way is highly improbable). More thorough tests are needed in order to be able to conclude in the matter.

Tests were also conducted to see whether an iron cylinder attached to the magnets would increase the total magnetic field. The magnets were attached to the cylinder (cylinder diameter $10mm$ and height $19.8mm$) and the field strength was measured at the magnets. Table 4 shows that the field obviously

becomes stronger with the iron cylinder attached.

Note that these tests are not extremely precise, as for instance the placement of the measurement probe might be a bit different in each test, especially with the "subtraction" tests, where it was extremely difficult to maintain the position of the magnets. However, the *qualitative* result is pretty conclusive in that field summation seems to work, that field subtraction *might* work (though the fields most probably are deflected), and that that introducing an iron cylinder increases the magnetic field. More tests has to be done concerning the field subtraction.

| *# Magnets top* | 1 | 2 | 2 |
|---|---|---|---|
| *# Magnets bottom* | 1 | 1 | 2 |
| *Top magnets* | $238mT$ | $370mT$ | $350mT$ |
| *Bottom magnets* | $-253mT$ | $-270mT$ | $-394mT$ |
| *Total magnetic field* | $-14mT$ | $\approx 110mT$ | $-66mT$ |
| *Difference (Tot-top-bottom)* | $1mT$ | $10mT$ | $-22mT$ |

**Table 3:** Magnetic field "subtraction". The total magnetic field is *measured*. Top and bottom points to the place of the magnets at the measurement probe.

| *# Magnets* | 1 | 2 | 3 | 4 | 5 |
|---|---|---|---|---|---|
| *Without cylinder, B:* | $260mT$ | $375mT$ | $437mT$ | $460mT$ | $476mT$ |
| *With cylinder, B:* | $334mT$ | $420mT$ | $479mT$ | $495mT$ | $500mT$ |
| *Difference,* $\Delta B$ | $74mT$ | $45mT$ | $42mT$ | $35mT$ | $24mT$ |

**Table 4:** Tests with and without an iron cylinder attached to the magnets.

### 4.4.4 Pipe diameter $1mm$

First, the test rig had a pipe with inner diameter $1mm$. The tests conducted with that pipe diameter proved to be nearly impossible to get anything sensible from. The initial length of the pipe was about $9cm$, but had to be cut to about $5cm$ in order to get anything flowing at all. In addition, the pressure needed to be at least $4kg/cm^2$(approximately $392kPa$) in order to push any fluid through. However, at $5kg/cm^2$, the o-ring used to seal the top of the reservoir slipped, causing a leakage of air and a minor heartattack to the person standing next to it. Therefore, for safety reasons, the maximum pressure had to be $4kg/cm^2$. In addition, the flow stopped when the magnets were close to the pipe, at much lower field strengths than assumed prior to the tests. Approximately $20-30mT$ was all that was needed in order to stop the flow. As an example, with $4kg/cm^2$ inlet pressure, and a field strength of $5.7mT$, it took about 14 minutes to reach $2dl$, which is really too slow. In addition, with a field of $9.8mT$, it took about $11min46s$ to fill up $2dl$, so it is clear that the flow was highly irregular. It was then discovered that the flow occasionally stopped for some time, before starting again. This might be due to poorly mixed fluid, combined with the slow flow making it easy to clot. Inevitably, the results had to be discarded due to their obvious unreliability.

So, the tests showed that even $5kg/cm^2$ was not enough in order to get the fluid flowing at a satisfactory rate. This is rather high, as the pressure on the lid then corresponds to $250kg$. It is clear that, for safety reasons, the pressure should be lower. Therefore, the design of the test rig had to be changed. Building a test rig that could take even higher pressures was not an alternative, as it seemed that the pressure needed to be a lot higher in order to get a satisfactory flow rate. This higher pressure would inevitably lead to a more complex design and the need for other pressure supplies (the pressure regulator used to supply the inlet pressure could give up to $6kg/cm^2$). In addition, there were the time and cost aspect, that prevented a substantial change in the design. Therefore, the easiest (and possibly the best) solution was to get a pipe with a larger diameter. The experiences from the tests conducted with the $1mm$ diameter pipe suggested that there would be no

problem at all in getting the magnetic field strong enough even with a larger diameter. Hence it was decided to try with a pipe diameter of $3mm$.

### 4.4.5 Pipe diameter $3mm$

New tests were then conducted with a wider pipe; this time the inner diameter of the pipe was $3mm$, with its length being about $5cm$ as before, see Figure 50. In addition, the pipe was magnetic, as opposed to the previous pipe that was made of copper and not magnetic. The larger diameter led to a higher flow rate at a lower pressure, as predicted. The flow at zero inlet pressure (only gravity "dragging" the fluid through the pipe) still was too low to measure (almost no flow), but at $0.5kg/cm^2$, things were speeding up a bit. At that inlet pressure, it took about $1min35s$ to get $2dl$ fluid through the pipe. The tests were only carried out up to an inlet pressure of $2.5kg/cm^2$ due to the relatively fast flow at that point; $2dl$ was reached in only about $17s$.

The first measurement in each of the tests unfortunately had to be discarded due to the high probability of measurement error (the points in marked as blue dots in the figures). The reason why these first measurements sometimes are quite far from the other might be due to several reasons. One reason might be the fact that the fluid has got a somewhat high viscosity and therefore, at the first measurement (at about $1dl$), might not have exactly the same height around the receiver. The base was probably not perfectly level, so the container might have tilted slightly to one side. Therefore, at that small volume, the difference in the height of the fluid in the receiver would be more distinctive than later. In addition, it was a bit more difficult to read the level due to residues of the fluid on the wall of the receiver making it harder to see the height of the fluid at $1dl$.

Please note that, as previously mentioned, the inlet pressure $p_i$ supplied by the pressure regulator equals the pressure difference $\Delta p$ between the inlet and the outlet, since the initial pressure at the inlet and at the outlet is assumed equal to the atmospheric pressure. The pressure supplied by the pressure regulator then becomes an additional pressure at the inlet.

The first experiments were carried out *without* any magnetic field. As can be seen in Figure 54, the increase of flow rate with the inlet pressure is close to linear, which is as expected; the theoretical model is the Hagen

Poiseuille equation [18](see Section 4.2.2):

$$\Delta p = \frac{12\eta QL}{\pi r^4}$$
$$\Rightarrow Q = \frac{\Delta p \pi r^4}{12\eta L} \tag{15}$$

It was first tried with 8 instead of 12 in the numerator, but 12 fittet way better. Therefore, this will be used from now on, and supports the fact stated in Section 4.2.2 that the equation in [18] does not tell the whole truth. The length of the pipe was calculated after the first experiment using the above equation, since all the other parameters were known except the total length of the pipe. This was a bit difficult to measure because of the valve and the other arrangements at the outlet of the reservoir, having unknown internal geometries. The calculated length is the equivalent length of a pipe with diameter $3mm$ all the way from the outlet of the reservoir to the outlet of the pipe, ignoring the valve. $\Delta p$ is the inlet pressure, Q was measured in the experiment, and r was measured with a slide caliper. With $\Delta p = 2.0kg/cm^2 = 196133Pa$, Q measured to be $\approx 10.38 \cdot 10^{-6} m^3/s$, and $r = 1.5mm = 0.0015m$, the length of the pipe is calculated to be $L = \frac{\Delta p \pi r^4}{12\eta Q} = 0.0894m$, which seems reasonable since it is a bit shorter than the real length of the pipe and the valve – the valve has a larger inner diameter than the pipe. Plotting the model from Equation (15) in the same plot as the results from the experiments gives a near *perfect match*, see the uppermost plot in Figure 54 which indicates that the model fits rather well.

Applying a magnetic field to the fluid, it quickly became clear that high magnetic fields was not needed. Only one magnet was actually enough to stop the flow. However, it was possible to get quite sensible measurements with only the one magnet, as long as it was kept at a certain distance from the pipe and the magnetic field was kept under about $100mT$. For the magnetic fields tested, the response proved to be quite close to linear, as can be seen in the centre plot in Figure 54. The deviation from the linear approximation is most probably due to measurement errors in the measurement of the magnetic field. These inaccuracies stems from the slightly inaccurate placement of the measurement probe used to measure the magnetic field. A slight change in the position of the probe could lead to a change in the magnetic field field of up to $10mT$. Notice that the field was measured *inside* the magnet holder (through the slit in the holder, shown in Figure 51) and hence making it nearly impossible to see the position of the probe – the placement had to be made based on *feeling* whether the position was right or not. However, as far as possible, the placement of the probe was subject to the outmost

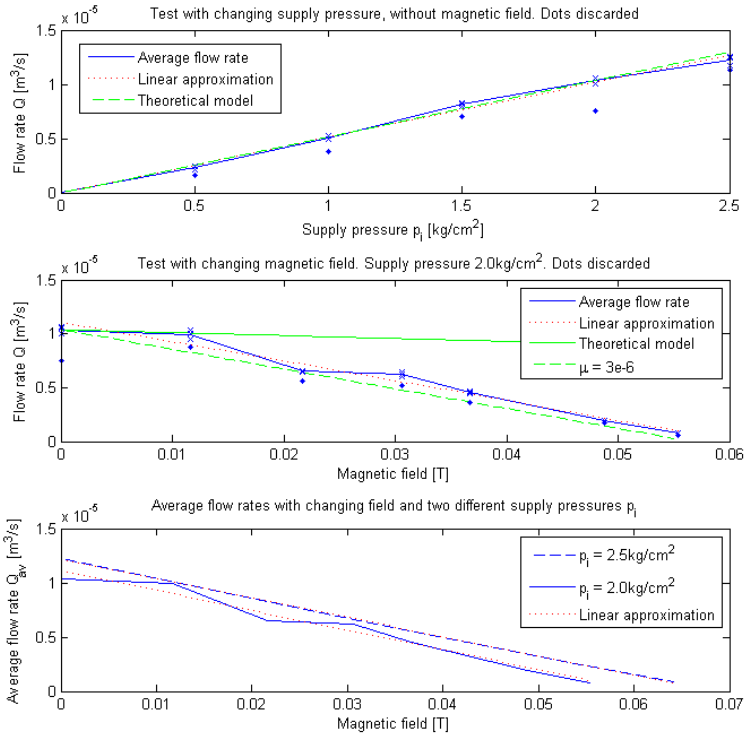


**Figure 54:** Plot of the tests with changing supply pressure and with changing magnetic field. The points visualized as blue dots were discarded due to the high probability of measurement error. The green lines show the theoretical models.

thoroughness. Still, there is no guarantee that the probe was placed at *exactly* the same place each time, which might explain some of the deviations from the linear approximation. The linearity of the results are as expected, since the yield-stress vs magnetic field intensity curve is close to linear for small fields (see Figure 46).

In Figure 54, the theoretical model is plotted green. As a reminder, the model is repeated here (see Section 4.2.2), with $T^* < 0.5$ (this is the case for

the tests below, calculated in Matlab):

$$\Delta p = \frac{12\eta QL}{\pi r^4} + 3\frac{L_m}{h}\tau_y$$
$$\Rightarrow Q = \frac{\Delta p \pi r^4}{12\eta L} - \frac{3L_m \pi r^4}{h 12\eta L}\tau_y \quad (16)$$

where $\Delta p$ is the inlet pressure, r is the radius of the pipe, $\eta = 0.28Pas$ is the (dynamic) viscosity of the fluid, L is the length of the pipe, $L_m = 1cm$ is the length of the pipe under the influence of the magnetic field (the diameter of the magnets), $h = r$ (see Section 4.2.2), and $\tau_y$ is the yield stress of the fluid, dependent on the magnetic field intensity ($\tau_y = \tau_y(H)$). In [5] a linear approximation with $\tau_y(H) = k_\tau H = 0.3H$ was used. However, in this case the field is below $100mT$, i.e., below $50000A/m$ (see the typical magnetic properties of the fluid in Figure 32). Therefore, a more accurate linear approximation can be utilized, with $\tau_y(H) = 0.52H$, see Figure 46. Note that the approximation may not be entirely correct since the curve does not pass through the origin even though it should, so the curve is probably a bit inaccurate (for a "clean" figure, please see Appendix D). In addition it is stated in the fluid technical data sheet that the values are *typical* values as not all tests are run on each lot of material produced (see Appendix D).

Since the measurements of the magnetic field is in Tesla (magnetic flux density), the permeability of the fluid is needed in order to convert this into $A/m$ (the magnetic field intensity). The figure showing the typical magnetic properties of the fluid is shown in Figure 32. However, it is a bit difficult to get good readings from the curve for small magnetic fields, and in addition the curve seems not to pass through the origin, but rather to pass $H = 0$ at $B \approx 80mT$. Since most of the tests are carried out at fields below that, the permeability is very difficult to find, if not impossible. The figure with the typical magnetic properties is clearly not trustworthy. Anyway, by using the tangent to the curve at $H = 0$, the permeability $\mu = \frac{B}{H}$ was found to be about $2.0 \cdot 10^{-5} N/A^2$, which corresponds to a relative permeability of $\mu_r = \frac{\mu}{\mu_0} = \frac{2.0 \cdot 10^{-5}}{4\pi \cdot 10^{-7}} \approx 16$. Conversion between the magnetic flux density $B$ and the magnetic field intensity $H$ is then done by $H = \frac{B}{\mu} = \frac{B}{2.0 \cdot 10^{-5}}$. However, as can be seen in the centre plot in Figure 54 (the solid green line), the theoretical model with the previously found permeability fits rather poorly. The permeability that seems to fit the best is $\mu = 3.0 \cdot 10^{-6}$, corresponding to a relative permeability of $\mu_r \approx 2.4$, which is almost 7 times smaller than calculated. The difference might be related to the difficulty of reading the typical magnetic properties graph, perhaps in addition to poor mixing of the

fluid, and some can certainly be related to the fact that the magnetic field is measured at only one point, in air, and that the magnetic field might be different in the presence of both the magnetic pipe and the fluid, and varying with the distance from the magnet.

In the bottom plot in Figure 54, some experiments with a higher supply pressure ($2.5kg/cm^2$) are plotted, together with the plots from before. These tests proved to be almost as close to linear as possible. In addition, the difference in flow rates between the two supply pressures seems to be fixed, since the distance between the two plots stays the same when the magnetic field varies.

Figure 55 shows how the flow rate changes when the magnetic field, starting from about $53.2mT$, is reduced by introducing another magnet with an "opposite field" in a step-by-step manner. As before, the first measurement for each experiment was discarded due to the high probability of measurement error (blue dots). The dotted line shows the ideal line, taken from the centre plot in Figure 54, of how the fluid responds to a certain magnetic field, only influenced by the magnetic field from *one* magnet (a "clean" magnetic field, so to speak). Clearly, the performance for the field subtraction is rather poor. It can also be seen that if the "zeroed field" increases (i.e. the initial field is higher), the flow rate decreases. This is rather logical since the overall magnetic field increases. In addition to the field between the magnets, the field on top of the magnet holder was measured, i.e., the perpendicular field that will act tangential to the pipe in the direction of the fluid flow. The field was measured at the hole for the pipe in the magnet holder, shown in Figure 51. The measurements showed, quite logically, that this perpendicular field increased as the total magnetic field increased. The literature states that the best effect from the magnetic field is achieved when the magnetic field is perpendicular to the fluid flow, but says little or nothing about how large the effect of having the field tangential to the flow direction is. The problem might get smaller with a smaller pipe diameter, as a percentual larger area of the pipe will have a magnetic field close to zero, but this is not for certain. Notice that the field is measured to be zero at *one* point, and will increase beyond that point (there will always be some field "skulking about" in the corners).

The fact that the flow rate apparently changes very little during the field "subtraction" is not necessarily negative. It means that field subtraction does not work the way wanted, but it does work! It can be compared to having no change whatsoever in the magnetic field at the pipe that is subjected to the subtraction, but an increase of magnetic field at the side that has an addition of field. For instance, the effect of the magnetic field at the left pipe

can increase while the effect of the magnetic field at the right pipe stays the same. The effect is hence sort of halved. If there had been no subtraction effect whatsoever, the magnetic field would have been strengthened at both sides and there would be no pressure difference between the pipes and nothing would have happened. Again, the principle still works, though a bit poorer than first assumed.

An interesting result was discovered at the beginning of the subtraction experiments, after the "benchmark" was set at $B = 53.2mT$: To reduce this field, another magnet was pushed into the magnet holder at the opposite side of the already present magnet. However, the iron cylinder was not used to push it in. The result was actually a slightly *lower* flow rate than before, even though the field was apparently reduced to about $37.1mT$ (seen in Figure 55 as blue dots at $B = 0.0371T$). But, when the iron cylinder was inserted, the flow rate *increased*. A theory to why this happened is that the magnetic field was led to the iron cylinder instead of remaining in the fluid, since the iron cylinder has got about 1000 times higher permeability than the fluid and was relatively close to the fluid. This emphasizes the importance of deflecting the magnetic field from the areas it should not be, i.e. the magnetic field should ideally only influence the fluid between the magnets, and not any other place. Therefore, it could be an idea to have some iron around the pipe to lead the magnetic field away from the fluid if the field should be deflected. However, this is only a theory that should be kept in mind when further investigating the concept, and should be more extensively tested before a conclusion can be made. Bear in mind that the field should not be "removed" from between the magnets.

The last thing that was tested was the constriction of the pipe. Two "pins" (actually two welding rods), one of them with diameter $1.1mm$ and the other with diameter $1.9mm$ were mounted on a piece of plexiglass each, and placed in such a way that the end of the pin was inside the pipe by a measured distance, becoming the constriction length $L_c$. For each test, a piece of the pin was cut off before doing the experiment over again, then having a shorter constriction. The results are shown in Figure 56, plotted together with the theoretical model (green lines), which is calculated by using Poiseuille's law $\Delta p = \frac{12\eta QL}{\pi r^4}$ as above, slightly modified to take the

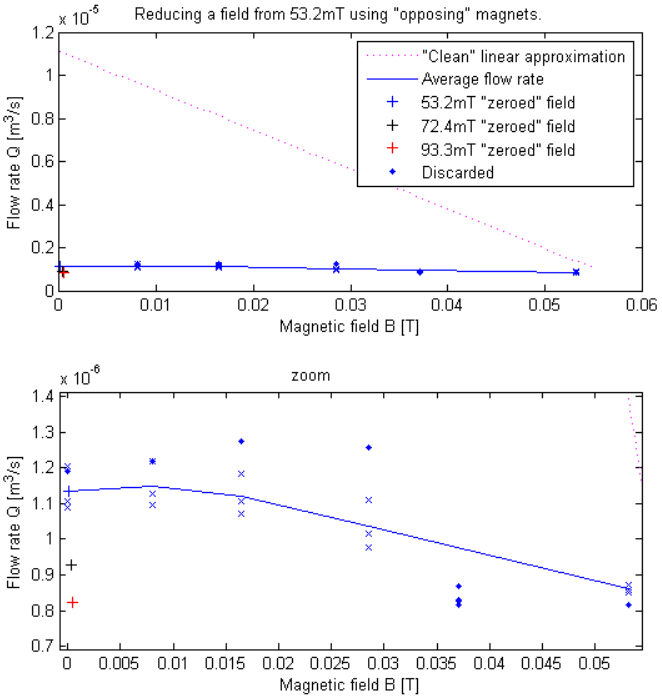


**Figure 55:** Plots with the magnetic field reduced from about $0.055T$ to zero by an "opposing" field. The dotted line is the result from the "clean" test, without any opposing fields. The first measurement in each experiment is discarded due to the high probability of measurement errors. The dots at $0.0357T$ were discarded due to a different test method (the test was done without the iron cylinder). The bottom plot is a close-up of the upper plot.

constriction into account:

$$\Delta p = \frac{12\eta Q(L-L_c)}{\pi r^4} + \frac{12\eta Q L_c}{A_c h^2} = \frac{12\eta Q(L-L_c)}{\pi r^4} + \frac{12\eta Q L_c}{\pi(r^2-r_{cyl}^2)(r-r_{cyl})^2} \tag{17}$$

$$r_{con} = (r^2-r_{cyl}^2)(r-r_{cyl})^2 \tag{18}$$

$$\Rightarrow Q = \frac{\Delta p \cdot \pi r^4 r_{con}}{12\eta r_{con}(L-L_c) + 12\eta L_c r^4} \tag{19}$$

with $A_c = \pi r^2 - \pi r_{cyl}^2 = \pi(r^2 - r_{cyl}^2)$ being the cross-sectional area of the pipe minus the constriction) and the "height" between the cylinder constriction

and the pipe being $h = r - r_{cyl}$ (see Figure 24 and the calculations performed in Section 4.2.2). The theoretical model is slightly above the test results, but not very far. This might be due to measurement errors in either the constriction length, $L_c$, or in the cylinder constriction diameter, $2r_{cyl}$. The theoretical model was calculated all over again with some other cylinder diameters in order to see if the test results would fit better. In the upper plot in Figure 56, the diameter $1.3mm$ for the cylinder constriction fitted better than the measured value of $1.1mm$. As for the second plot, the difference is slightly smaller with a best-fit of $2mm$ for the cylinder constriction, while it was measured to be $1.9mm$. These differences are small enough to be measurement errors, especially for the thickest constriction. For the smallest diameter, some of it must be due to a measurement error in the constriction length too, because that diameter in reality was rounded up to $1.1mm$. The measurement error in the constriction length must in that case be that the length should be longer, i.e., the test results in Figure 56 perhaps should be moved a bit to the right. Anyway, the results are close enough to conclude that the mathematical model agrees quite good with the test results.

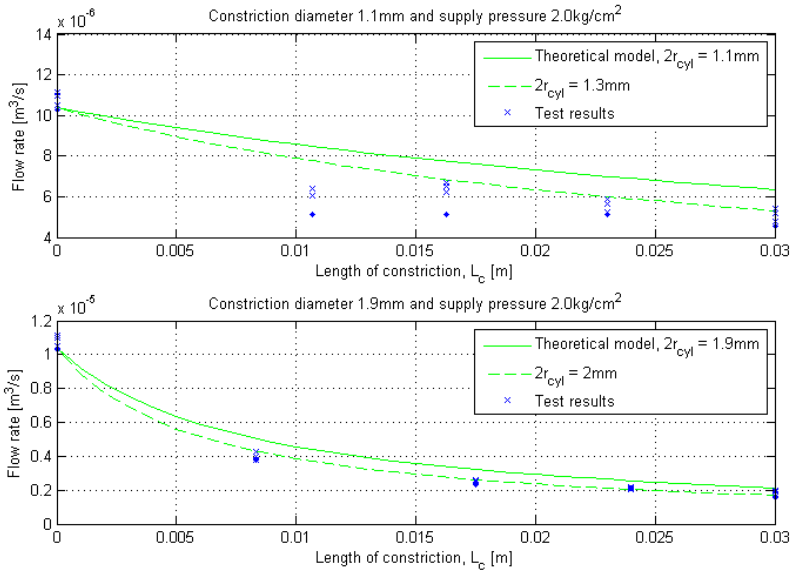


**Figure 56:** Constriction tests with two different constriction diameters. Test results marked as blue dots are discarded due to their high probability of measurement errors.

### 4.4.6 New Comsol dynamic simulations

Since it seems as if field subtraction works rather poorly, some new dynamic simulations were conducted in Comsol, this time without subtraction of the field (the field being static). The field is added at one side, but on the other side nothing happens, i.e., $H_1 = H_{pm} + H_{el}$ while $H_2 = H_{pm}$. The results are shown in Figure 57, illustrating that the slope is reduced. The linear approximations to the slopes are now as follows:

- $\underline{2r_c = 0.15mm}$: $\Delta x = 4.5 \cdot 10^{-8} \cdot H_{el}$ [m]
- $\underline{2r_c = 0.25mm}$: $\Delta x = 1.5 \cdot 10^{-8} \cdot H_{el}$ [m]
- $\underline{2r_c = 0.35mm}$: $\Delta x = 0.575 \cdot 10^{-8} \cdot H_{el}$ [m]

from which can be seen that the slope is halved if you compare to the linear approximations from before (Section 4.3.4). The result is that the maximum displacement of the piston is also nearly halved:

- $\underline{2r_c = 0.15mm}$: $\Delta x_{max} = 4.5 \cdot 10^{-8} \cdot H_{elmax} * 2 = 7.2mm$
- $\underline{2r_c = 0.25mm}$: $\Delta x_{max} = 1.5 \cdot 10^{-8} \cdot H_{elmax} * 2 = 2.4mm$
- $\underline{2r_c = 0.35mm}$: $\Delta x_{max} = 0.575 \cdot 10^{-8} \cdot H_{elmax} * 2 = 0.92mm$

with $H_{elmax} = 80000A/m$, as before.

Note that the stiffness of the actuator is the same as before due to the fact that it does not depend on the magnetic field, but on the constriction.

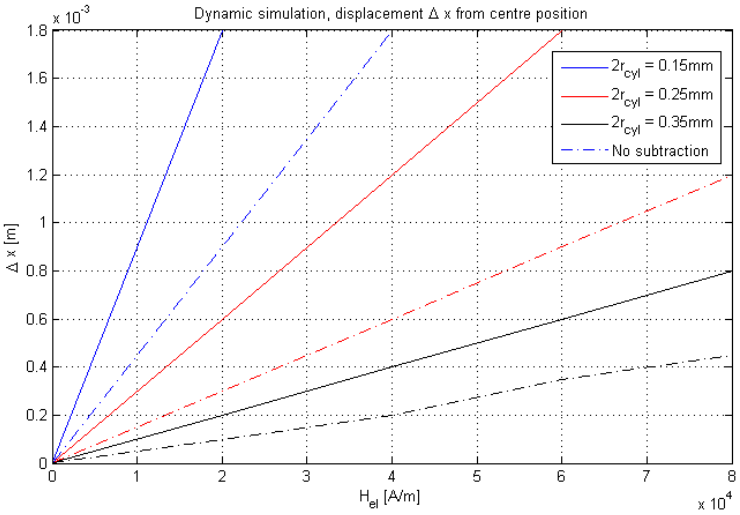


**Figure 57:** Comsol dynamic simulations without subtraction of magnetic fields (i.e., $H_1 = H_{pm} + H_{el}$, $H_2 = H_{pm}$) shown dotted. The slope is almost exactly halved, consequently the maximum displacement is nearly halved.

### 4.4.7 Discussion

It is a suitable question to ask whether the fluid is too thick (has a too high viscosity) for the purpose. The fluid was chosen because it had the highests attainable yield stress, and hence was the most powerful fluid. With a pipe diameter of $1mm$ and length $5cm$, it was nearly impossible to get a free flow of fluid even with an inlet pressure of up to $5kg/cm^2$. Since the diameter of the pipe perhaps should be even smaller, it is fair to ask whether the pressure needed to drive the fluid through at a needed flow rate will be too high. But, a fluid with a lower dynamic viscosity will have a lower attainable yield stress, and hence will create a lower flow resistance (less performance). However, the simulations done in Comsol had an inlet pressure of about $10bar$, while the real tests had a maximum of about $5bar$. In addition, the Comsol simulations were carried out at a pipe diameter of only $0.5mm$. That seemed to work well, so it is not certain that a fluid with a lower viscosity needs to be used. This has to be considered when or if the problem arises.

The fact that the contribution from the weight of the fluid is neglected in the inlet pressure, i.e. $p = \rho gh$ is neglected, is thought not to lead to large errors, since it has little contribution to the pressure at the outlet of the reservoir compared to the pressure from the pressure regulator.

As earlier mentioned, it was made a note of the time at four different fluid heights (volumes): at about $1dl$, $2dl$, $3dl$, and $4dl$. Notice that these might not be exact volumes due to the fact that the base (the table) probably was not perfectly level and the possibility of inaccuracies in measuring and marking these volume marks on the receiver. Still, the inaccuracies are believed to be consistent throughout the experiments.

A potential source of error lies in the calculation of the length of the pipe in the test rig. Ideally, this should have been *measured* along with the internal geometries of the valve, but due to the difficulties in doing so, this was not done. Still, judging by the comparison between the theoretical model and the test results in Figure 54, the error is rather small.

The tests with a changing supply pressure and no magnetic field proved to be dead on the theoretical model, see the upper plot in Figure 54. This indicates that the Hagen-Poiseuille equation with 12 in the numerator (Section 4.2.2) is the right equation to use for fluid flow through a pipe with no applied magnetic field.

The greatest uncertainty is linked to the fluid's magnetic permeability, which proved to be very difficult to find from the typical magnetic properties curve (see Figure 32). This is probably the reason why the difference is as large as it is between the theoretical model and the test results in the centre plot in Figure 54. The theoretical model of the flow rate with a certain magnetic field at the best-fitting magnetic permeability is slightly below the linear approximation of the test results as can be seen in the centre plot in Figure 54. This can be the result of measurement errors in the tests, but might also be due to measurement errors in the variables used in the theoretical model. Another reason to the differences might be insufficient mixing of the fluid leading to another density, or other magnetic properties, possibly also causing cloting of the fluid. In addition, the pressure regulator had an analogue pressure gauge, so the inlet pressure might have been slightly different in the various experiments. A last reason might be the base of the receiver, which could have been poorly leveled.

When it comes to the field subtraction tests in Figure 55, they indicate that the subtraction of fields is not possible the way first assumed, with "perfect" subtraction $H_{pm} - H_{el}$. The field might seem to be "zeroed" since the magnetic field *measurements* shows zero field, but the measurement is only valid for one point. Most likely the fields are deflected and placed at other parts of the fluid, parallel to the flow direction. It seems as if it could be advantageous to find a way to lead these deflected fields away from the fluid, since the flow rate increased when the an iron cylinder was placed close to the fluid. Note that there might be other reasons to why the flow

rate increased, such as measurement errors, but the result is rather logical; leading the deflected field away from the fluid will lead to less magnetic field in the fluid. It seems as if there is a slight *increase* in the flow rate as the field is "zeroed", which means that the subtraction effect is present but extremely small. However, it is unknown how this effect will be with higher magnetic fields. Still, from the results in Figure 55, it seems as if the magnetic field subtraction works, but has an extremely small effect. The results implies that the range of operation (magnetic field range) will be smaller than previously believed, since it is not possible to zero the magnetic field entirely.

The fact that the magnetic field should be guided away from the parts of the fluid where it should not be is rather logical, and could perhaps improve the effect of the magnetic field subtraction. However, it is difficult to point out excactly what has to be done before the final design of the actuator is determined. Still, it could be an idea to have a magnetic material around the pipes at the places the magnetic field does not have to be. But, this must not interfere with the regions where the magnetic field must be in order to create the needed effects in the fluid. It will be a bit of a challenge to find the best way to lead the deflected magnetic field away from the fluid at the same time as making sure that the wanted field remains where it should.

The measurements done in relation with the constriction tests might have been slightly inaccurate. The diameter of the cylinder constrictions, $2r_{cyl}$, was measured with a slide caliper and is accurate down to about $\pm 0.1mm$. But, the measurement of the constriction *length* was a bit more difficult to get correct. To measure this length correctly, the constriction had to be placed in the base of the receiver (Figure 52) and into the pipe of the reservoir. This led to very little space to do the measurements, it was virtually impossible to find room to measure anything. Fortunately, there was some residue of fluid left in the pipe such that it was possible to see what part of the cylinder constriction had been into the pipe and then measure that part. However, this was a somewhat inaccurate measurement due to the fact that it is a bit difficult to know whether there was fluid residues only at the part of the cylinder that had been inside the pipe. In addition, the method to measure the constriction length as it was decreased, was to measure the parts of the cylinder that were cut off and subtract these from the initial length. This might also have introduced some measurement errors. Still, these are not thought to be large errors; judging by the similarity between the theoretical model and the tests, it seems as if the measurement was not very far from reality (see Figure 56). Slight adjustments to the radius of the constrictions had to be made for the theoretical model to agree with the test results. The largest error was with the smallest constriction diameter, but this might be

due to other measurement errors like the length of the constriction. Looking at the test results at constriction length $10.7mm$ and constriction diameter $1.1mm$ in Figure 56 (upper plot), it seems as if they might be wrong since the results are quite far from the theoretical model compared to the other test results. Since the other results are quite close to the theoretical model, this could be the result of some kind of human error, perhaps forgetting to reduce the length of the constriction before doing the test. There could also of course be some kind of measurement error, like starting the timer too late. Still, all in all, the theoretical model of the constriction of a pipe (Section 4.2.2) seems to agree quite well with the test results.

### 4.4.8 Conclusion

It might be advantageous to use another magnetorheological fluid with a lower dynamic viscosity, but remember that this will be at the account of the movement since a fluid with a lower viscosity produce a smaller flow resistance due to its lower "performance". This has to be decided when the full design of the actuator is tested.

The theoretical models used in Section 4.2.2 seem to be suitable for the purpose since they are quite consistent with the real tests. The differences can be accounted to measurement errors or simplifications in the equations.

The field subtraction does not work as well as previously assumed. There is a tiny, though almost neglectible, effect of the field subtraction. So the concept works, just poorer than first assumed. Provided the results are correct, the movement of the piston is halved if this is taken into account.

More investigations into how to lead the deflected magnetic field away from the fluid at the same time as leaving the required field where it should be, has to be carried out. This might lead to a better performance of the field subtraction and hence a larger movement of the piston.

### 4.4.9 Summary

A pipe diameter of $1mm$ in the test rig proved to be too small, so the diameter had to be increased to $3mm$. The tests proved to be quite close to the theoretical models found in Section 4.2.2, even though some deviations were found.

The subtraction of magnetic fields proved not to work very well in reality, probably due to the fact that the deflected magnetic field remained at other parts of the fluid. Still, the main principle works though a bit poorer than first assumed.

Simulations with no field subtraction showed that the movement of the piston was almost exactly halved compared to if the subtraction had worked perfectly.

# 5 Discussion

The chosen product development methodology seems to have fitted the project quite well, though it was not possible to utilize the methodology to its full extent due to the relatively low complexity level of this project.

When it comes to the choice of concept, this was rather easy when the idea to use a cylindrical constriction emerged. Maybe some more concepts should have been invented and investigated, but there would probably not have been enough time to do so anyway. And with the magnetic concept (electromagnetic coil and permanent magnets) working as well as it seems from the simulations, there seem to be no need to explore any other magnetic concepts.

In order to compare the test results to the goal, the specifications are repeated here:

*Ideal values*:

- $10mm$ movement
- Stiffness $5N/mm$
- 2mm diameter

*Marginally acceptable values*:

- $5mm$ movement
- Stiffness $1N/mm$
- 5mm diameter

The differences between the Comsol simulations and the mathematical model calculations might be due to the simplification in the mathematical models – assuming separate inlet pressures for the two pipes (or more precisely, assuming the resistance from the inlet to the pipe branching close to zero). The calculations from the mathematical models indicate a stiffness of about $0.59N/mm$ and a movement of about $2cm$ with a 70% constriction of the pipes, while the simulations in Comsol indicate a stiffness of about $1.77N/mm$ and a movement of only $1.6mm$ at the same constriction. It seems as if the constriction should have a larger diameter judging by the calculations and a smaller diameter judging by the simulations. All in all, it seems as if the mathematical model calculations are somewhat more optimistic than the simulations in Comsol. This can most probably be accounted to the already stated fact that the calculations were carried out assuming

separate pipe branches with a separate inlet pressure, whereas the simulations took the "pressure travel" between the two pipe branches into account since the pipes had a mutual inlet pressure. In addition, there might have been some discrepancies between the geometries in the Comsol simulations and the mathematical model calculations, especially when considering that the Comsol simulations were carried out in only two dimensions. There is also a possibility that the Comsol simulations were not entirely correct because of the sudden leap in the viscosity model from the parts of the fluid not influenced by the magnetic field to the parts with a magnetic field (remember that the magnetic field was not simulated, but *assumed* to have certain magnitude). Another possibility is that the mathematical model might contain errors not yet discovered. Nevertheless, the results are not extremely far from each other, so it is reasonable to believe that it can be possible both to achieve a stiffness of $1N/mm$ at the same time as having a movement of $5mm$. This is under the ideal values of the movement and the stiffness set in the specifications, but at the marginally acceptable values. The calculation of the forces were done assuming an actuator diameter of $4mm$ and a pin diameter of $1mm$. This is above the ideal value of a total diameter of $2mm$, but was necessary in order to get the forces a bit higher. There are then two ways of getting higher forces: Either increasing the diameter of the actuator or increasing the inlet pressure. However, both the simulations in Comsol and the mathematical model calculations indicate that the movement of the piston will decrease as the inlet pressure increases. This means that there is a trade-off between higher forces and the movement of the piston, and indeed between the size of the actuator and the forces (which by the way did not come as a surprise). Another possibility might be to reduce the pipe length (see further down).

These were the results when assuming a perfect, ideal magnetic field subtraction. New simulations in Comsol indicate that it would be possible to achieve a stiffness of over $0.5N/mm$ at the same time as having a movement of up to and perhaps over $5mm$ even though the field subtraction should fail to be perfect. The tests showed that the subtraction of fields worked the way intended, but with an extremely small impact on the flow resistance. This would lead to a near halving of the movement of the piston, but no considerable impact on the stiffness of the actuator since the stiffness is mostly related to the constriction of the pipes and not the magnetic field. However, the tests were carried out at relatively small magnetic fields, so it is difficult to know what would happen at higher fields. The results are *below* the marginally acceptable values, but the results might be improved by increasing the diameter of the piston from $4mm$ to the marginally acceptable

value $5mm$, by reducing the length of the pipes, or by any other means described in this thesis. So, the marginally acceptable values might still be within reach.

Note that the yield stress of the fluid is approximated with a linear approximation that constantly is below the real curve (see Figure 46), $\tau_y = 0.3H$ when the whole range of magnetic field is simulated. This means that the movement of the piston in reality is a bit larger. The reason why this linear approximation was made was to have a kind of "worst-case" scenario, to be certain that the results did not get better than in reality. This linear approximation also led to a linear behaviour of the actuator, which in reality would be more nonlinear. Again this means that the simulations and calculations only can be viewed as approximate. Nevertheless, the results are good hints as to whether the concept is viable or not.

It is clear that the supply pipes should be made as short as possible in order to leave most of the pressure change to the constriction or to the magnetic field. A large part of the pipes not being directly linked to either the constriction or to the magnetic field would lead to a larger part of the pressure drop from inlet to outlet happening outside the constriction or the magnetic area and hence they would have a much smaller impact. The results show that longer pipes leads to a smaller stiffness.

The magnetic field calculations indicate that there should be no problem in getting the required magnetic field intensity from an electromagnetic coil at the given size. However, the thickness of the wires and windings has not been taken into account when considering the size of the coil. Therefore, the coil might get thicker than first thought. This must be considered when further exploring the concept.

A problem that has not been thought of in the simulations or calculations is that there might be some problems when the piston get closer to one of the pipes and the magnets; it might get drawn towards the magnets. This can be solved by making sure the piston does not get too close to the magnets or by having the piston made of a non-magnetic material.

If the movement or stiffness should prove to be too small, there is another concept that could be investigated; the "amplifier" concept shown in Appendix B. Due to a lack of time this concept has not been further investicated.

Finally, note that the actuator seems to be stable provided the constriction is balanced to the pressure difference created by the magnetic field.

# 6 Conclusion

Even with a poor magnetic field subtraction, it seems as if it will be possible to reach a stiffness of $0.5N/mm$, a movement of over $5mm$, and a diameter of the actuator below $5mm$. This is below the marginally acceptable value for the stiffness, but it seems as if it can be improved to reach the marginally acceptable value. It is clear that there is a trade-off between the stiffness of the actuator and its range of movement. A higher stiffness will lead to a smaller movement and vice versa. The ideal movement can be reached if a lower stiffness can be accepted, and the ideal stiffness can be reached if an (extremely) low movement can be accepted. All in all, it seems as if the concept is viable. The constriction concept with a cylinder constriction moving in and out of the pipe seems to be the best choice in order to achieve the best range of movement and the most uniform/linear movement. The required movement of the pin can be "controlled" by adjusting the stiffness of the actuator (the constriction), and the overall force can be increased by either increasing the diameter of the actuator or increasing the inlet pressure. Notice that a higher inlet pressure leads to a smaller movement.

It may seem as if the ideal values (together) might be out of reach. However, it should be possible to improve the results. For instance, more thorough investigations into leading the deflected magnetic field away from the fluid should be carried out. In addition, the pipes should be as short as possible in order to leave most of the pressure drop to the areas with a magnetic field or with a constriction. This way the the magnetic fields and the constrictions would have a greater impact on the system. Also, if the diameter of the actuator could be accepted to be a bit larger, the forces would increase.

Anyway, the conclusion must be that the results are positive enough in order to justify the creation of a prototype to test the concept in its full range. There are still a few open questions as to how the concept will behave in a full-scale model, especially concerning the placement of the permanent magnets and the electromagnetic coil and the behaviour of the field subtraction at high fields. In order to be certain about how the actuator will behave, a full-scale model should be tested, either as 3D simulations in Comsol, or as a prototype test.

## 6.1 Future Work

Further work should include detail design of the actuator, especially focusing the attention on the permanent magnets and the electromagnetic coil, and

the magnetic field path. Something should be figured out concerning leading the deflected field (in the field subtraction case) away from the fluid, at the same time as not reducing the field at the places it should be. Finding ways to improve the field subtraction is the best way of achieving a better performance of the actuator.

The next step must be either three-dimensional simulations in Comsol, or building a full-scale prototype.

# References

[1] C.R. Beverly and R.I. Tanner. Numerical analysis of extrudate swell in viscoelastic materials with yield stress. *Journal of Rheology*, 33(6):989–1009, 1989.

[2] Don DeRose. Proportional and servo valve technology. *Fluid Power Journal*, pages 8–15, 2003.

[3] Hans Petter Hildre et al. Mekatronikk metodikk. Technical report, NTNU/SINTEF, 1996.

[4] H. Douglas Garner. Method and device for producing a tactile display using an electrorheological fluid. United States Patent no. 5 496 174, March 1996.

[5] Dag Sverre Grønmyr. Modelling and simulation of a rheological servomechanism. Project work TTK4500 Medical Cybernetics, NTNU, December 2007.

[6] H.A.Barnes, J.F.Hutton, and K.Walters. *An Introduction to Rheology*, volume 3. Elsevier, 1989.

[7] Allan R. Hambley. *Electrical Engineering Principles and Application*, chapter 15. Prentice Hall, second edition, 2002.

[8] J.Huang, L.J.Fu, and G.C.Wang. Properties and applications of magnetorheological fluids. In *Proceedings of SPIE – ICMIT 2005: Mechatronics, MEMS, and Smart Materials*, volume 6040, March 2006.

[9] Lord Corporation, USA. [web page] http://www.mrfluid.com. [Accessed 11 May 2008].

[10] Moog – Industrial Controls Division. *Electrohydraulic Valves... A Technical Look.* Retrieved May 6, 2008 from http://www.moog.com/media/1/technical.pdf.

[11] M. Mouret, M. Bouanini, A. Bascoul, and A. Sellier. Hydrodynamic simulation of non newtonian fluid in an agitated vessel. In *Proceedings of the COMSOL Users Conference 2006 Paris*, 2006.

[12] Muturi G. Muriuki and William W. Clark. Design issues in magnetorheological fluid actuators. In *Proceedings of SPIE – Smart Structures and Materials 1999: Passive Damping and Isolation*, volume 3672, pages 55–64, June 1999.

[13] Maria Vatshaug Ottermo. *Virtual Palpation Gripper*. PhD thesis, Norwegian University of Science and Technology, 2006.

[14] Ahmad Shakeri. *A methodology for development of mechatronic systems*. Doktor ingeniøravhandling, NTNU, 1998. Institutt for telematikk.

[15] B.F. Spencer, G. Yang, J.D. Carlson, and M.K. Sain. "smart" dampers for seismic protection of structures: A full-scale study. In *Proceedings of the Second World Conference on Structural Control*, pages 417–426, June 28-July 1 1998.

[16] A.V. Srinivasan and D. Michael McFarland. *Smart Structures, Analysis and Design*, chapter 4. Cambridge University Press, 2001.

[17] Karl T. Ulrich and Steven D. Eppinger. *Product Design and Development*. McGraw-Hill, fourth edition, 2008.

[18] Wikipedia, the free encyclopedia. Hagen-Poiseuille equation. Retrieved April 24, 2008 from http://en.wikipedia.org/wiki/Hagen-Poiseuille_equation.

[19] Wikipedia, the free encyclopedia. Permeability (electromagnetism). Retrieved February 28, 2008 from http://en.wikipedia.org/wiki/Magnetic_permeability.

[20] Wikipedia, the free encyclopedia. Saturation (magnetic). Retrieved February 28, 2008 from http://en.wikipedia.org/wiki/Magnetic_saturation.

# A M-TEST 3205 Digital Teslameter

For measuring magnetic fields, the Teslameter pictured in Figure 58 was used, the *M-TEST 3205 Digital* made by Maurer Magnetic AG.


**Figure 58:** The teslameter used for measuring the magnetic fields.

# B Description of the "amplifier" concept

Figure 59 shows a sketch of a concept that should act as an amplifier. If the movement of the tested concept should prove to be too small, this design could perhaps be utilized. The main principle is the same as before, with distribution of pressure caused by a difference in magnetic field at the pipes.

The idea is that a small movement by the left piston should lead to a larger movement of the right piston sort of as a two-stage servomechanism.

If for instance the electromagnetic coil has got a north pole to the right and a south pole to the left, in such a way that the right pipe is "constricted" and the left pipe is "opened". Then, piston 1 (the left piston, see Figure 59) would start moving to the left due to an increase of pressure in area 2 and decrease in area 1. Further, the right nozzle will become more constricted because the cylinder constriction moves longer into the pipe and the left nozzle will be less constricted. This leads to an even higher pressure in area 2 and lower pressure in area 1. This is then a (deliberate) positive feedback effect, and piston 1 will probably saturate, meaning it will stop at the right pipe. But, since the pressure in area 2 also acts on piston 2, this piston will also move and with a higher force than piston 1 since the effective area is larger. Then, with an appropriately stiff spring between piston 1 and 2, piston 2 will eventually drag piston 1 from being saturated to having a certain equilibrium displacement. Hence the spring will act as the feedback mechanism, just as the feedback wire in the traditional servo valve (Figure 9). Note that area 1 is connected with area 3.

The difference between this concept and a larger version of the previous concepts is the spring and the positive feedback effect. The spring should be adjusted appropriately.

It is difficult to see how the stiffness will be compared to the other concepts in this thesis before some more thorough investigations are carried out. But, there are no indications that the stiffness will be lower. The drawback with this concept is that the servo mechanism will become larger, both longer and wider.

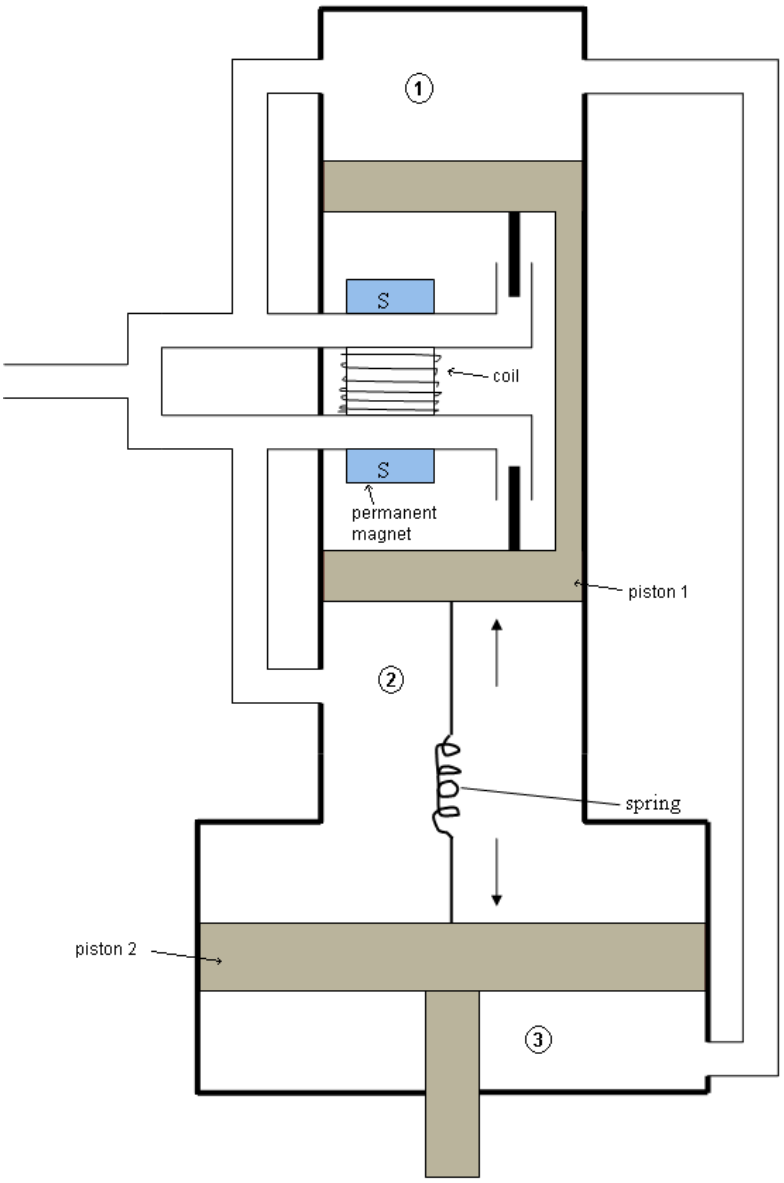


**Figure 59:** Sketch of the amplifier concept.

# C Comsol Screenshots

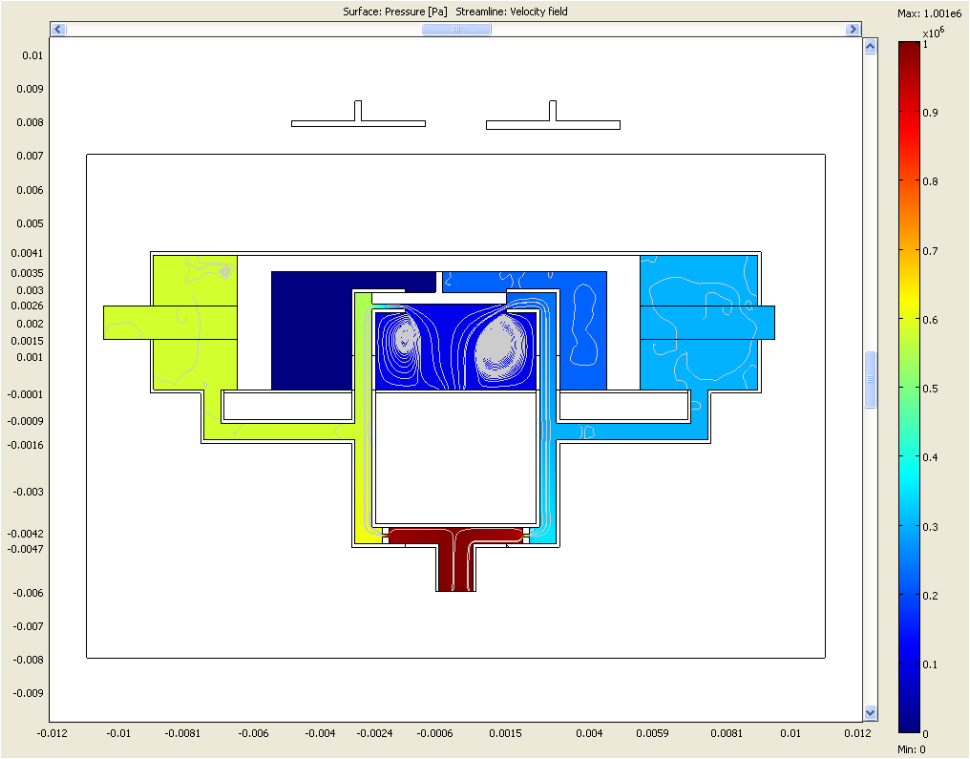


**Figure 60:** The Comsol model used to simulate constrictions. The figure shows the largest constriction ($0.35mm$) with the piston at its leftmost. Notice that the nozzles are pointing inwards, a necessity in order to avoid crossing pipes (Comsol cannot handle crossing pipes like in Figure 15 c)). It can be seen that the pressure is higher in the left chamber than in the right chamber. The streamlines show the velocity field of the fluid, while the colours indicate the pressure (see the bar at the right-hand side of the figure).

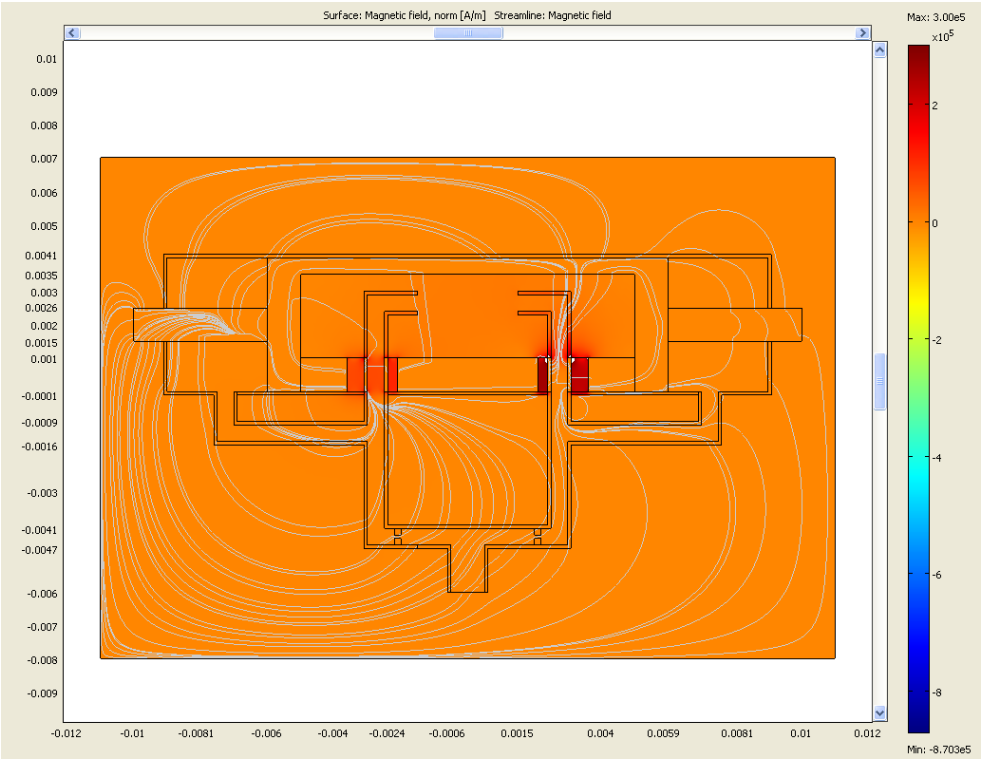


**Figure 61:** Tests with permanent magnets at each side of the pipes and an electromagnetic coil in the middle, with its poles simulated as permanent mangets. The fields are the same in all magnets. The colours symbolize the norm of the magnetic field intensity, H, while the streamlines symbolize the magnetic field lines. At the left side there is a north pole vs. a south pole, while the right side has got a north pole vs. a north pole, hence field addition at the left side and field "subtraction" at the right side.

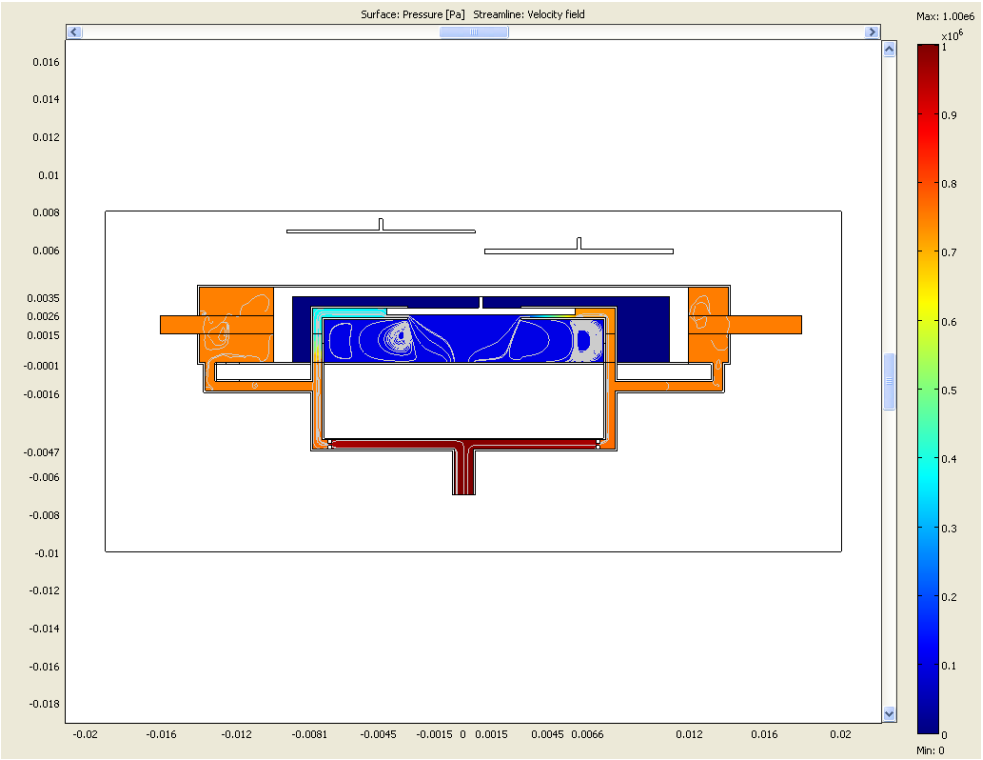


**Figure 62:** Dynamic simulation with the largest cylinder constriction ($r_{cyl} = 0.35mm$) and the largest difference in magnetic field intensity between the two pipes (left side $H_1 = 160000A/m$, right side $H_2 = 0A/m$, assumed magnetic fields). The pressure is equal in the leftmost and the rightmost chamber, so the piston is in "equilibrium". The colours show the pressure distribution while the streamlines show the velocity field of the fluid. The inlet pressure is $p_i = 10 \cdot 10^5 Pa$, while the outlet pressure is the atmospheric pressure.

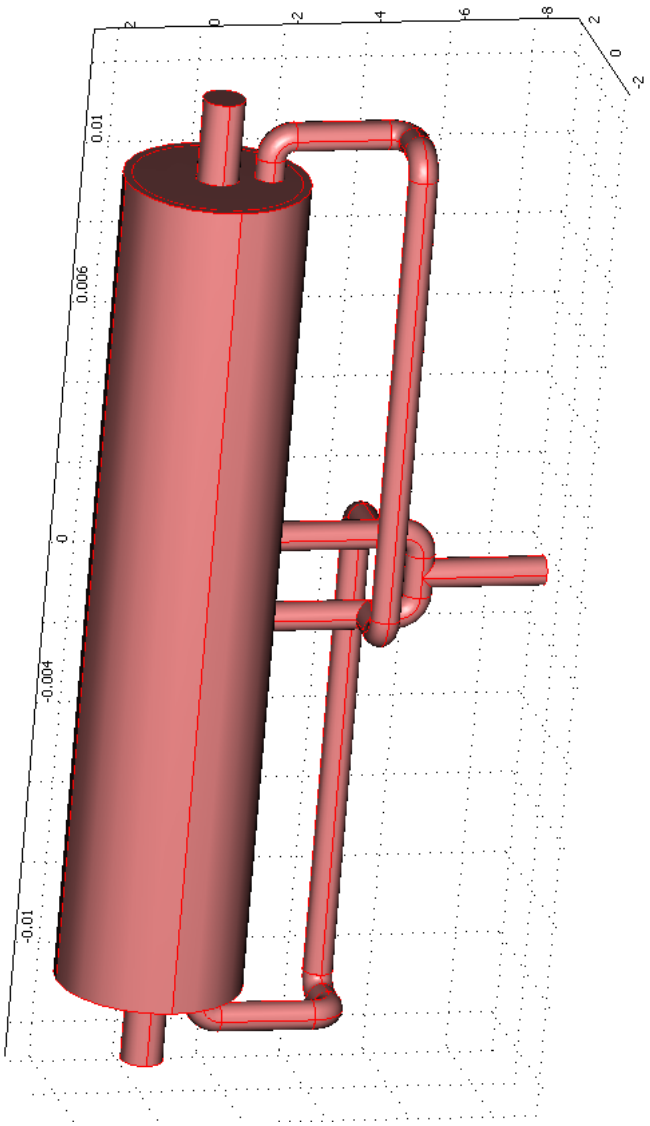


**Figure 63:** Comsol 3D model of the actuator.

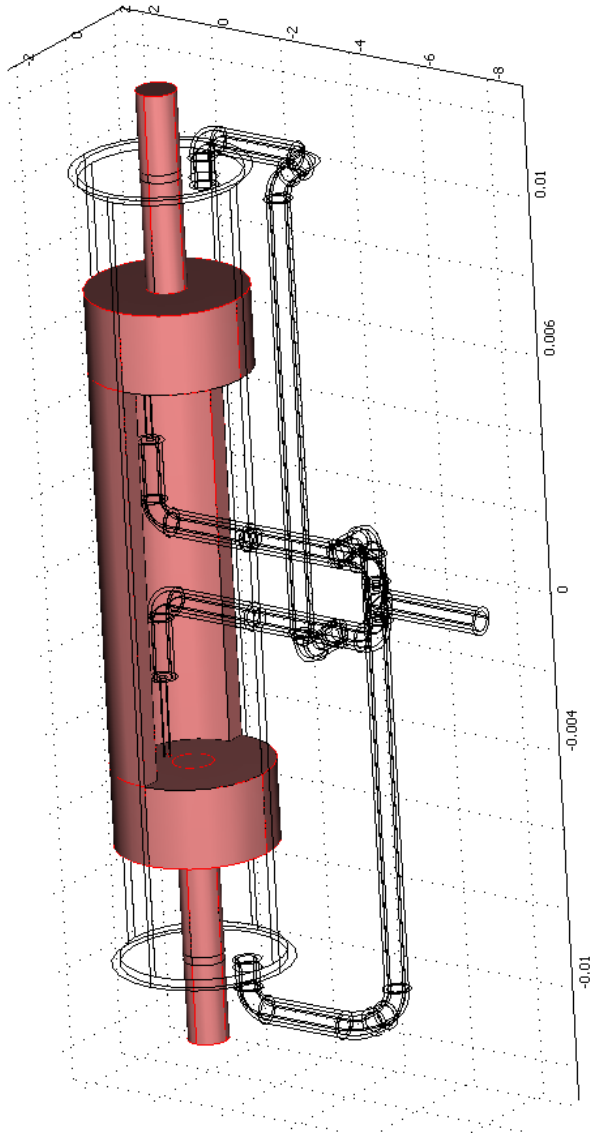


**Figure 64:** Comsol 3D model of the actuator, the piston highlighted.

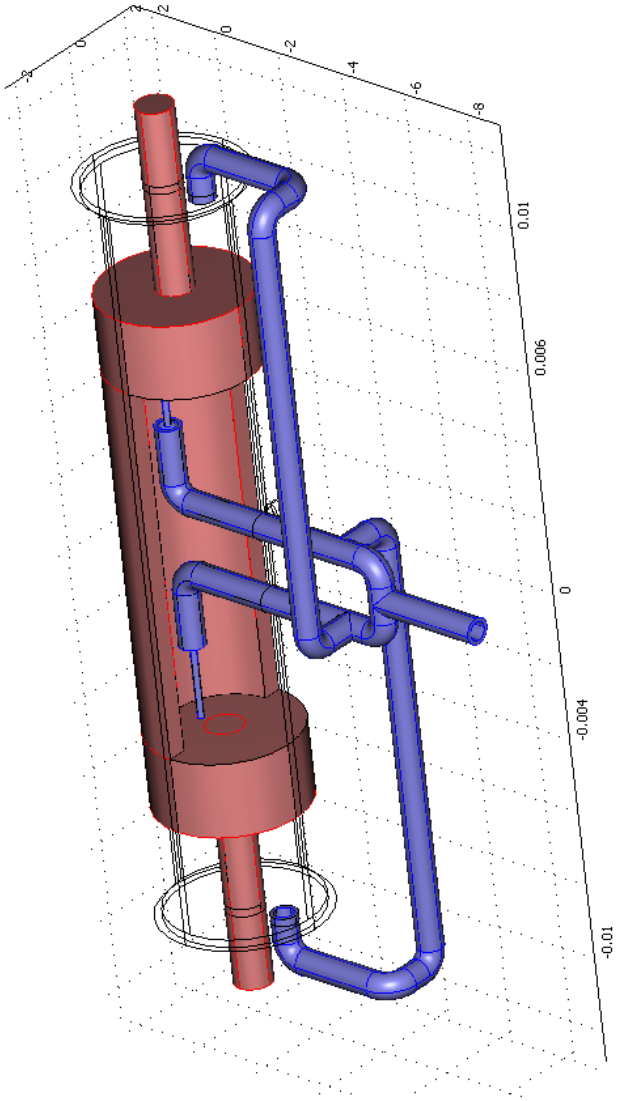


**Figure 65:** Comsol 3D model of the actuator, the pipes and the piston highlighted.

# D Fluid Technical Data

LORD TECHNICAL DATA

## MRF-140CG Magneto-Rheological Fluid

### Description

LORD MRF-140CG fluid is a hydrocarbon-based magneto-rheological (MR) fluid formulated for general use in controllable, energy-dissipating applications such as shocks, dampers and brakes.

MRF-140CG fluid is a suspension of micron-sized, magnetizable particles in a carrier fluid. When exposed to a magnetic field, the rheology of MRF-140CG fluid reversibly and instantaneously changes from a free-flowing liquid to a semi-solid with controllable yield strength. Altering the strength of the applied magnetic field precisely and proportionally controls the consistency or yield strength of the fluid.

MRF-140CG fluid can be used in *valve mode* (fluid flowing through an orifice) or in *shear mode* (fluid shearing between two surfaces). In the absence of a magnetic field, MRF-140CG fluid flows freely or allows free movement. Upon application of a magnetic field, the fluid's particles align with the direction of the field in chain-like fashion, thereby restricting the fluid's movement within the gap in proportion to the strength of the magnetic field.

### Features and Benefits

***Fast Response Time*** – responds instantly and reversibly to changes in a magnetic field.

***Dynamic Yield Strength*** – provides high yield strength in the presence of a magnetic field and very low yield strength in the absence of a magnetic field; allows for a wide range of controllability.

***Temperature Resistant*** – performs consistently throughout a broad temperature range, meeting the requirements of demanding applications such as automotive shock absorbers.

***Hard Settling Resistant*** – provides high resistance to hard settling; easily redispersed.

***Non-Abrasive*** – formulated to not abrade the devices in which the MR fluid is used.

### Application

For more information on MR technology, refer to the MR Design Guides located on www.lord.com/mr.

***Mixing*** – Under common flow conditions, no separation is observed between particles and the carrier fluid. However, a degree of separation may eventually occur under static conditions. If needed, use a paint shaker to redisperse the particles into a homogeneous state prior to use.

### Storage

Keep container tightly closed when not in use.

### Typical Properties*

| | |
|---|---|
| Appearance | Dark Gray Liquid |
| Viscosity, Pa @ 40°C (104°F)<br>Calculated as slope 800-1200 $sec^{-1}$ | 0.280 ± 0.070 |
| Density | |
| $g/cm^3$ | 3.54-3.74 |
| (lb/gal) | (29.5-31.2) |
| Solids Content by Weight, % | 85.44 |
| Flash Point, °C (°F) | >150 (>302) |
| Operating Temperature, °C (°F) | -40 to +130 (-40 to +266) |

*Data is typical and not to be used for specification purposes.

LORD
AskUsHow™

# LORD TECHNICAL DATA

## Cautionary Information

Before using this or any LORD product, refer to the Material Safety Data Sheet (MSDS) and label for safe use and handling instructions.

*For industrial/commercial use only.* Not to be used in household applications. Not for consumer use.

***Shear Stress as a function of Shear Rate with no Magnetic Field applied at 40°C (104°F)***

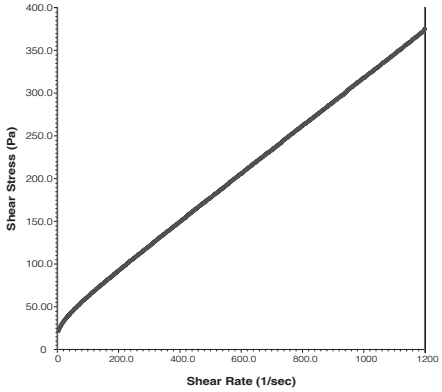


***Yield Stress vs. Magnetic Field Strength***

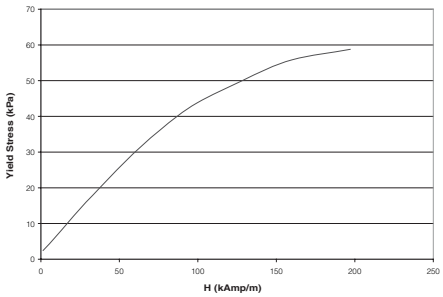


***Typical Magnetic Properties***

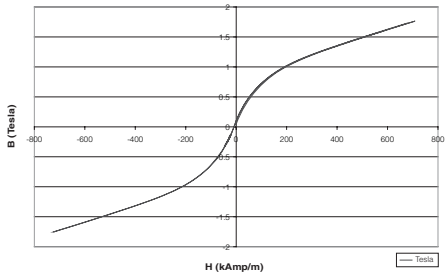


Values stated in this technical data sheet represent typical values as not all tests are run on each lot of material produced. For formalized product specifications for specific product end uses, contact the Customer Support Center.

Information provided herein is based upon tests believed to be reliable. In as much as LORD Corporation has no control over the manner in which others may use this information, it does not guarantee the results to be obtained. In addition, LORD Corporation does not guarantee the performance of the product or the results obtained from the use of the product or this information where the product has been repackaged by any third party, including but not limited to any product end-user. Nor does the company make any express or implied warranty of merchantability or fitness for a particular purpose concerning the effects or results of such use.



LORD provides valuable expertise in adhesives and coatings, vibration and motion control, and magnetically responsive technologies. Our people work in collaboration with our customers to help them increase the value of their products. Innovative and responsive in an ever-changing marketplace, we are focused on providing solutions for our customers worldwide . . . Ask Us How.

**LORD Corporation**
**World Headquarters**
111 Lord Drive
Cary, NC 27511-7923
USA

**Customer Support Center**
+1 877 ASK LORD (275 5673)

www.lord.com



LORD Ask Us How™

# E Test Photos

**Figure 66:** Picture of the magnet holder when mounted on the pipe. Notice the (manual) valve at the outlet of the reservoir.

**Figure 67:** Picture of the magnet holder to the left, with the cap and iron cylinder used to push the magnets, and the cylinder constriction to the right. The constriction is a welding rod mounted on a piece of plexiglass.

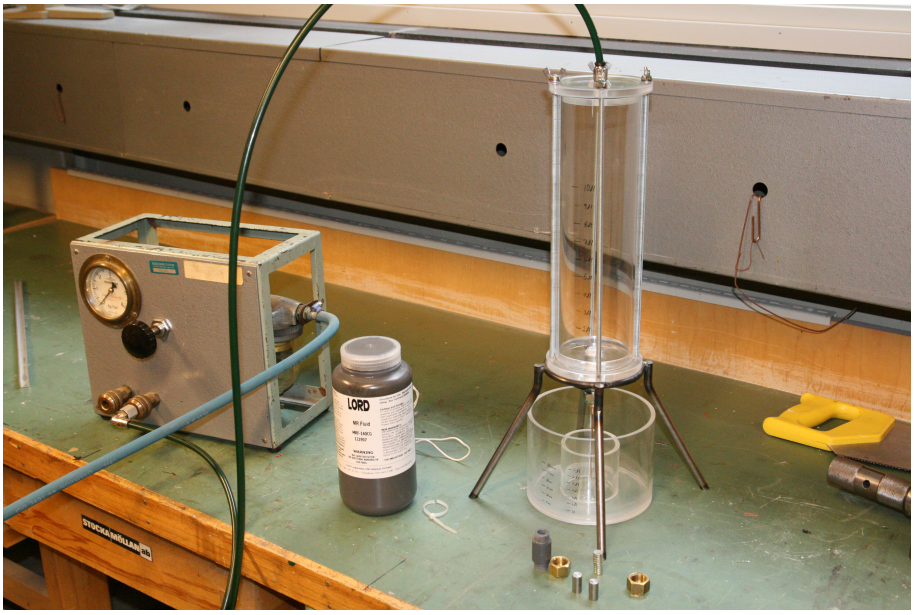


**Figure 68:** Picture of the whole test rig, with the (compressed air) pressure regulator to the left, the fluid in the middle, the reservoir and the receiver to the right, and the magnet holder in front of the reservoir.

# F Matlab Scripts

## F.1 mathematicalModel.m

```
%Finding p_11 and p_12

p_o = 100000;       %outlet pressure
p_i = 10e5;         %inlet pressure
eta = 0.28;         %(dynamic) viscosity
r_t = 0.00025;      %pipe radius 0.25mm
r_cyl = 0.000175;   %radius of cylindre constriction, 2r_cyl = 0.35mm
d = 0.001;          %length of the magnetic field interaction  1mm
l_21 = 0.001;       %see figure 1mm
l_22 = l_21;
l_n = 0.001;        %"nozzle" length
l_ic = 0.0002;      %length of inlet constriction 0.2mm
r_ic = 0.00005;     %radius of inlet constriction, 2r_ic = 0.1mm
R_ic1 = (12*eta*l_ic)/(pi*(r_ic^4));
R_ic2 = R_ic1;
R_i1 = (12*eta*0.004)/(pi*(r_t^4));
R_i2 = R_i1;
x = 0.0005:0.00001:0.001;

H_pm = 80000;          %preload made by the Permanent magnet
H1 = 0;
H2 = 0;
k_tau=0.3;             %yield stress proportionality constant
tau_y1 = k_tau*H1;     %yield stress at pipe 1
tau_y2 = k_tau*H2;     %yield stress at pipe 2

den = pi*(r_t^2-r_cyl^2)*(r_t-r_cyl)^2;
R_p1 = R_ic1+R_i1+ (12*eta*d)/(pi*(r_t^4)) + (12*eta*(l_21+l_n-x))/(pi*(r_t^4))
        + (12*eta*x)/(den);
R_p2 = R_ic2+R_i2+ (12*eta*d)/(pi*(r_t^4)) + (12*eta*(l_22+x))/(pi*(r_t^4))
        + (12*eta*(l_n-x))/(den);
Q1 = (p_i-p_o-(3*tau_y1*(d/r_t))./(R_p1);
Q2 = (p_i-p_o-(3*tau_y2*(d/r_t)))./(R_p2);

p_11 = Q1.*((12*eta*d)/(pi*(r_t^4)) + (12*eta*(l_21+l_n-x))/(pi*(r_t^4))
        + (12*eta.*x)./(den)) + 3*tau_y1*(d/r_t) + p_o;
```

```
p_12 = Q2.*((12*eta*d)/(pi*(r_t^4)) + (12*eta*(l_22+x))/(pi*(r_t^4))
        + (12*eta*(l_n-x))/(den)) + 3*tau_y2*(d/r_t) + p_o;
dP = p_11-p_12;

A_p = (pi*0.002^2)-(pi*0.0005^2);
F = dP*A_p;

dx = x-0.0005;

%Plots
figure(1)
subplot(2,1,1)
plot(dx,F3,'g')
hold on
grid on
plot(dx,F2,'r')
plot(dx,F1)
hold off
title('Plot of the force versus the displacement of the piston')
xlabel('\Delta x [m]')
ylabel('F [N]')
legend('2r_c_y_l = 0.35mm','2r_c_y_l = 0.25mm','2r_c_y_l = 0.15mm')
xlim([0,5e-4])
subplot(2,1,2)
plot(dx,dP3,'g')
hold on
grid on
plot(dx,dP2,'r')
plot(dx,dP1)
hold off
title('Plot of the differential pressure versus the displacement of the piston')
xlabel('\Delta x [m]')
ylabel('\Delta P [Pa]')
legend('2r_c_y_l = 0.35mm','2r_c_y_l = 0.25mm','2r_c_y_l = 0.15mm')
xlim([0,5e-4])
```

## F.2 magneticCalculations.m

```
%Magnetic field calculations
```

```
r_t = 0.0005;       %radius of the pipe 0.5mm   (1mm diameter)
r_core = 0.0005;    %radius of the electromagnetic coil core
d = 0.001;          %magnet height
l_f = 0.002;        %length of the two fluid gaps
mu_f = 5e-6;        %permeability of fluid
A_f = d*(2*r_t);    %cross-sectional area of fluid gap - no fringing
l_ret = 0.02;       %length of flux return path  2cm
%l_ret = 0:0.0001:0.02;
mu_ret = 5000e-6;   %permeability of flux return path
%mu_ret = 0:1e-4:25000e-6;
A_ret = 1e-6;       %cross-sectional area of flux return path...
%A_ret = 0:1e-8:5e-6;
l = 0.005;          %length of coil windings 5mm
%l = 0:0.0001:0.01;
mu = 5000e-6;       %permeability of iron
%mu_c = 0:250e-6:25000e-6;   %the permeability in the coil core
mu_c = mu;
l_c = l;             %length of coil core
N=50;                %#windings in the coil
%N = 0:1:250;
%i=1;
i = 0:0.001:2;       %current in the coil
Fmmf = N*i;
A_c = pi*r_core^2;      %cross-sectional area of coil core
%A_c = 0:1e-8:1e-6;
%H = 440;               %saturation limit of iron
H = Fmmf./l;            %Field intensity from windings

R1 = l_f/(mu_f*A_f);        %Reluctance of fluid gap
R2 = l_ret./(mu_ret.*A_ret);  %Reluctance of flux return path

Rc = l_c./(mu_c.*A_c);             %Reluctance of the coil core

H_f = (R1./(R1+R2+Rc))*Fmmf./l_f;     %field intensity over fluid gap
H_c = (Rc./(R1+R2+Rc))*Fmmf./l_c;     %field intensity in coil core

H_ret = (R2./(R1+R2+Rc))*Fmmf./l_ret

x = ((1e-5)*H_f + 2)/1000;      %divide by 1000 to get meters
```

```
figure('Name','Various core properties etc..','NumberTitle','off')
subplot(2,1,1)
plot(i,H_f)
grid on
xlabel('i [A]')
ylabel('H_f [A/m]')
title('Field intensity in the fluid vs the current, with N=50')

subplot(2,1,2)
plot(i,H_c)
grid on
xlabel('i [A]')
ylabel('H_c [A/m]')
title('Field intensity in electromagnetic coil core vs the current')
```

# G CD

Contents of the CD:

- *Comsol Models*
  - *3Dmodel.mph* – the preliminary 3D model.
  - *2Dmagnetic.mph* – the model used in the magnetic simulations.
  - *2Dmagnetic.mph* – the model used in the constriction simulations with short pipes.
  - *2Ddynamic.mph* – the model used in the dynamic simulations with longer pipes.
- *Matlab Scripts*
  - *magneticCalculations.m* – the script used for calculating the magnetic fields.
  - *mathematicalModel.m* – the script used in the pressure calculations.
  - *realTests.m* – the script used for displaying the results of the tests and compare this with the mathematical model (Figure 54).
  - *realTestsSubtraction.m* – used for displaying the subtraction tests (Figure 55).
  - *realTestsConstriction.m* – used for displaying the constriction tests and compare with the mathematical model (Figure 56).
- *References* – Some of the references in the reference list
- *Test Photos* – Different photos from the tests